SECOND QUARTERLY REPORT

REUSABLE NUCLEAR STAGE ADVANCED STRUCTURES STUDY

CONTRACT NAS8-27191

REPORT PERIOD: JULY 26 — OCTOBER 25, 1971

NOV 1971
RECEIVED

MCDONNELL DOUGLAS ASTRONAUTICS COMPANY

FACILITY FORM 602

N71 76484
(ACCESSION NUMBER)
(THRU)
121
(PAGES)
None
(CODE)
CR-121036
(NASA CR OR TMX OR AD NUMBER)
(CATEGORY)

MCDONNELL DOUGLAS CORPORATION

SECOND QUARTERLY REPORT

REUSABLE NUCLEAR STAGE ADVANCED STRUCTURES STUDY

CONTRACT NAS8-27191

REPORT PERIOD: JULY 26 -- OCTOBER 25, 1971

PREFACE

This document represents the second informal quarterly report prepared under Contract NAS8-27191 entitled "Reusable Nuclear Stage Advanced Structure Development Study." The work is being performed for the National Aeronautics and Space Administration's Marshall Space Flight Center under the cognizance of Mr. J. M. Walters, the Contracting Officer's Representative. The study will define an advanced structural concept for Reusable Nuclear Stage (RNS) modules capable of being launched into earth orbit within the cargo bay of the Space Shuttle and which will be operational in the 1980's and beyond. The major contributors to this report and their area of concentration are summarized below:

L. B. Goda -- Study Manager
Task 2, Design Concept Study

R. J. Holl -- Coordination

E. A. Grant -- Manufacturing

J. S. Evangelides -- Inspection and Testing

G. Markus -- Costing

R. M. Washburn -- Task 4, Materials Investigation

CONTENTS

Section 1	INTRODUCTION AND SUMMARY	1-1
	1.1 Study Objectives	1-1
	1.2 Previous Study Results	1-1
	1.3 Study Plan and Status	1-5
	1.4 Baseline RNS Configuration	1-6
Section 2	TASK 2 -- DESIGN CONCEPT STUDY	2-1
	2.1 Task 2.1 -- Design Criteria	2-1
	2.2 Task 2.2 -- Concept Formulation	2-4
	2.2.1 Stabilization System	2-4
	2.2.2 Tank Penetrations	2-10
	2.2.3 Propellant Feedline	2-11
	2.2.4 Pressurization Duct	2-13
	2.2.5 Tank Sump	2-15
	2.2.6 Fiber Reinforcement Layup	2-15
	2.2.7 Thermal Insulation	2-19
	2.3 Task 2.3 -- Concept Definition	2-21
Section 3	TASK 3 -- MANUFACTURING FEASIBILITY AND COST ASSESSMENT	3-1
	3.1 Manufacturing Feasibility Assessment	3-1
	3.1.1 Tooling	3-1
	3.1.2 Manufacturing Plan	3-6
	3.1.3 Inspection and Testing	3-15
	3.2 Cost Analysis	3-30
	3.2.1 Bases for Cost Estimates	3-30
	3.2.2 Recurring Costs	3-36
	3.2.3 Nonrecurring Costs	3-40

Section 4 TASK 4 -- MATERIALS INVESTIGATION 4-1

4.1 Materials Summary 4-1

4.2 Organic Matrix 4-2

4.2.1 Requirements 4-2
4.2.2 Candidate Matrix Materials 4-4
4.2.3 Low Temperature Fracture Toughness 4-6
4.2.4 Processing 4-7
4.2.5 Properties of the Organic Matrix 4-13

4.3 Filamentary Reinforcement 4-15

4.3.1 Requirements 4-15
4.3.2 Candidate Reinforcement Materials 4-16
4.3.3 Evaluation 4-21
4.3.4 Assembly Concept 4-23

4.4 Tank Liner 4-25

4.4.1 Requirements 4-25
4.4.2 Candidate Liner Materials 4-26
4.4.3 Evaluation 4-26
4.4.4 Selected Concept 4-28

References R-1

Figures

Number		Page
1.2-1	Individual Module Concept	1-2
1.2-2	Space Frame Concept	1-4
1.3-1	Study Schedule	1-5
1.4-1	Baseline RNS Configuration	1-6
1.4-2	RNS Propellant Module	1-7
2.1-1	Limit Bending Moment Distribution, Engine Operation	2-2
2.1-2	Limit Axial Load Distribution, Engine Operation	2-2
2.2-1	Internal Support, Eight Peripherial Struts	2-5
2.2-2	Internal Umbrella Support	2-7
2.2-3	External Support	2-9
2.2-4	Feed Through Redesign	2-11
2.2-5	Original Sump Design	2-16
2.2-6	Revised Sump Design	2-16
2.2-7	Membrane Layup Sequence	2-18
2.2-8	Stretch Weave Concept	2-19
2.2-9	Insulation Joint Location	2-20
2.3-1	Baseline Configuration	2-22
3.1-1	Propellant Module Subassemblies	3-2
3.1-2	Supported Inflatable Mandrel (Option 1)	3-4
3.1-3	Non-Inflatable Mandrel (Option 2)	3-7
3.1-4	Manufacturing Flow Plan	3-8

Figures (Cont'd)

Number		Page
3.1-5	Feed Through Installation	3-10
3.1-6	Flow Plan for Intermodule Thrust Structure	3-12
3.1-7	Ultrasonic Properties of a Pyrolyzed Unidirectional Carbon-Carbon Composite	3-23
3.1-8	Holographic Inspection of 15 cm Titanium Pressure Vessel	3-25
3.1-9	Typical Acoustic Emission Response of Carbon-Carbon Composite in Tensile Test	3-28
3.1-10	Correlation Between Strength and Attenuation For Plate-Slap Tested Composite	3-29
3.2-1	Work Breakdown Structure	3-32
4.2-1	Crack Propagation by Craze Formation and Breaking	4-6
4.2-2	Thermal Effects on Epoxy Resin	4-8
4.3-1	Contraction Curves for Potential Materials	4-24
4.4-1	Total Materials Selection for RNS Tank Wall	4-28

Tables

Number		Page
1.4-1	RNS Weight Comparison	1-8
2.2-1	Support System Weights	2-10
2.3-1	Structural Weight	2-32
3.1-1	Propellant Tank Acceptance Test Program	3-15
3.1-2	Manufacturing Testing Sequences	3-17
4.3-1	Present and Predicted 1980 Fiber Properties (SI Units)	4-17
4.3-2	Present and Predicted 1980 Fiber Properties (English Units)	4-18
4.3-3	Present and Predicted 1980 Composite Properties (SI Units)	4-19
4.3-4	Present and Predicted 1980 Composite Properties (English Units)	4-20

Section 1

INTRODUCTION AND SUMMARY

This report summarizes the technical work performed during the second quarter on the Reusable Nuclear Stage Advanced Structures Study, under Contract NAS8-27191. Following a summary in this section the balance of the report is organized according to the task breakdown structure used in the study.

1.1 STUDY OBJECTIVES

The primary objective of this study is to define an advanced structure design concept for the Reusable Nuclear Stage (RNS) with modules adapted for transport to orbit by the space shuttle. Additionally, the study is to perform a feasibility assessment of the selected concept and identify the major technology developments required. The technology level utilized in this study is for the 1980's and beyond. This allows the use of very advanced structural materials and introduces the option of space fabrication. These factors are most significant for the RNS performance due to the low density mono-propellant LH_2 employed and the limited volume available in the space shuttle cargo bay.

1.2 PREVIOUS STUDY RESULTS

Phase A definition studies were conducted under NASA contract to define RNS configurations capable of being launch into earth orbit within the cargo bay of the space shuttle. These studies utilized a 1973 technology level and resulted in multiple modules fully fabricated on the ground with dimensions limited by those of the space shuttle cargo bay. Due to these limited dimensions approximately 8 discrete propellant modules were required to provide the reference propellant loading of 136,000 Kg of LH_2. Additionally, due to the early level of technology these modules were fabricated from aluminum alloy.

The concept identified by MDAC under Contract NAS8-24714 is shown in Figure 1.2-1 (Reference 1.1). Three distinct types of modules, all configured for launch to orbit inside the 4.57 m (15 ft) diameter by 18.3 m (60 ft) long cargo bay of the space shuttle, are employed in this vehicle. All modules are completely fabricated on the ground and can be assembled and disassembled in space to form the RNS vehicle. The propulsion module contains NERVA and a small run tank of propellant. This facilitates replacement of NERVA as might be required because of failure or to extend the lifetime of the RNS vehicle beyond that of the engine. Primary propellant is contained in the 8 propellant modules shown. Each propellant tank contains 16,600 Kg (36,500 lbs) of LH_2. The modules have a docking system on each end and are assembled in the clustered configuration shown by first accomplishing an end-to-end docking and then rotating the outboard module into position with the aid of deployed hinge mechanism and space tugs. An automated deployment

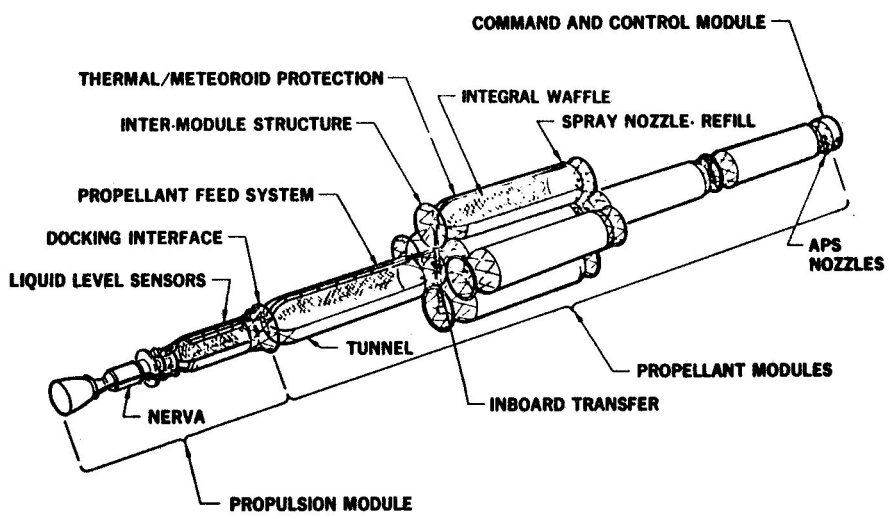

Figure 1.2-1 INDIVIDUAL MODULE CONCEPT

system is used to connect the main propellant and electrical lines between modules. The command and control module (CCM) is located at the forward end of the vehicle. This module contains most of the functional equipment and all of the expendables except mainstage LH_2. It is replaced between missions in earth orbit, thereby effecting a replenishment of expendables and all scheduled maintenance.

The vehicle configuration was selected to optimize the combined effects of biological shield weight, which favors maximum vehicle length; maximum stability and controllability, which favors minimum length; and minimum assembly operations from the fewest outboard modules. The configurations shown employs 4 tandem modules which, in conjunction with the small solid angle subtended by the run tank, precludes the requirements of any biological shield. An adequate margin of safety is maintained for vehicle stability and controllability with this configuration.

The Lockheed modular concept developed under Contract NAS8-24715 is shown in Figure 1.2-2 (Reference 1.2). After transportation to earth orbit by the space shuttle, the modules are assembled in the configuration shown. This system is also completely fabricated on the ground and consists of a space frame, 6 propellant modules, and a propulsion module. They are configured in two tiers with a central void within the space frame in the forward tier. The space frame is hexagonal and provides the basic load carrying structure of a RNS. The outboard propellant modules are side docked to this space frame for vehicle assembly. An equipment module is located at the forward end of the space frame and is stowed inside the space frame during launch. It has 6 equipment bay areas and contains the major stage functional equipment. Hinged panel doors or hinged trays provide accessibility to the equipment within the structure. Service of the module is performed via EVA in orbit.

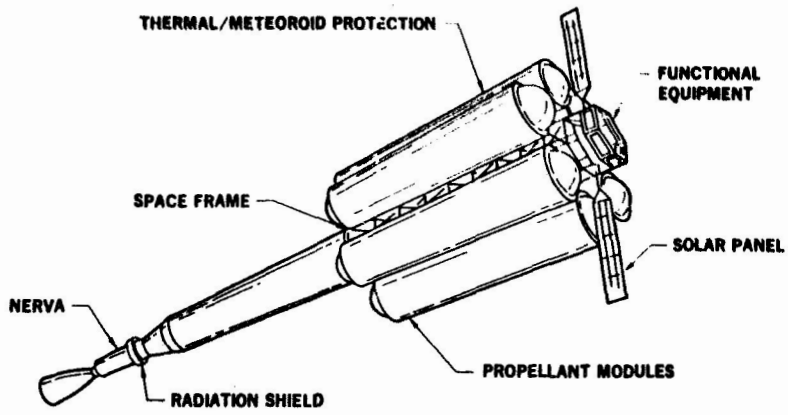

Figure 1.2-2 SPACE FRAME CONCEPT

Examination of these concepts shows that the major impact of the limited space shuttle cargo bay dimensions is on the propellant module configuration. Additionally, virtually all stage structural weight is concentrated in the propellant module. For these reasons the advanced structural study will seek a light weight alternative to these propellant module configurations. The baseline approach will retain the use of the propulsion module and the CCM from the MDAC configuration.

1.3 STUDY PLAN AND STATUS

The study schedule is shown in Figure 1.3-1. The initial Task 1 activity selected a baseline configuration for the RNS. This task was completed and documented in the preceding quarterly report. The unique expandable structures concept resulting from Task 1 (summarized in the following subsection) was carried forward to Task 2 for further design definition. Task 2 was organized to treat the unique features as individual trade studies or topics for analysis. These features were then assembled to provide a baseline RNS configuration. This task has proceeded on schedule and will be completed during the next month. The new material requirements for the advanced RNS configuration were evaluated under Task 4, Materials Investigation. This task was completed during the

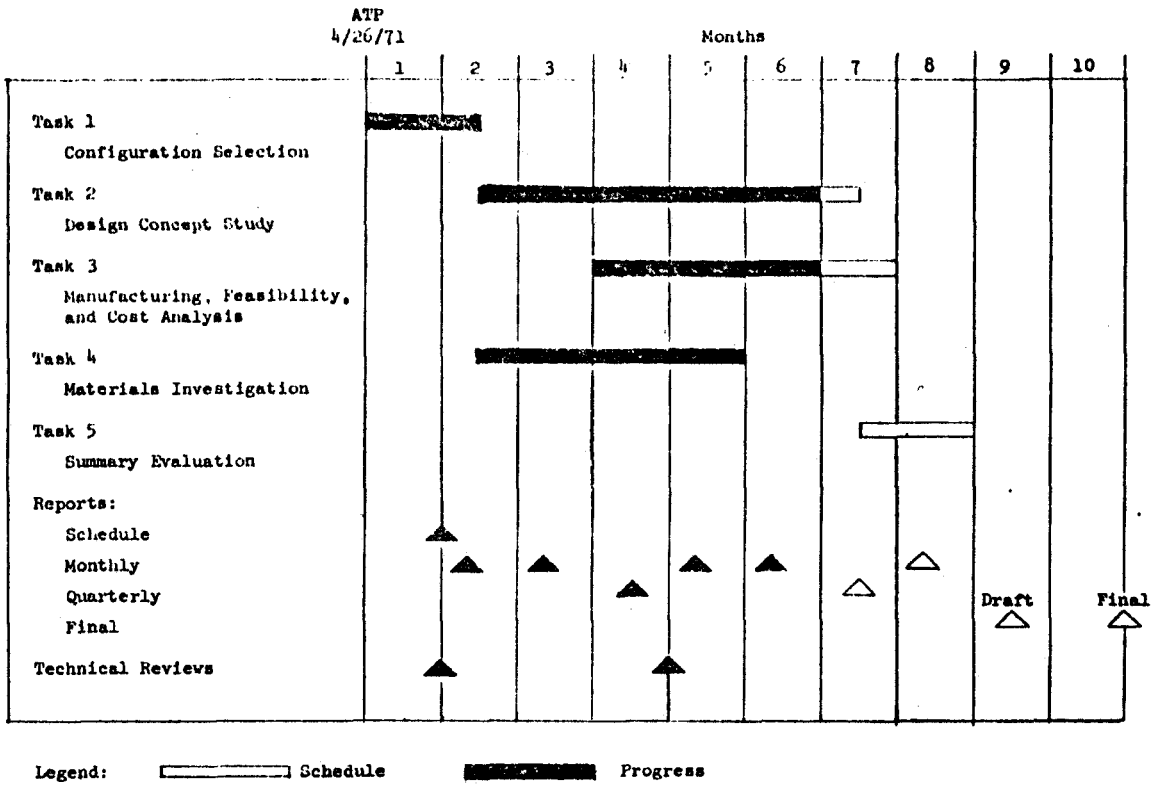

Figure 1.3-1 STUDY SCHEDULE

past quarter and resulted in the definition of a new concept for a multi-layer tank liner as well as the requirements for a space curable organic matrix tank wall composite. Task 3 was initiated during the past quarter and produced a tooling and manufacturing plan and established the basis for an inspection and testing plan and a costing analysis. Task 5, Summary Evaluation, is scheduled to begin during the next month and will produce a concept feasibility assessment, an over all evaluation, and a preliminary development program plan.

1.4 BASELINE RNS CONFIGURATION

The baseline RNS configuration defined in this study is shown in Figure 1.4-1. As can be seen the propulsion module and CCM from the preceding study results were retained. The full RNS propellant capacity is contained within the three propellant modules shown in a tandem configuration. The length of these modules is limited to the 18.3 m dimension of the space shuttle cargo bay; however, through the use of expandable tankage material a module diameter of 7.53 m is obtained. The individual propellant module is shown in Figure 1.4-2. The operational configuration shows the module fully deployed

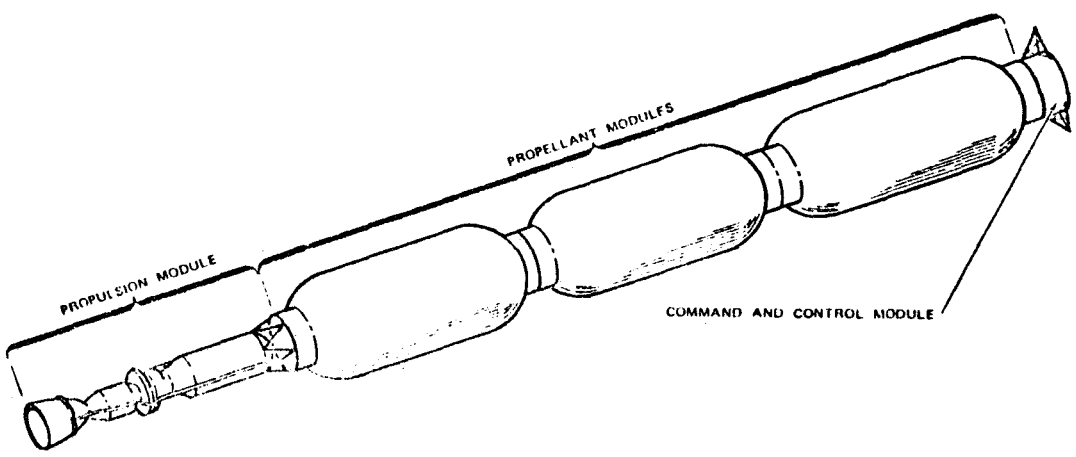

Figure 1.4-1 BASELINE RNS CONFIGURATION

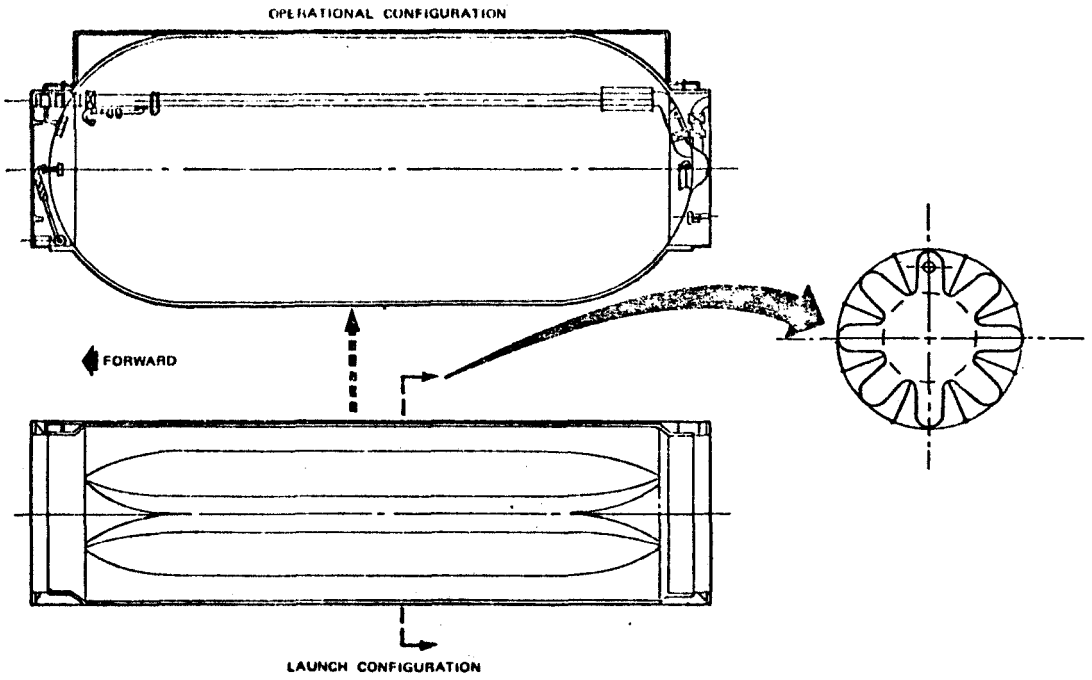

Figure 1.4-2 RNS PROPELLANT MODULE

as in the preceding figure. The launch configuration shows the module folded into an 8 pointed star shape to fit within the cargo bay of the space shuttle. The basic materials requirement imposed by this concept is for a pliable tank wall material which can be folded into the configuration shown for launch. An organic matrix composite tank wall is used to meet this requirement. The matrix undergoes a first stage cure to a pliable non-tacky condition for folding prior to launch. Once in orbit the tank wall is expanded to its operational configuration via internal pressurization and a final cure operation is performed to rigidize the tank. Composite reinforcement is provided by fibers of PRD-49-3. An integrally bonded tank liner is composed of 5 layers of urethane elastomer, each coated with vacuum deposited nickel. An integral seamless liner is provided in this way. The module end domes contained within the launch configuration are rigidized on the ground. All module instrumentation and equipment

as well as the inter-module thrust structure and docking systems are assembled on the ground to these rigid end domes. Thus, the expansion and cure operation in earth orbit produces a fully functional propellant module.

A weights comparison between this advanced configuration and the earlier MDAC concept is shown in Table 1.4-1. It can be seen that a potential weight reduction exceeding 11,000 Kg is available from this advanced concept. This is divided about equally between the improved materials properties of the advanced composite and the increased efficiencies due to reducing the number of modules from 8 to 3.

Table 1.4-1

RNS WEIGHT COMPARISON

Element	Weight (Kg)	
	Current (NAS8-24714)	Advanced Concept
Command and Control Module	2,130	2,130
Propulsion Module (W/O Disk Shield)	13,860	13,860
Propellant Modules:		
Tankage	2,820	8,600
Other Structure	1,065	4,320
Equipment	1,290	3,600
Thermal/Meteoroid Protection	3,050	4,520
Contingency	660	1,040
Disk Shield	1,210	--
Propellant Residuals	2,310	1,880
Total Operational Weight	28,395 (61,600 lb)	39,950 (87,900 lb)

Section 2

TASK 2 -- DESIGN CONCEPT STUDY

Design of the baseline RNS propellant module continued during this report period. Additional design criteria are given in Subsection 2.1. Specific design features selected for analysis or trade studies are contained in Subsection 2.2 while the overall module definition is summarized in Subsection 2.3.

2.1 TASK 2.1 -- DESIGN CRITERIA

The baseline configuration bending moment and axial load diagrams are shown in Figures 2.1-1 and 2.1-2 for mission operation with the engine gimbaled hardover at 0.079 rad (4.5 degrees) under full thrust 34,000 Kg (75,000 lb). These represent limit load conditions and were generated by the MDAC SB-15 "Structural Load Histories" computer program. They are for the most severe condition which is with all modules filled with LH_2. In the figures the gimbal point is at station 106 and the forward end of the command and control module is at station 45.5.

The maximum bending moment of 335,000 N-m (3.1×10^6 in. lb) occurs at station 67. In addition a thrust or compression load of 18,000 Kg (40,000 lb) is produced at this station. This results in a combined ultimate load of 22,000 N/m (126 lb/in) for the tankage which was analyzed to determine if it could resist engine operation loads in an unpressurized condition. Reference 2.1 was employed to perform the analysis and produced a bending allowable of 3,430 N/m (19.6 lb/in) and a compression allowance of 1,315 N/m (7.5 lb/in). These values are well below the design loads, therefore, the tankage must be pressurized to at least 4,470 N/m^2 (0.65 psi) operation to prevent buckling.

A meteoroid survival probability of 0.995 over the reference 27 day round trip lunar shuttle mission was assigned. This is consistent with the Phase III and Phase IV Reusable Nuclear Stage Definition Studies. Since tank pressurization is required for load transfer during engine operation, this criteria was applied to all module, full or empty, for the full mission duration.

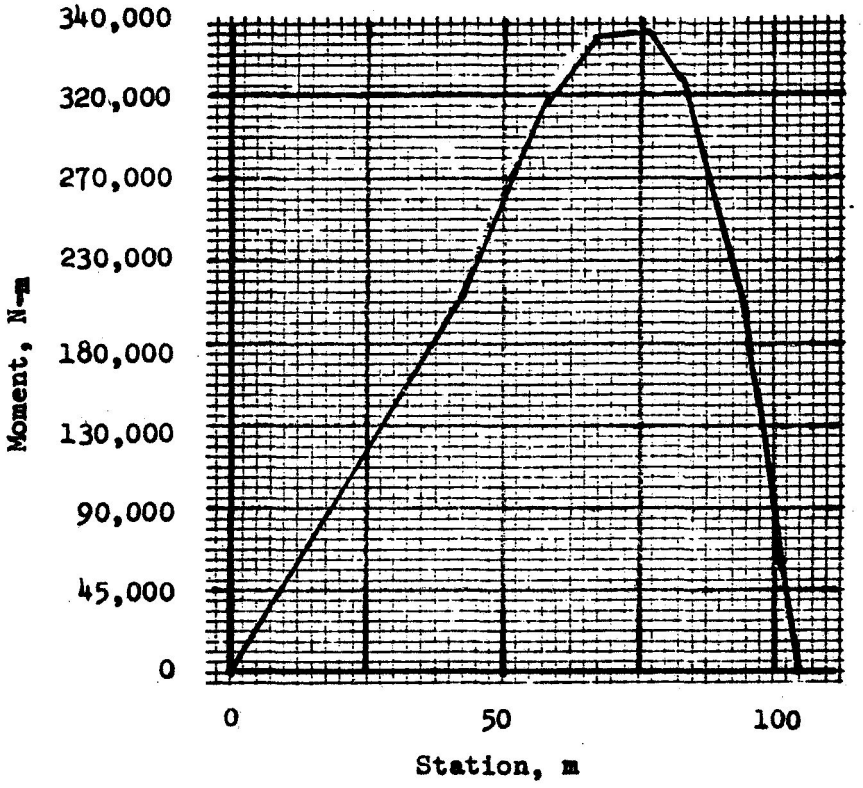

Figure 2.1-1 LIMIT BENDING MOMENT DISTRIBUTION, ENGINE OPERATION

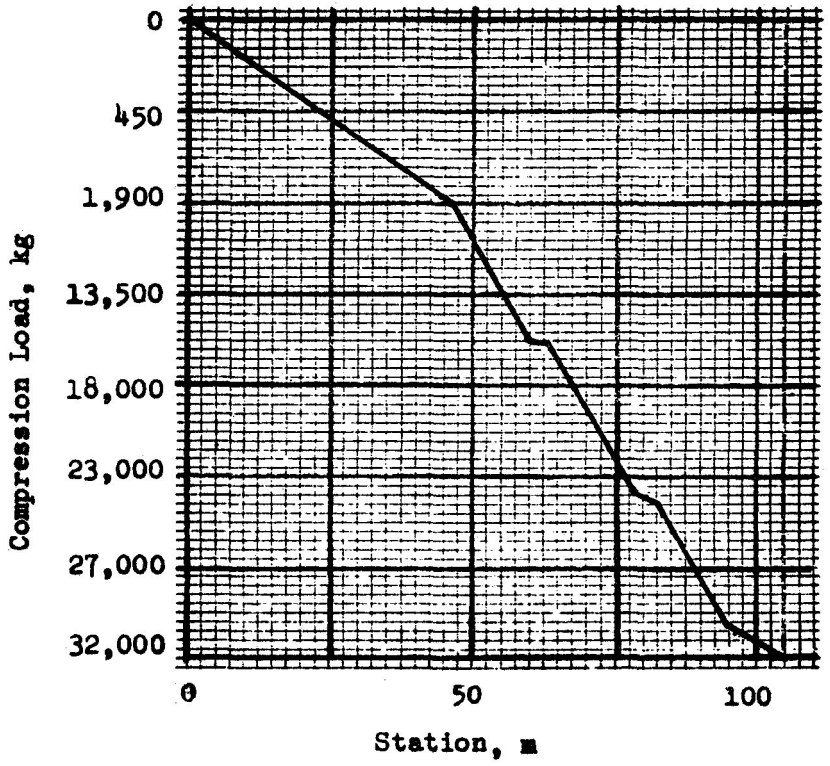

Figure 2.1-2 LIMIT AXIAL LOAD DISTRIBUTION, ENGINE OPERATION

The space meteoroid environment from Reference 2.2 was used. The meteoroid flux-mass model for the range of interest is described mathematically as:

$$\log N_t = -14.37 - 1.213 \log m$$

where N_t = number of particles/meter^2 - sec having mass m or greater and m = meteoroid mass in grams. The meteoroid density is 0.5 g/cm^3 and the average velocity is 20 km/sec. Additionally, the appropriate gravitational defocussing factor and planetary shielding factor as defined in the reference were applied over the course of the design mission.

2.2 TASK 2.2 -- CONCEPT FORMULATION

During this report period the stabilization system for space curing of the tankage composite was selected. As the baseline design progressed tank penetrations were redesigned to improve liner integrity, the propellant and pressurization lines were revised to improve system reliability for relative deflections between the tankage and the lines, and the sump was redesigned because of access requirements. In addition, requirements for the reinforcing fiber were reviewed and the fiber selection changed to PRD 49-3. At the same time a fiber reinforcement layup was determined.

The design problems associated with the insulation system were reviewed with the personnel conducting the high-performance insulation studies and tentative solutions arrived at for these problems.

2.2.1 Stabilization System

The candidate concepts for the support system required for the space curing of the tankage composite were reviewed. A new concept was developed for internal support of the interfaces and the external support system was redesigned because of inadequate clearances. The systems were sized based on the space shuttle acceleration load factors delineated in the design criteria section of the First Quarterly Report.

The internal support system developed during the first quarter is shown in Figure 2.2-1. It is comprised of eight struts that attach to stainless steel fittings bonded to the ground rigidized dome poles. The struts must be capable of moving with the tank as it is filled with LH_2 and subsequently pressurized. This is accomplished by employing a telescoping design whose sections are released by automatically pulling a pin.

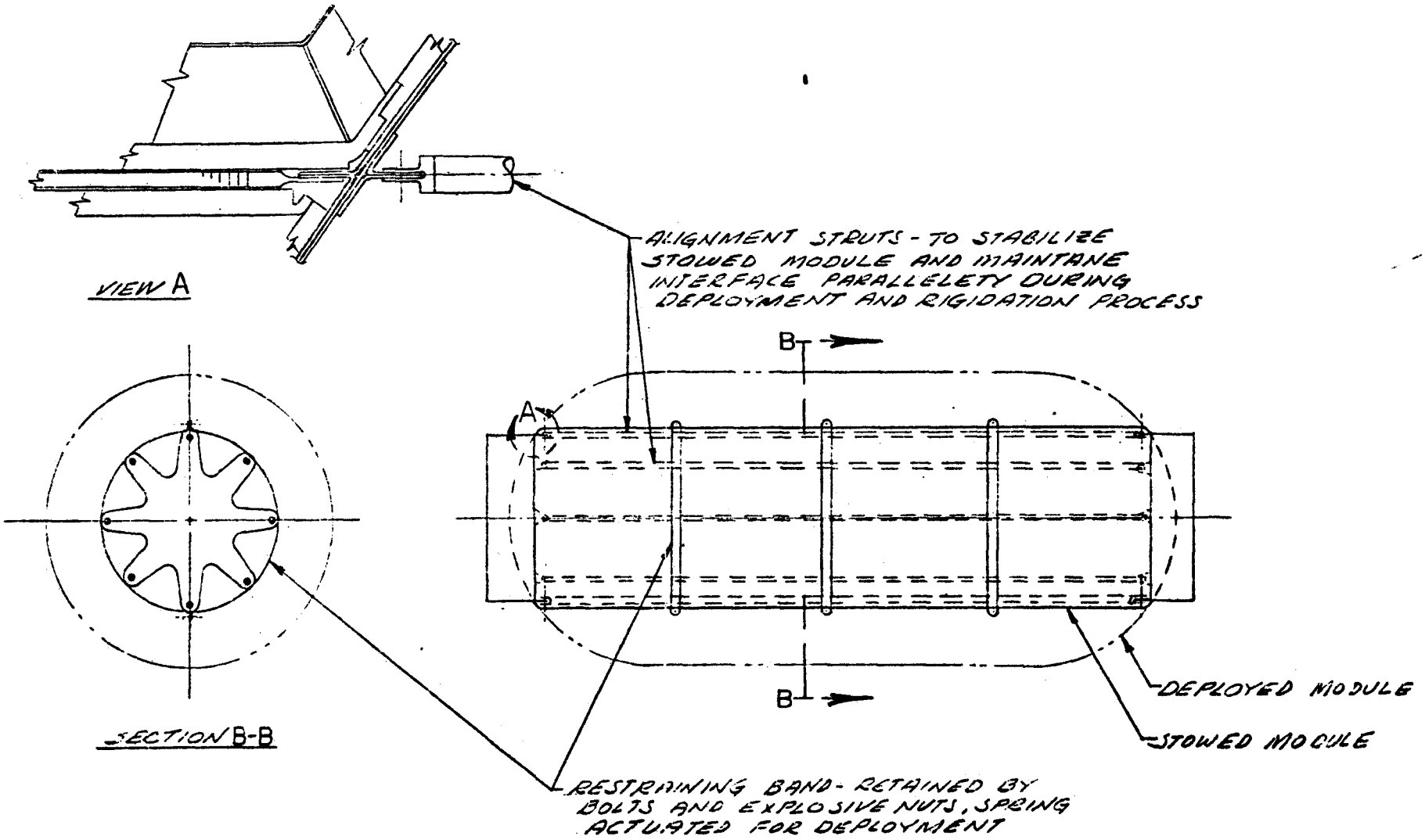

Figure 2.2-1 INTERNAL SUPPORT, EIGHT PERIPHERIAL STRUTS

The new internal support system, shown in Figure 2.2-2, consists of a central shaft which has a restraining ring attached at each end. Eight struts are installed to each ring. The struts bolt to stainless steel fittings which are bonded to the ground rigidized dome poles. To prevent racking or twisting of the system self-aligning bearings are not employed and a close tolerance is maintained between the support strut and the clevis of its attach fitting.

In order to ensure interface parallelity and perpendicularity with the center line, the system is installed and adjusted while the module is in its fabrication fixture. One of the restraining rings is attached to the central shaft by a pin equipped with an automatic pulling device. After the flexible tank composite has been cured in space the pin is pulled. This permits the restraining ring to move along the central shaft, thereby compensating for the expansion of the tank when it is filled with LH_2 and subsequently pressurized.

Foam blocks, which are attached to the restraining bands, were added to the internal support systems. These blocks are contoured to the valley of star fold and maintain the fold configurations. They are jettisoned with the restraining bands.

The disadvantages associated with this concept are: (1) the weight penalty incurred because the system is non-jettisonable and non-functionable after module rigidization, (2) the requirement for a pin puller inside the LH_2 tankage even though the number of pins has been reduced from eight to one, (3) the penetration of the impermeable liner and the attendant danger of liner cracking by the dome attach fittings and, (4) the probable requirement for a canister or shroud to support the uncured composite during ground operations and while the module is inside the space shuttle.

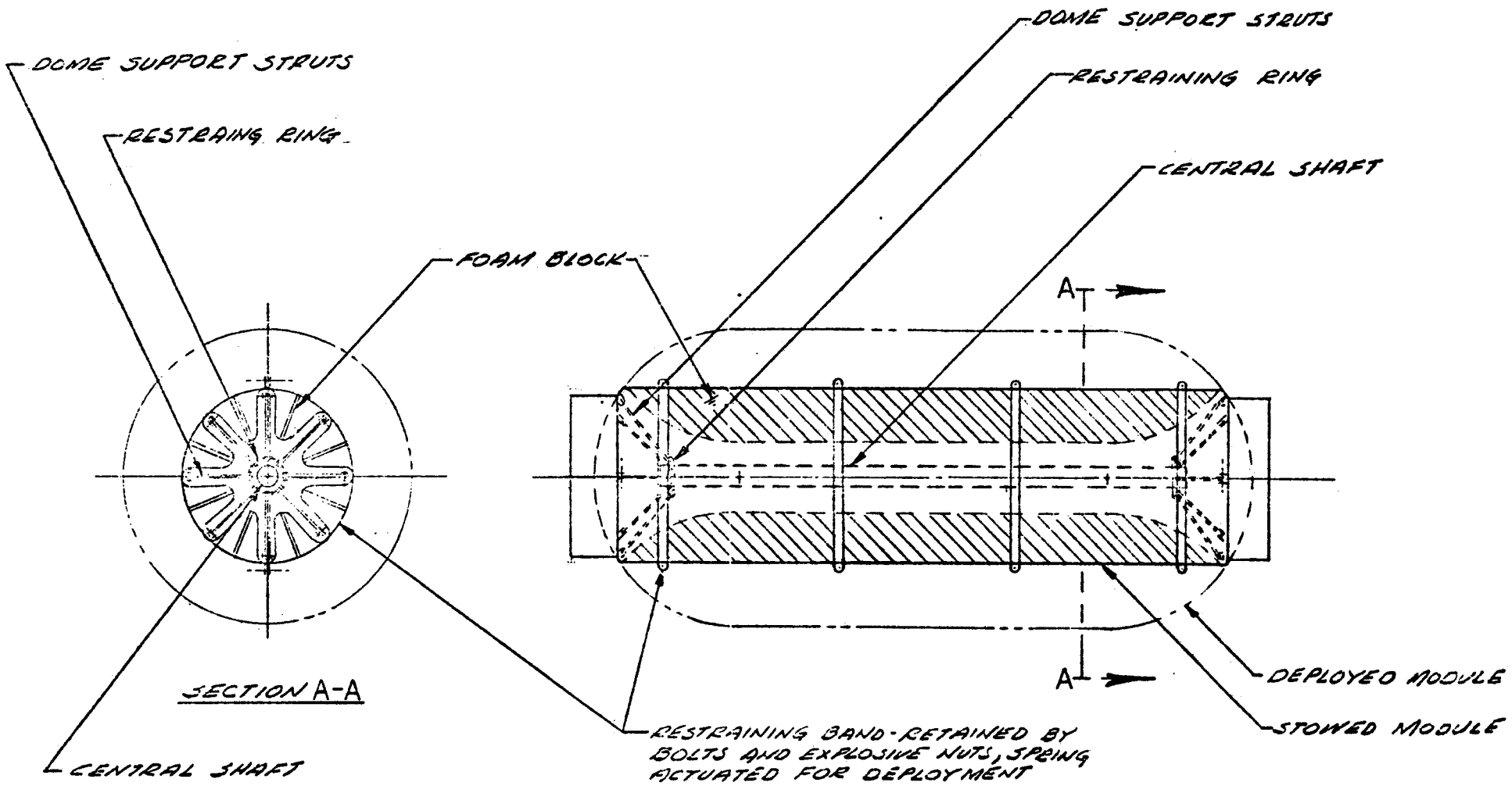

Figure 2.2-2 INTERNAL UMBRELLA SUPPORT

Since the support structure for the internal support concepts is non-jettisonable an aluminum graphite composite was selected for their construction. The properties used in the analysis were:

$$E = 18.3 \times 10^9 \ N/m^2 \ (26.5 \times 10^6 \ psi)$$
$$Ftv = 81.2 \times 10^6 \ N/m^2 \ (118{,}000 \ psi)$$
$$Fcy = 61 \times 10^6 \ N/m^2 \ (88{,}500 \ psi)$$
$$\rho = 2{,}220 \ Kg/m^3 \ (0.08 \ lb/in^3)$$

The main component of the revised design for the external support system (Figure 2.2-3) are eight L-shaped supports, two alignment support rings and two restraining bands. Each L-shaped support consists of four main members, two extending approximately the full length of the stage and two at 1.57 rad (90 degrees) to the longitudinal members. These traverse members attach to support fittings machined in the assembly support rings. For deployment the supports are rotated approximately 2.36 rad (135 degrees) about these fittings by a pulley and cable system. The supports are locked in their stowed position by the restraining bands which are jettisoned after the module has been deployed from the space shuttle. The inboard longitudinal members of the supports are formed to the contour of the valleys of the star fold to maintain the fold configuration. A truss framework is utilized to stabilize the longitudinal members.

Each of the alignment support rings is composed to two 3.14 rad (180 degrees) segments which are joined together with bolts and explosive nuts. The rings fit into grooves which are machined into the intermodular thrust structure interface rings. After the flexible composite has been rigidized, the explosive nuts are ignited and the alignment rings and supports are jettisoned by springs or a pyrotecnic device installed between the ring segments. An all aluminum construction was selected for this concept since the system is jettisoned after the tank is rigidized, thereby, imposing no penalty on the operational weight.

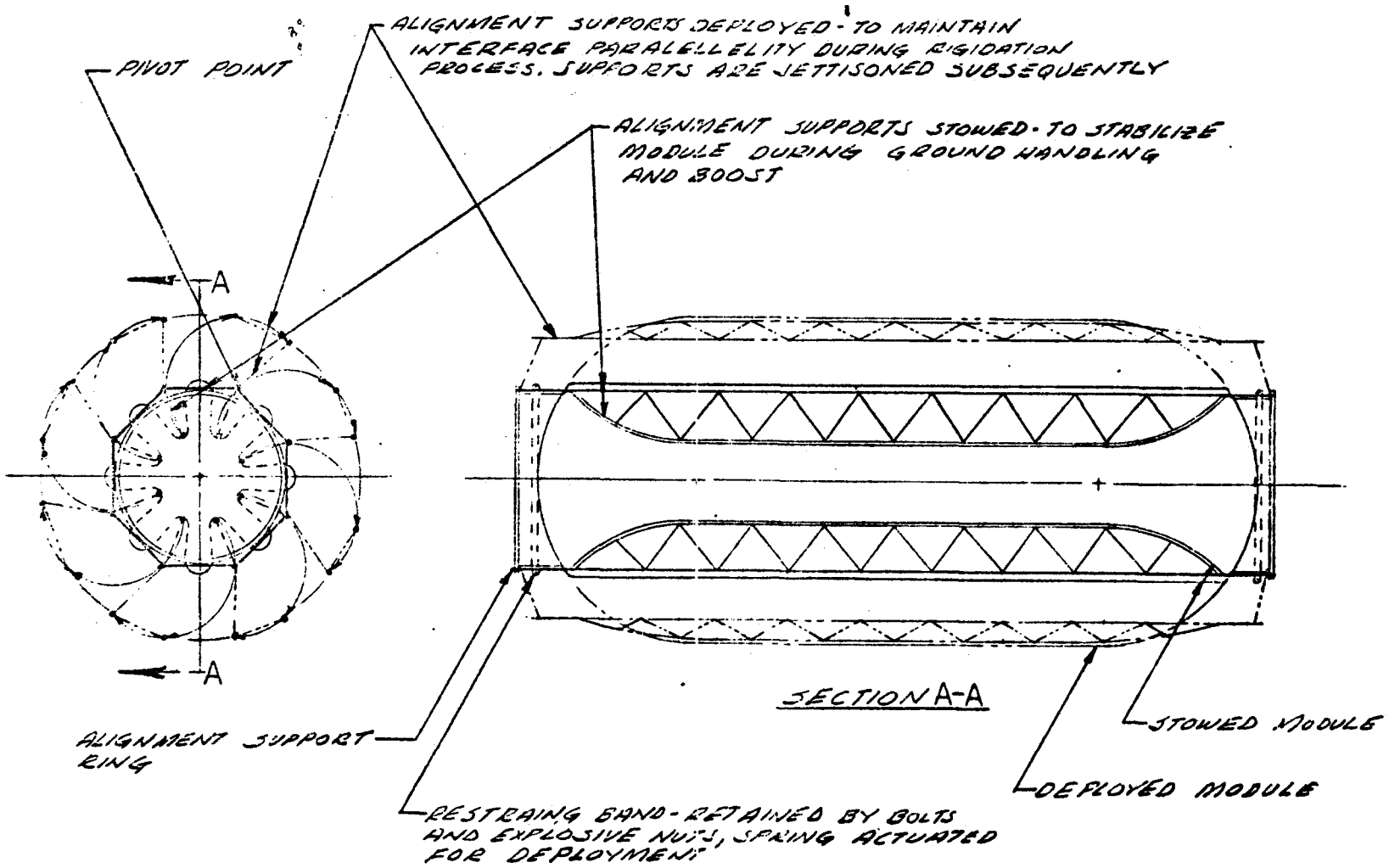

Figure 2.2-3 EXTERNAL SUPPORT

A weight statement for these three candidates is given in Table 2.2-1. The external support system was selected because: (1) it is jettisonable, therefore, having the least impact on operational weight, and (2) it does not require tank internal attach fittings which could cause cracks in the liner when loads are induced.

Table 2.2-1

SUPPORT SYSTEM WEIGHTS

System	Weight, Kg (Lb)
Internal Support, Eight Peripherial Struts	80 (175)
Internal Umbrella Support	55 (120)
External Support	380 (835)

2.2.2 Tank Penetrations

The liner concept developed for this study is a seamless membrane that can easily accommodate dome compound curvatures. It is fabricated by spraying a series of urethane layers on an inflatable mandrel. Each elastomer layer receives a coating of vacuum deposited nickle 600 to 1200 Å thick. 1200 Å is used as an approximate upper limit subsequent to which the coating become brittle.

In order to improve the integrity of the liner at tank penetrations the feed throughs were redesigned as shown in Figure 2.2-4. This design installs the feed through in the mandrel after the primary liner has been applied. A second, localized liner coating is then applied to the exterior, outboard edge of the feed through flange. This permits a metal to metal contact between the liner and the feed through flange and eliminates post applications of liner after the mandrel is removed as was the case with the previous design. After the liner has been fabricated the dome pole tankage composite is layed up and cured on the liner utilizing the same expandable mandrel as the liner.

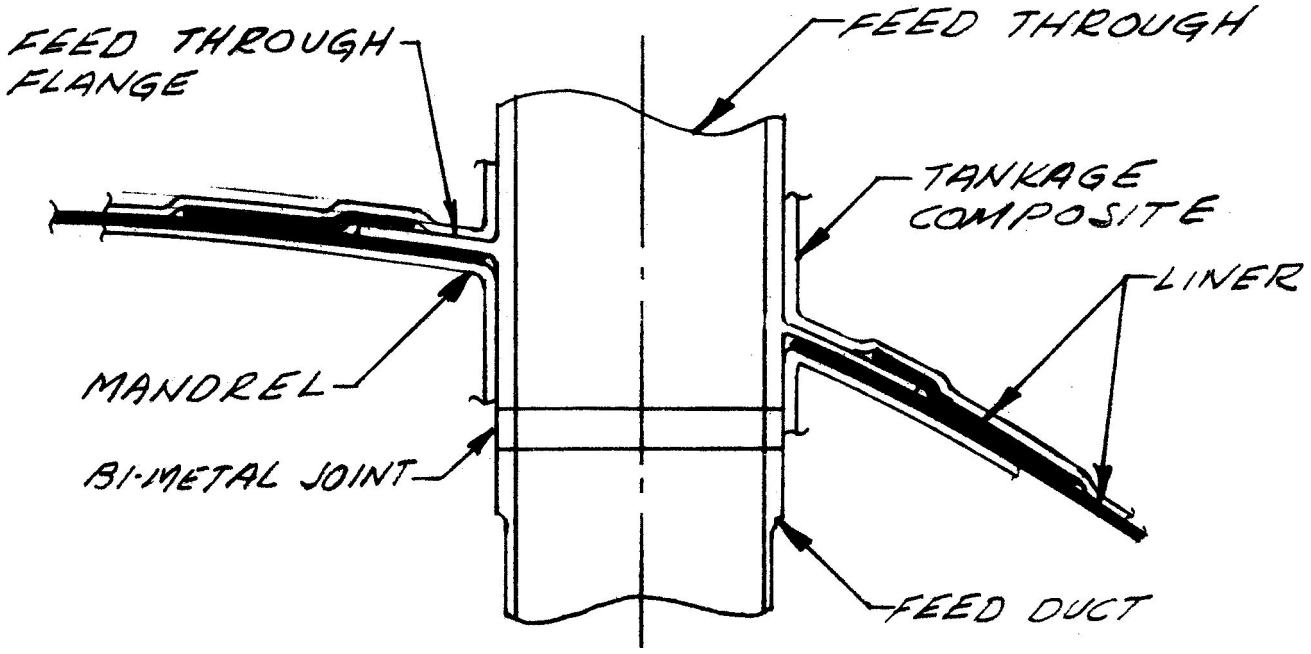

Figure 2.2-4 FEED THROUGH REDESIGN

The feed throughs were modified by incorporation of bi-metallic weld joints in place of bolted attach flanges internal to the tank. The external flange design was not changed because length requirements for the bi-metallic joint would decrease the tank length.

2.2.3 Propellant Feedline

Each propellant module contains an internal feed duct riser. This 12 in. diameter feed through duct is required for refueling and full thrust feed operating conditions. The duct traverses the entire length of the tank. Due to deployable requirements no support was available for this run. The duct basic material is aluminum and bi-metallic joining techniques will be utilized to transform to stainless steel wherever flexible elements are used so that no aluminum bellows will be utilized in the system. The duct design gages will be governed by collapse

considerations. This condition occurs during main feed system operation when the static pressure in the duct is less than the pressure in the tank through which the feed through is being accomplished.

The internal duct section must be capable of absorbing various working deflections. These deflections are installation tolerances, thermal deflections, and deflections due to tank pressurization. The differences in the duct parent material to tank material, make pressurization deflections predominant. The tank length relative to the duct will increase by 17.7 centimeters due to thermal and pressure effects. This large linear extension requirement in conjunction with the large unsupported duct length necessitated that the flexible elements used in this system provide the necessary structural stability as well as predictable end loading conditions. Various element schemes were investigated. A section of lined untied bellows was considered. This departs from being a pure tensile system, and therefore, introduces compressive end loading on the flanges. Since this condition could cause excessive bending moments due to the long unsupported length of the internal riser, it was discarded. Various dynamic sealing concepts were reviewed and discarded based on the same moment loading problems. The system selected utilizes a pressure volume compensator to absorb the large linear extension requirement. This type of a flexible element contains 3 sections of bellows which are inerted to eliminate the pressure separating load. This type of system will only transmit a load corresponding to the axial spring rate of the 3 sections of bellows. This provides for a predictable tensile loading system. The compensator in conjunction with two gimbals, one located at each end of the 60 ft. long riser, completes the system. The gimbals provide for flange misalignment and, in conjunction with the compensator, will provide the 5° freedom requirements of the system.

This pure tensile system also will be stable and therefore provide the required duct support. The gimbal joints and the pressure volume compensator both contain sections of convoluted metal bellows. A tentative selection for the material is 321 CRES. Expected low cycle requirements and the circumferential support obtained in the pressure volume compensator should reduce bellows squirm problems thus permitting the use of this conventional Austenitic steel. If high cycle requirements evolve, then various heat resistent alloys such as Inconel 718 must be investigated. Although some nickel-base alloys can present hydrogen embrittlement problems if ambient temperature regimes are prevalent.

2.2.4 Pressurization Duct

The pressurization line is a 2 in. diameter duct that runs external to the propellant tank. This duct conveys gaseous hydrogen at approximately 300°R and 800° psi from the engine tap-off to serve as expulsion pressurant. The duct assumes the shape of a double dog-leg and is supported on both ends on the tank intermodule thrust structures. Close to both supports on either end of the tank a swivel type joint is located. These joints provide a rotational deployment capability. The stowed position and the deployment motions are compatible with the stabilization system shown in Figure 2.2-3. The approximate 17 m unsupported length of this duct will require sufficient duct gage to ensure structural stability. The swivel type joints located on either end utilize a dynamic seal as well as sufficient guides to transmit the structural load into the tank support. This duct assembly must absorb operational deflections due to thermal and pressurization deflections relative to the propellant tank. The requirements are similar to those on the main propellant feed duct. There is a net increase in length of 15 centimeters due to the combined effects of the thermal and tank pressurization. The duct itself due to its relatively ambient surface temperature changes a very small amount. The various flexible elements were considered to achieve this deflection requirement with minimum tank loading and compatibility with the deployment requirements.

The configuration selected utilizes a sliding type joint with a dynamic seal to absorb the large linear extension requirement. The separation load induced by this dynamic seal is reacted by a rigid support where the duct penetrates the tank thrust structure. This solid support is a drill-on-assembly type support enabling the extension capability of the sliding joint to be used in conjunction with the two gimbal system to provide for installation tolerance absorption. The two gimbals provide a parallel offset capability, which in conjunction with the sliding joint provide the necessary 5° of freedom capability required of the system. A similar system is utilized on both ends of the dog-leg pressurant riser. Provisions will be made for teeing into the pressurization duct at the forward dome in order to provide a duct that will terminate at the interface between the modules. This tee will then enable pressurant to gas to be transferred to the next module in line. A pressure volume compensator was reviewed for this application and the major constraint being the increase in length requirement for such a flexible element.

Two other systems are currently still under reivew, and both look promising for this application. The first would utilize a basic 3 gimbal tensile system in the dog-leg portion of the duct. With the use of high angulation gimbals (15°) capability it is possible to absorb the full linear motion in a 3 gimbal angular system. The second alternative would be the utilization of two additional swivel type joints. This system introduces four more 90° bends which must be considered from a system impedence standpoint, but does afford a simple and direct routing. The addition of two more swivels with angulation capability will eliminate the necessity for the sliding joint and the two gimbal assemblies. This would reduce the loading problem at the penetration of the thrust structure. Since the current system uses swivel joints for deploying the pressurant duct loop, the addition of two more joints would be consistent with this philosophy. Although it should be noted that the unit loading on the dynamic seal in this type of joint would be high in order to achieve good leakage control. This would require a large force to rotate the joints.

The pressurization duct penetrates the tank from the forward dome area and terminates internal of the tank ullage in a pressurant diffuser which utilizes a nylon bag concept. The bag diffuser outlets prevent direct impingement of the warm pressurant gas into the cold liquid surface at the tank top.

2.2.5 Tank Sump

As the design of the mandrel progressed, it became evident the sump would have to be redesigned because of inadequate clearance for both mandrel removal and personal ingress and egress. In the original design shown schematically in Figure 2.2-5 the sump assembly consisted of a truncated cone and a cover which utilized a single conoseal. The sump body was integrated into the layup of the aft dome pole and had cloth layers bonded to both its flange and body. Since the propellant feed line elbow is welded to the sump body it infringes on the required clearance envelope.

A schematic of the redesigned version is shown in Figure 2.2-6. It consists of three components, the jamb, sump body and cover. Two conoseals are required for this design. The jamb is integrated into the layup of the aft dome pole and the sump body is bolted to the jamb after the mandrel is removed and there are no requirements for personal passage into the tank. The propellant feed line elbow is welded to the sump body in this case also but poses no clearance problems.

In the original design the cover was required to provide access to install both the anti-vortexing screen and to attach the feed line to the feed line elbow. With the revised version the anti-vortexing screen is installed prior to installation of the sump body and the cover is required only to provide access to make the final feed line connection.

2.2.6 Fiber Reinforcement Layup

A deflection check was conducted on the tankage to determine the motion caused by pressure and thermal loading. Results of the investigation showed that a tank constructed from fiber glass reinforcing filaments contracted 8 cm (3.15 in.) when cooled to LH_2 temperature and expanded 28.8 cm (11.37 in.) when pressurized to 20,700 N/m^2 (30 psi). This produced a total differential of 20.8 cm (8.22 in.) which is approaching

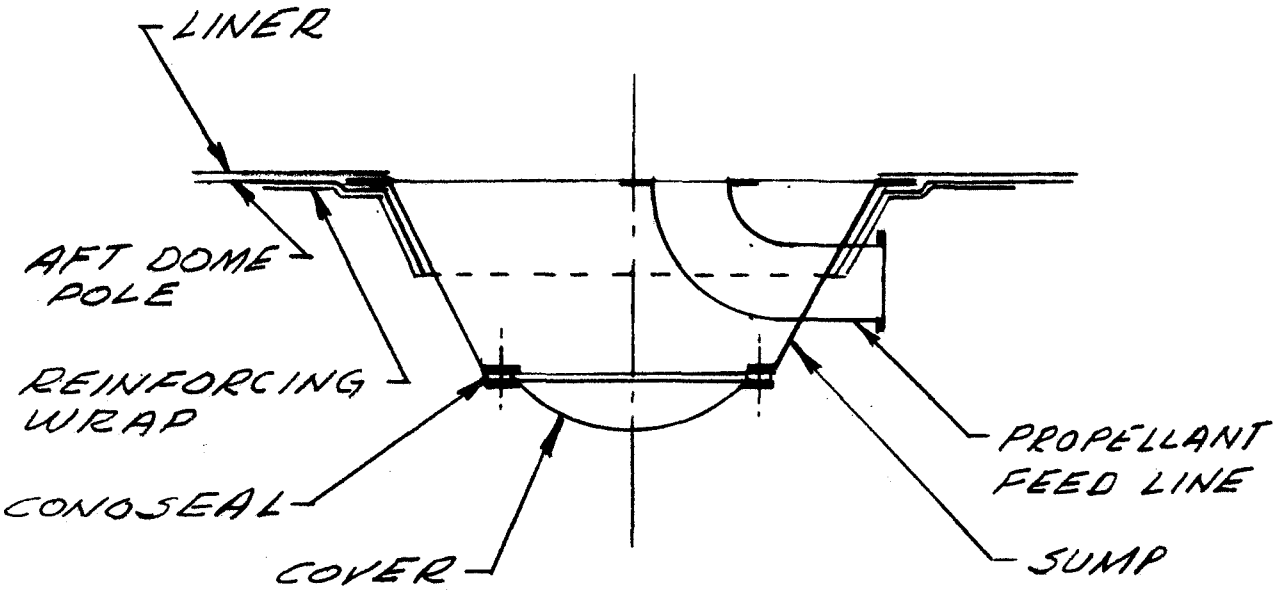

Figure 2.2-5 ORIGINAL SUMP DESIGN

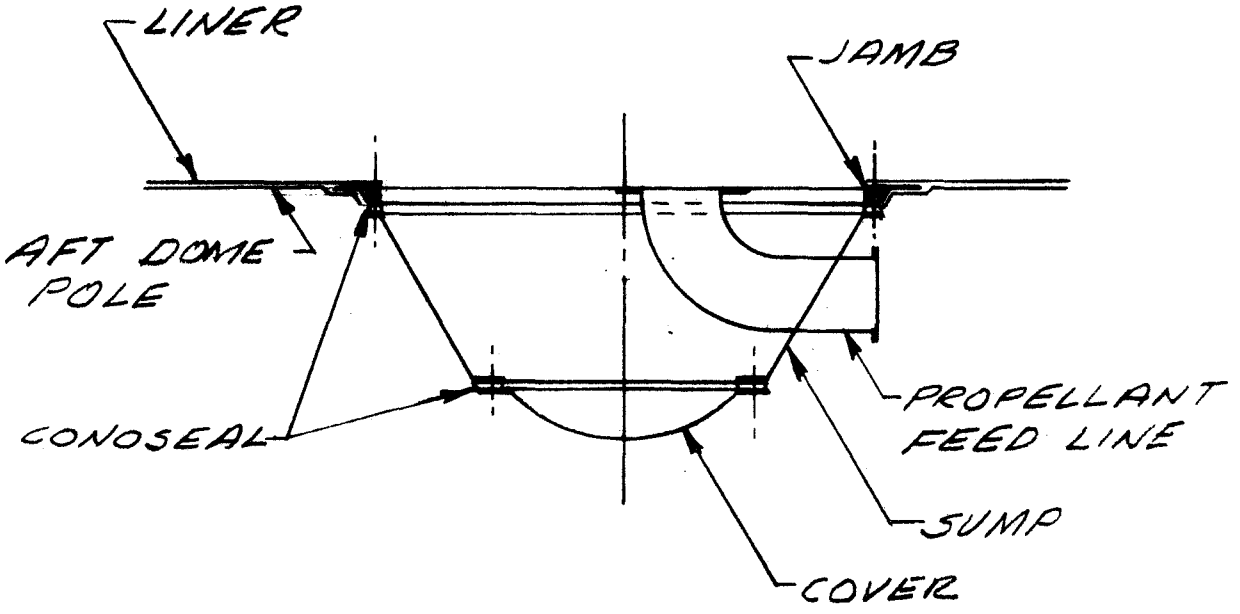

Figure 2.2-6 REVISED SUMP DESIGN

the two percent strain allowable of the matrix system. In an effort to reduce this value PRD 49-3 fibers were investigated because of their high modulus of elasticity. Even though this fiber exhibits a negative thermal coefficient of expansion, the total differential was reduced to 15 cm (5.9 in.). Based on the above results and its high specific strength, PRD 49-3 was selected for the reinforcing fibers (See Section 4 for material properties).

The longitudinally and circumferentially reinforced membranes are woven structures containing four per cent pic fibers. The neck area at one end of the longitudinally reinforced membranes is configured using an expansion weave which is designed to expand to the full diameter of the tank. They are installed over the liner, which contains an inflatable mandrel, per the sequence shown in Figure 2.2-7. After installation, the membranes are impregnated with the organic matrix and subjected to the first step cure. The membranes will be completely cured where they fasten to the intermodular thrust structure attach flanges. From this point through the transition zone they undergo a cure gradient to the first step cured area.

The weave required for the stretch portion of the membranes which have the majority of their reinforcing fibers oriented in the longitudinal direction was determined from a personal communication with Mr. W. Miller of Woven Structures. This will be accomplished by changing the characteristics of the fill yarn by plying it with an elastomeric yarn, pre-tensioned and served with S-glass fill yarn to give it a maximum expansion of 60 percent. Figure 2.2-8 is an illustration of the technique.

The requirements for integration 0.785 rad (45 degree) reinforcing fibers for shear transfer was investigated. Both practice and theory denote that only fibers oriented to react longitudinal and circumferential stresses are required. This has been shown by tests described in References 2.3 and 2.4.

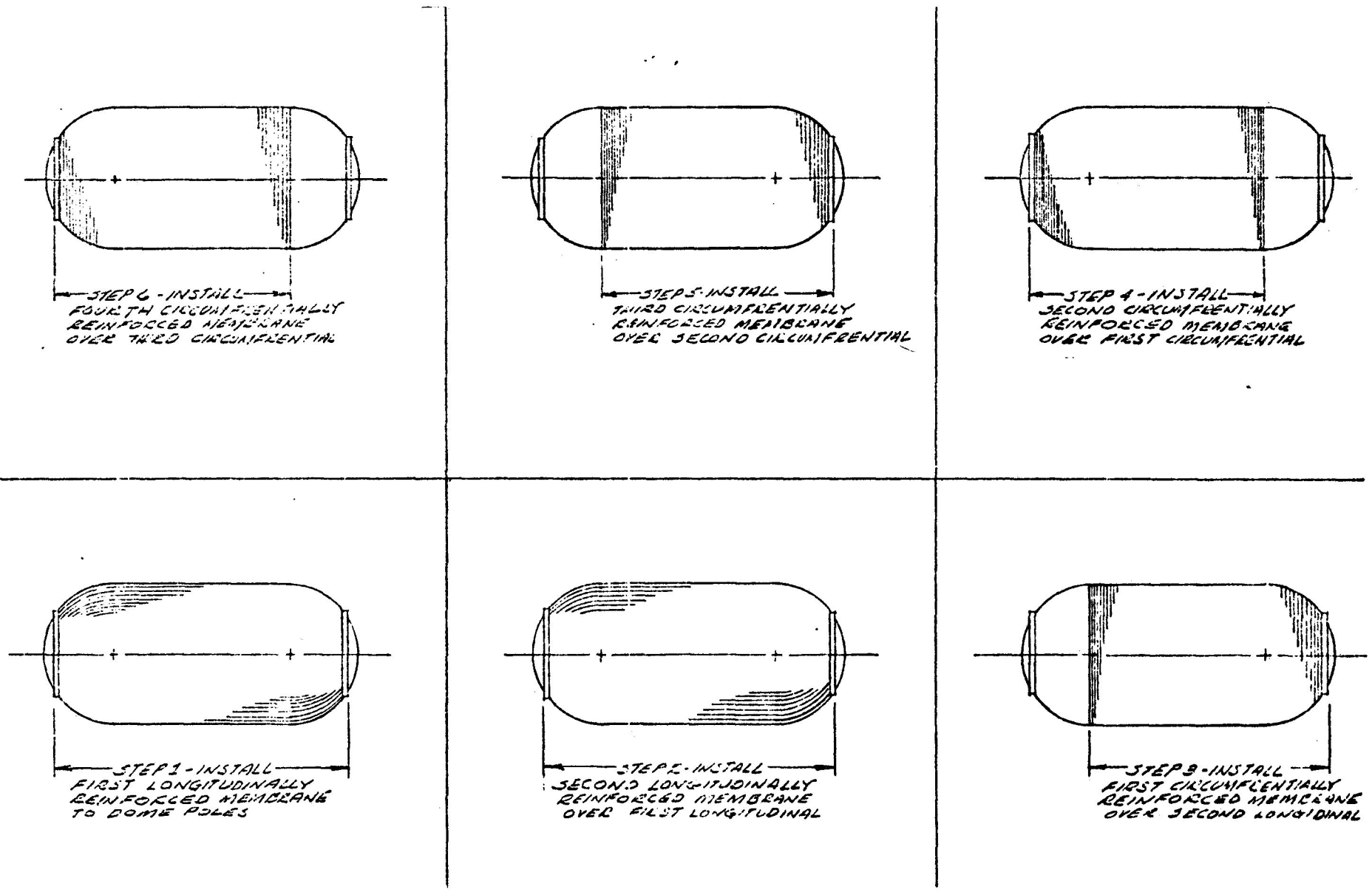

Figure 2.2-7 **MEMBRANE LAYUP SEQUENCE**

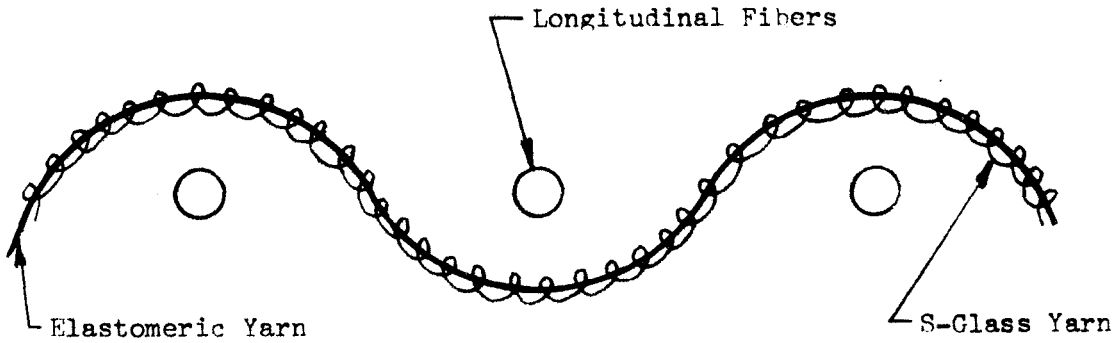

Figure 2.2-8 STRETCH WEAVE CONCEPT

2.2.7 Thermal Insulation

The insulation concept selected for this study was coordinated with the personnel conducting the study "Investigation of High-Performance Insulation Application Problems" under Contract NAS8-21400. During the discussion sheet tearing by the fastener or pin associated with the relative motion of the outer sheet with respect to the inner sheet of an insulation panel when folded to 25.4 cm radius and then expanded to a 3.76 m radius was investigated. Possible solutions arrived at were: (1) a pie-shaped slot in the panels which would permit the sheets of HPI to move with respect to each other without tearing the Mylar, (2) allow extra material for the inner sheets to accommodate the sheet tensioning effect upon deployment, and (3) space the fasteners at a greater distance in order to minimize relative motion.

The third solution appears to have the least impact on the present insulation blanket design and was selected for further investigation. The present design has fasteners spaced 30.4 cm (12 in.) on center; however, it would be possible to respace fasteners to twice this distance and retain structural integrity. Reference 2.5 presents test data by Lockheed and indicates that decompression loads on a butt-jointed blanket system are very low. The maximum measured differential pressure (Δp) was 83.7 N/m^2 (0.012 psi). This was for unperforated sheets. For perforated sheets which are employed in this concept, it would be possible to reduce this value by 50 percent. This would result in a fastener ultimate tension load of 2.2 kg (4.8 lb). Recent IRAD tests on the Butineer fastener, which is utilized for the panel design, produced tension allowables of 2.26 kg (5 lb). The inertia or g-loading affects on an insulation blanket is small. The ultimate load on each fastener would be 0.6 kg (1.3 lb). The allowable fastener shear load from Reference 2.6 is in excess of 0.91 kg (2 lb).

Some relative motion of the sheets without damage to the fastener holes can be tolerated by the blankets. A small test panel 1.2 by 0.61 m by 1.2 cm was fabricated using flat tooling. The panel was then installed to 10 m (33 ft) diameter sidewall mockup. The panel fit easily and there was no tearing at the fasteners (Reference 2.7).

The second area of discussion was that of joint gaping between panels when the module is deployed. The most viable solution for this problem would be to minimize joint travel and relative motion by increasing the panel width to approximately 2.96 m (115 in.) and to locate the joints on the centerlines of the star fold points (Figure 2.2-9). In addition, taping the inner sheets of the panels together at the joints would prevent rolling of the joint when the module is deployed.

The effect of the different coefficients of contraction of the tankage material and the insulation was also investigated. Since Mylar contracts and PRD 49-3 expands when cooled, the insulation blankets would be designed with an excess of material in both the longitudinal and circumferential direction to accommodate the movement of the tankage. In order to minimize the heat leak at joints circumferential joints would be eliminated. Individual insulation blankets would extend the full length of the tankage.

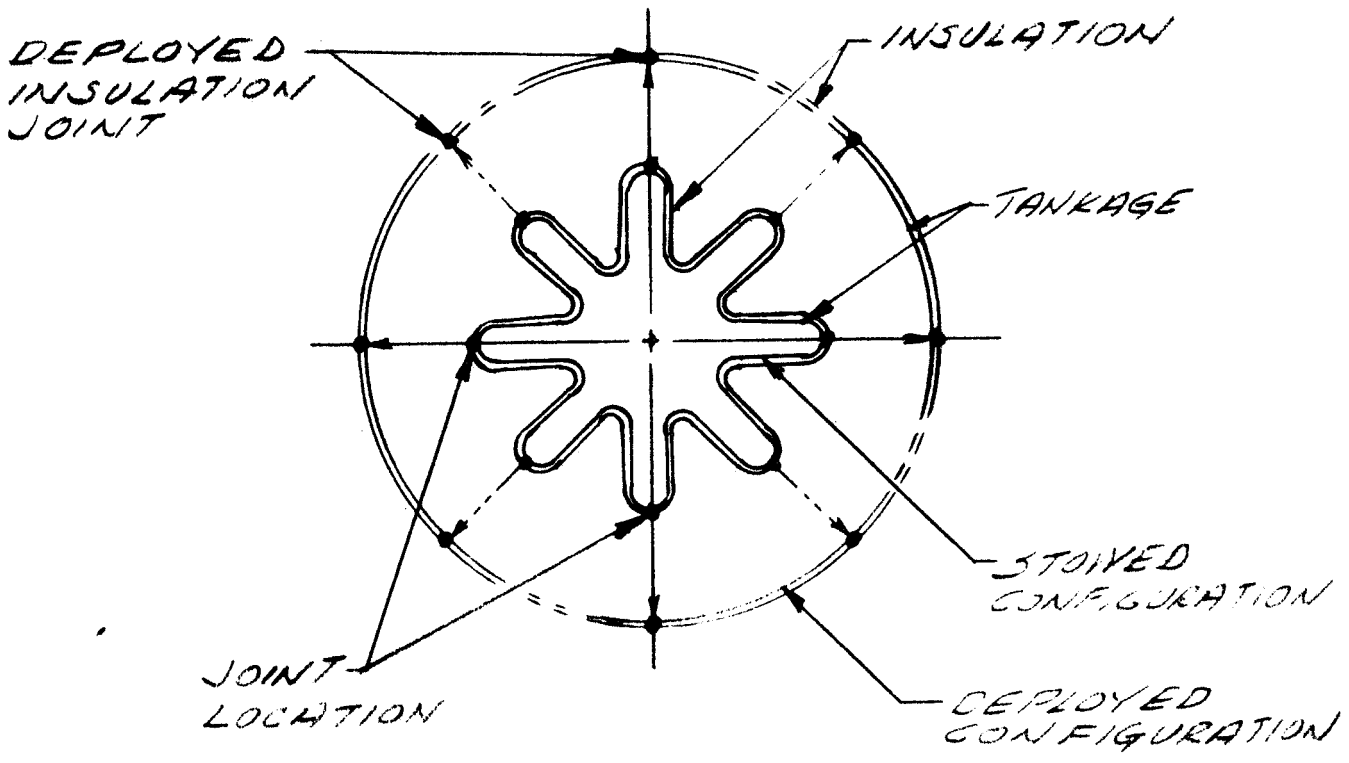

Figure 2.2-9 INSULATION JOINT LOCATION

2.3 TASK 2.3 -- CONCEPT DEFINITION

During the second quarter the baseline configuration drawing (Figure 3.2-1) was modified to incorporate the changes delineated in subsection 2.2. In Section B-B of Sheet 1, the propellant feed line, pressurization line and the vent line were revised. The bellows in the propellant feed line was replaced by a compensator and a gimbal joint was added to the forward end of the feed line to compensate for installation tolerances. The pressurization line was rerouted to its present 1.57 rad (90 degree) configuration because of clearance requirements when it is stowed. It no longer parallels the contour of the dome nor does it nest into one of the star fold valleys for stowage. Instead it traverses the module length adjacent to one of the points at the star fold. The vent line penetration was moved to the center of the dome to provide a port for the mandrel spindel. This also permits mounting of support brackets external to the tank, rather than internal, where they could cause damage to the liner.

The external support system required for curing of the tankage composite in space was added to view F and Section G-G of Sheet 2. The details of this system will be described subsequently as new views and sections are presented. Views C and E of Sheet 3 were modified for the new tank penetration/liner design and by replacement of the internal bolted flange connection for the feed through and propellant line with a bi-metallic weld joint. This joint is welded to the feed through prior to its installation in the mandrel. Elimination of flange provisions simplifies the mandrel design. View E shows the application of the liner to both the inside and outside surfaces of the feed through attach flange. It also shows the layup of the dome pole composite to the feed through.

View H of Sheet 4 was changed to reflect the rerouting of the pressurization line. It is shown in its stowed position in the view. View J was completely revised to incorporate the sump redesign. The jamb is installed in the mandrel after the liner has been applied to it. A second localized liner coating is then applied to the outboard surface of the jamb. A bolted connection is utilized to attach the jamb and a metallic gasket is used to seal the mating surfaces.

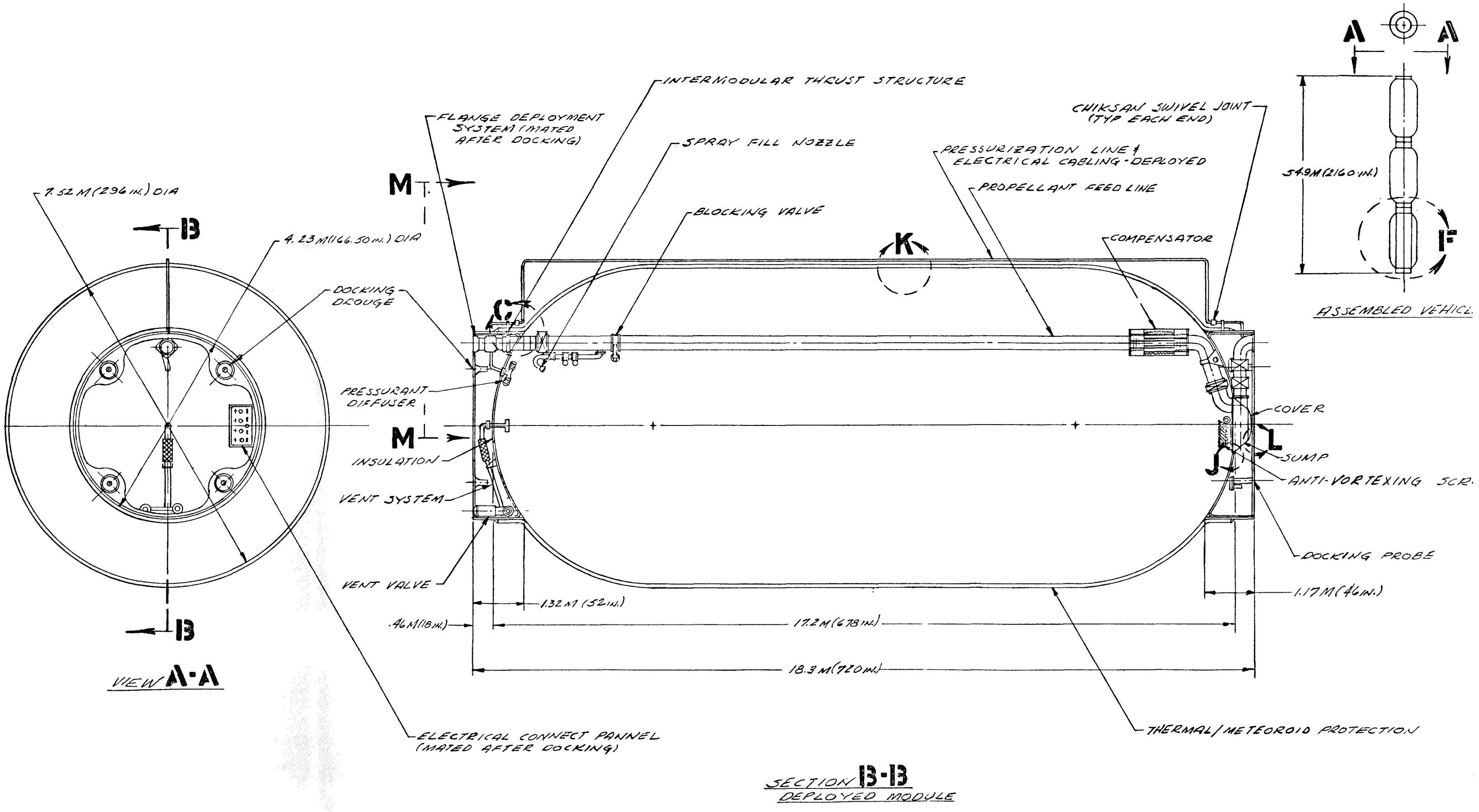

FIGURE 2.3-1 BASELINE CONFIGURATION (SHEET 1 OF 8

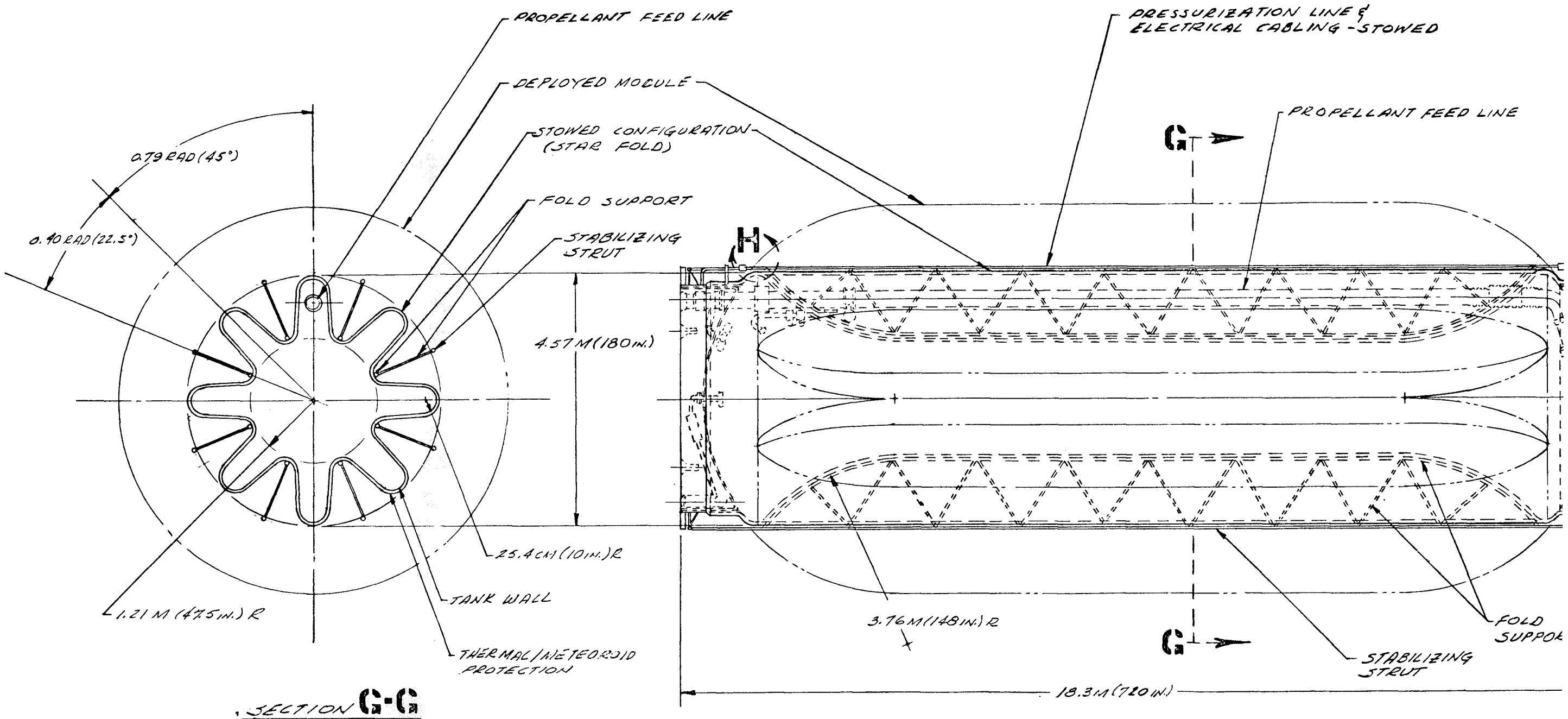

FIGURE 2.3-1 BASELI

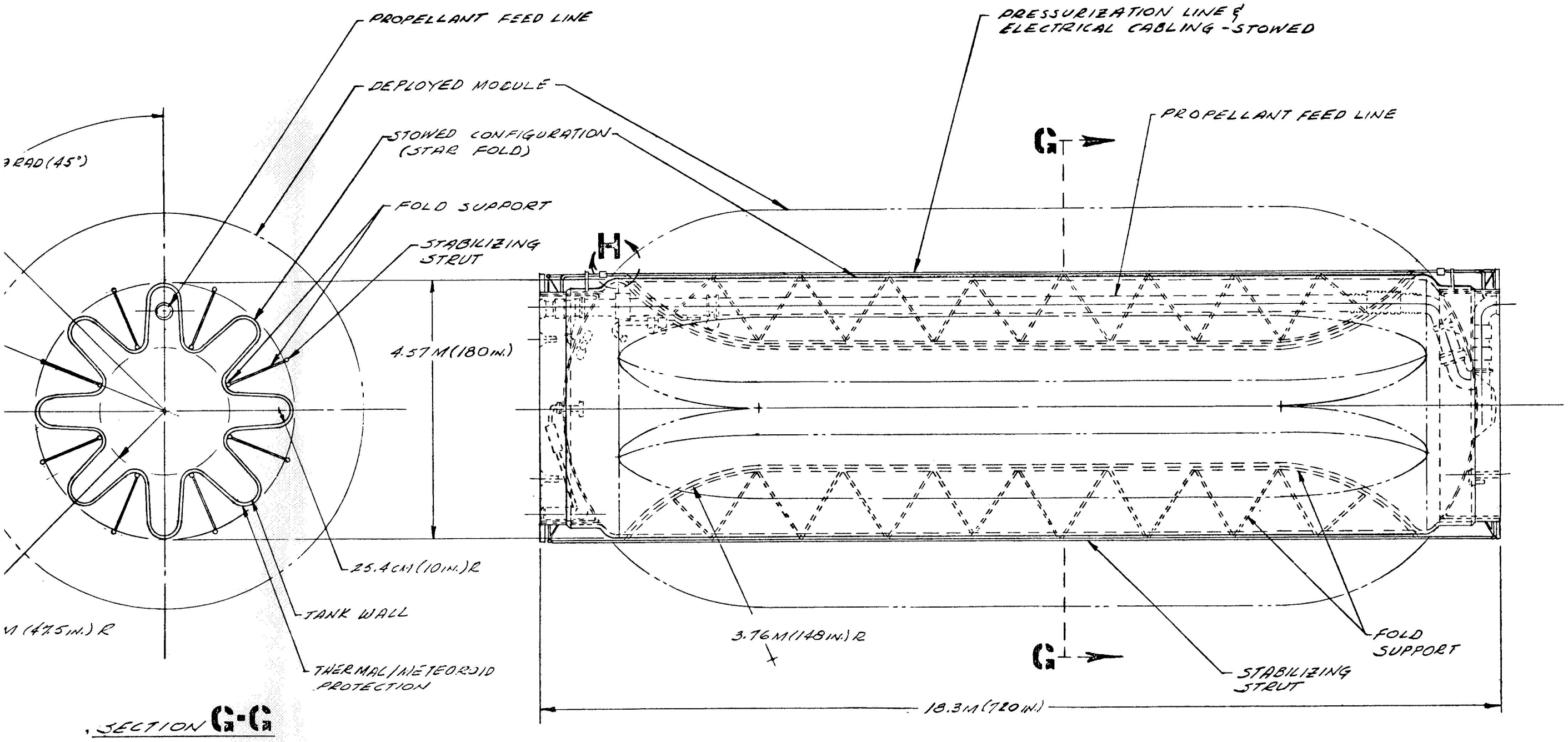

FIGURE 2.3-1 BASELINE CONFIGURATION (SHEET 2 OF 8)

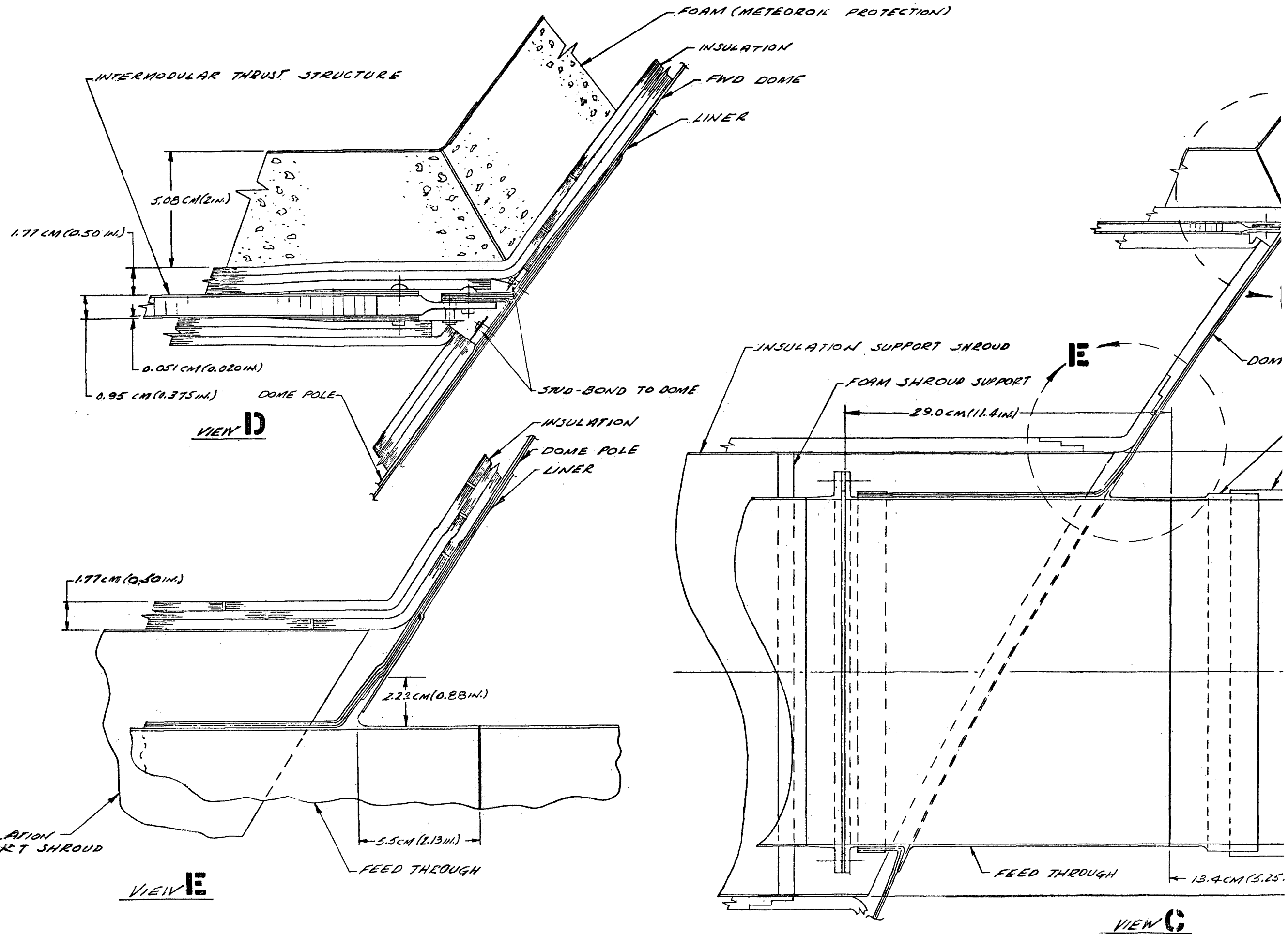
FOAM (METEOROID PROTECTION)
INSULATION
FWD DOME
LINER
INTERMODULAR THRUST STRUCTURE
5.08 CM (2 IN.)
1.77 CM (0.50 IN.)
0.051 CM (0.020 IN.)
0.95 CM (0.375 IN.)
DOME POLE
STUD-BOND TO DOME
VIEW D
INSULATION
DOME POLE
LINER
1.77 CM (0.50 IN.)
2.22 CM (0.88 IN.)
INSULATION SUPPORT SHROUD
5.5 CM (2.13 IN.)
FEED THROUGH
VIEW E
INSULATION SUPPORT SHROUD
FOAM SHROUD SUPPORT
29.0 CM (11.4 IN.)
E
FEED THROUGH
13.4 CM (5.25
VIEW C

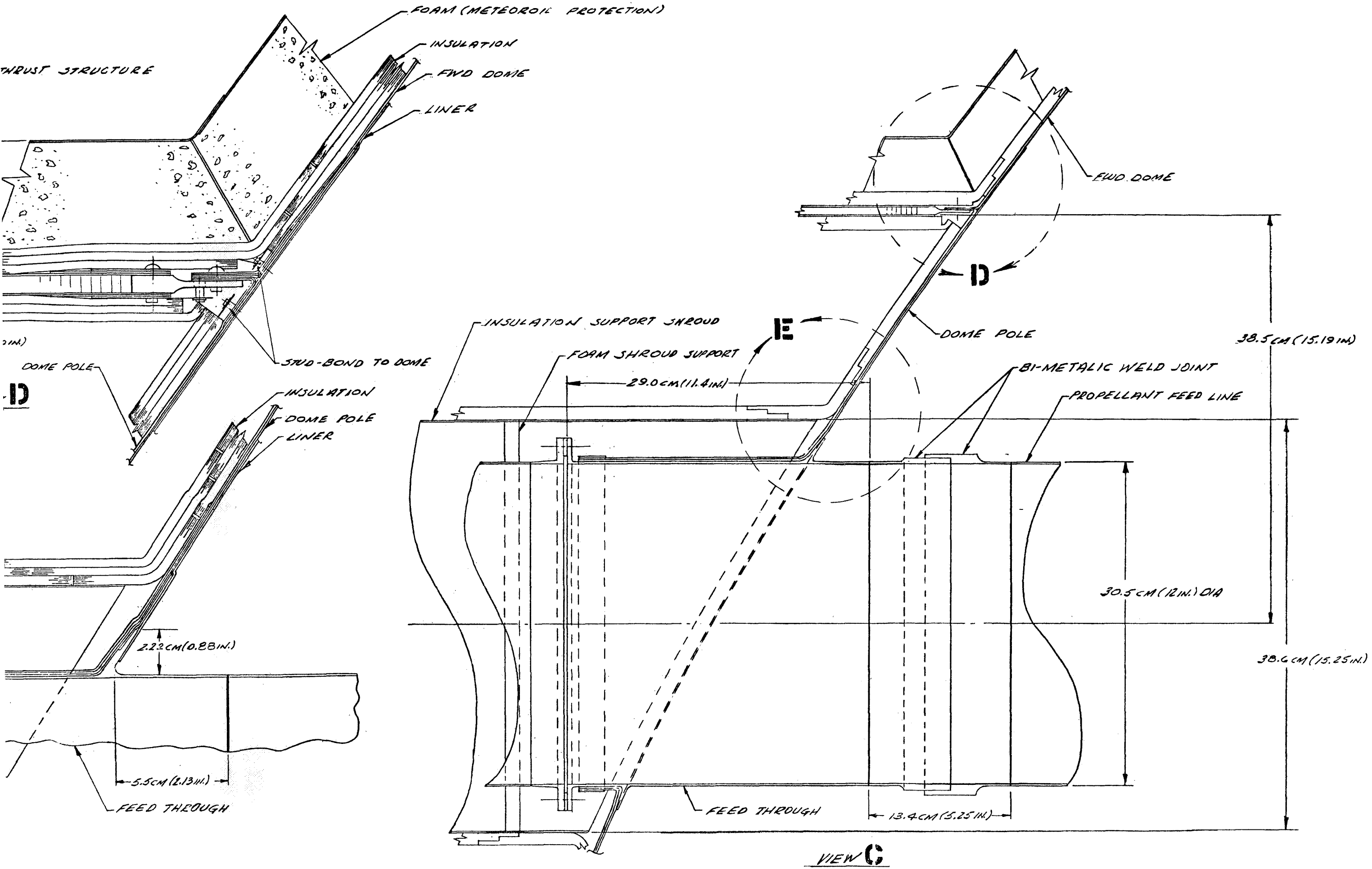

FIGURE 2.3-1 BASELINE CONFIGURATION (SHEET 3 OF 8)

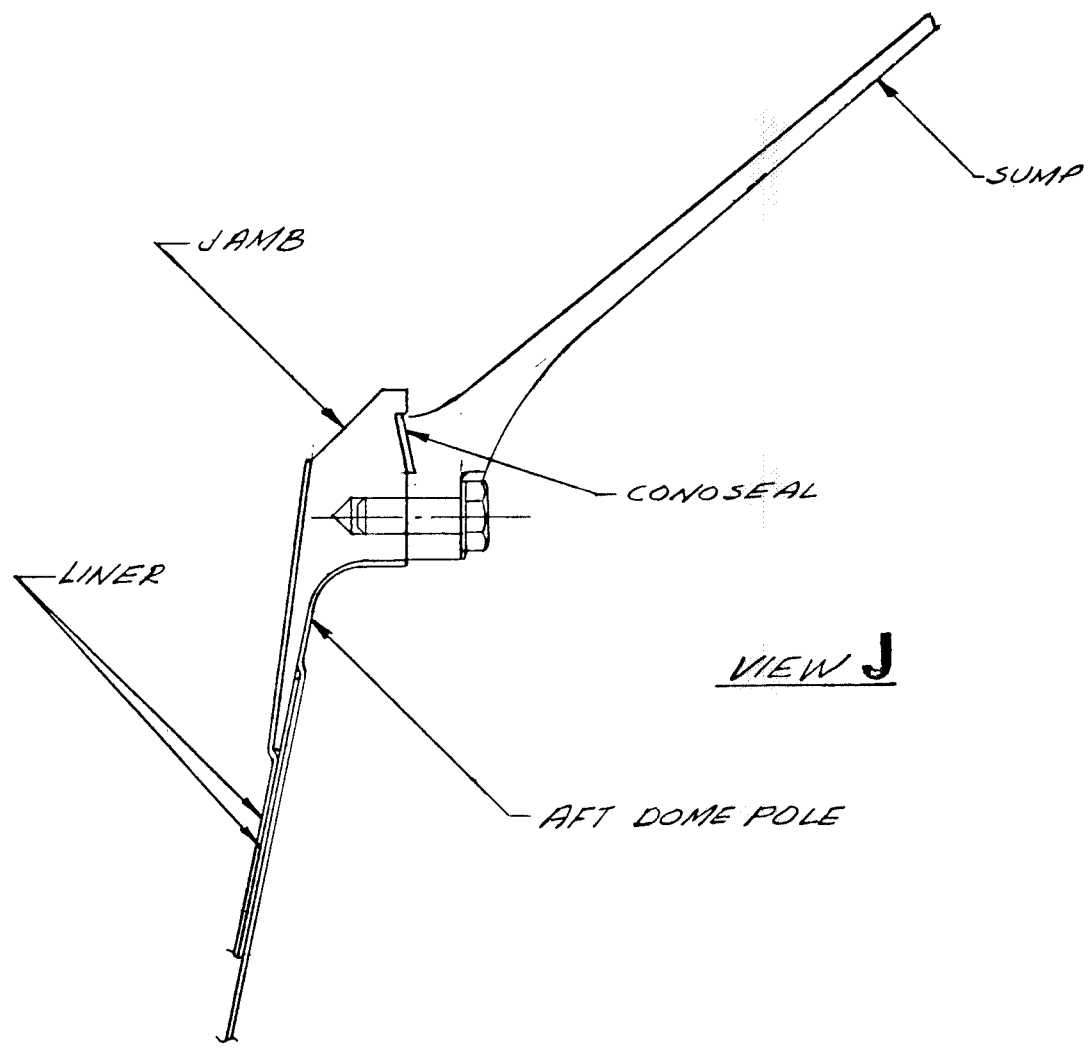
SUMP
JAMB
CONOSEAL
LINER
AFT DOME POLE

VIEW J

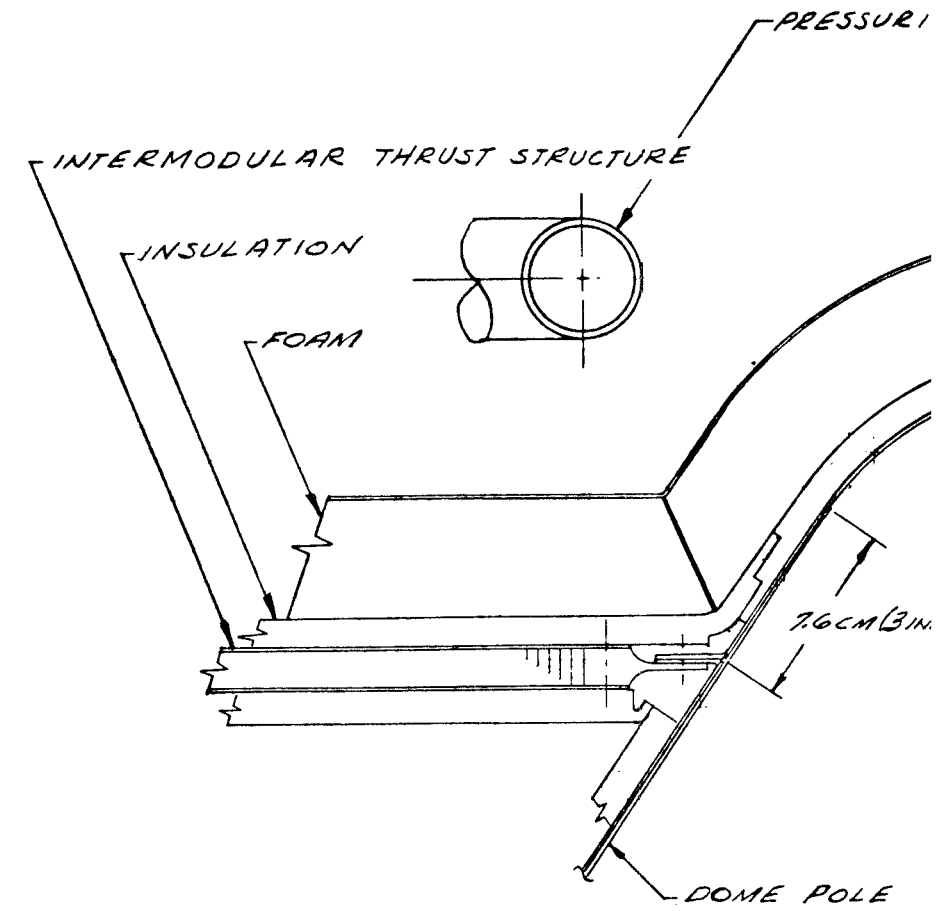
PRESSURI
INTERMODULAR THRUST STRUCTURE
INSULATION
FOAM
7.6CM(3IN.
DOME POLE

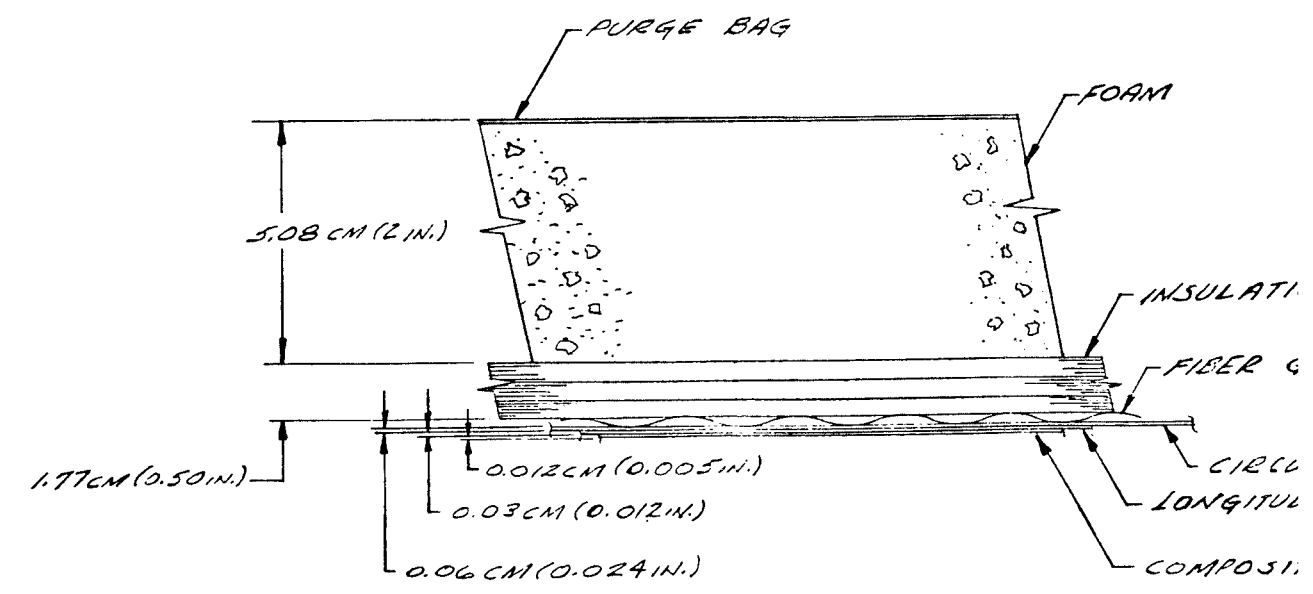
PURGE BAG
FOAM
5.08 CM (2 IN.)
INSULATI
FIBER G
CIRCU
LONGITUD
COMPOSI
1.77CM (0.50 IN.)
0.012CM (0.005 IN.)
0.03CM (0.012 IN.)
0.06 CM (0.024 IN.)

VIEW K

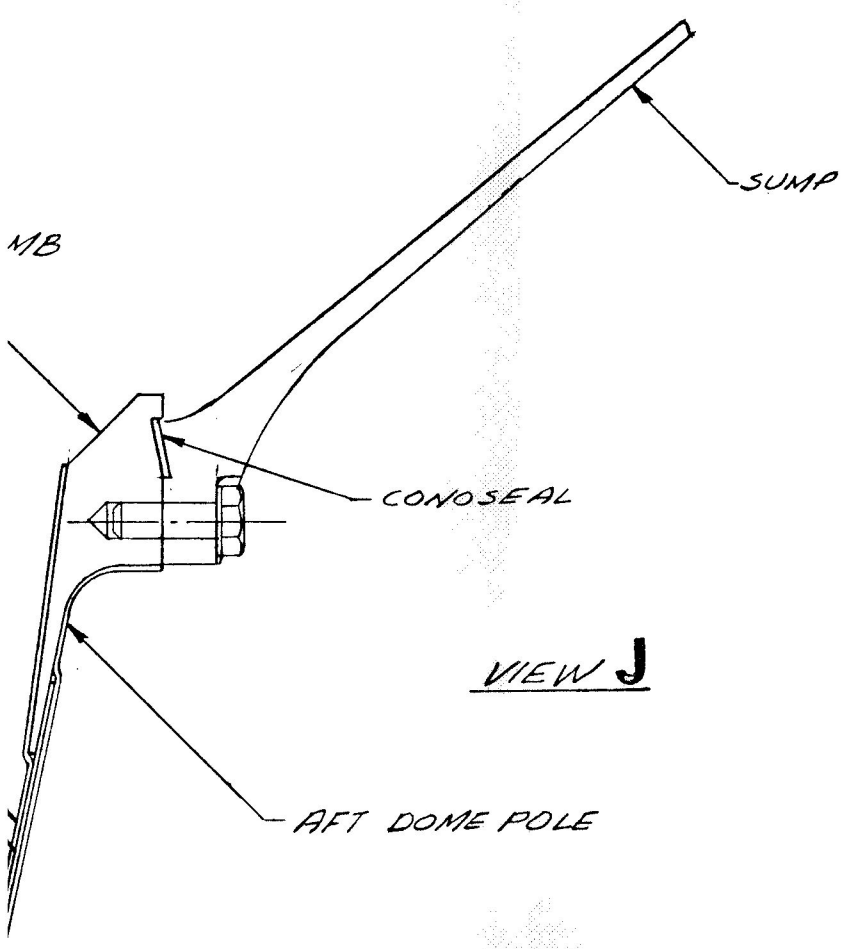

VIEW J

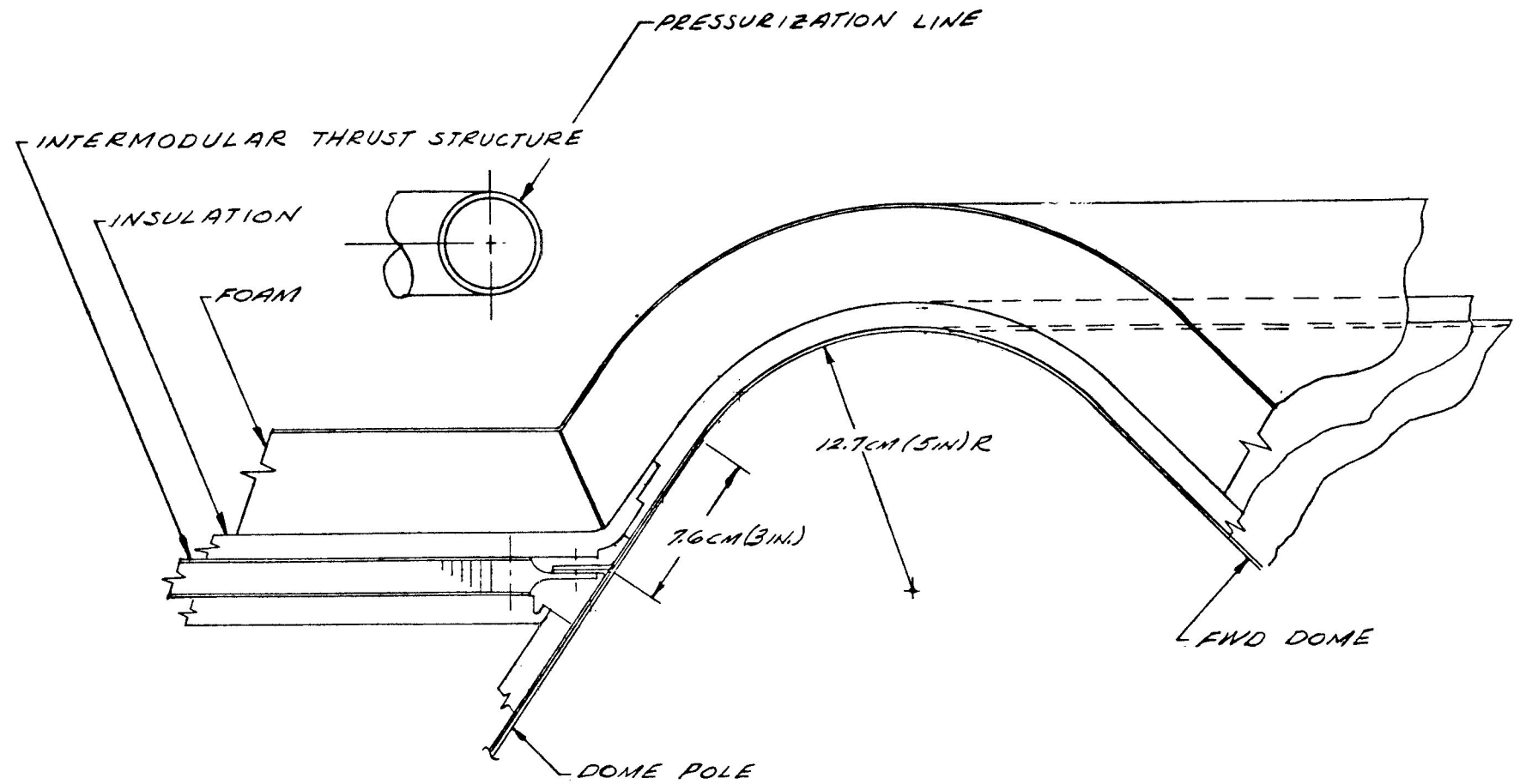

VIEW H

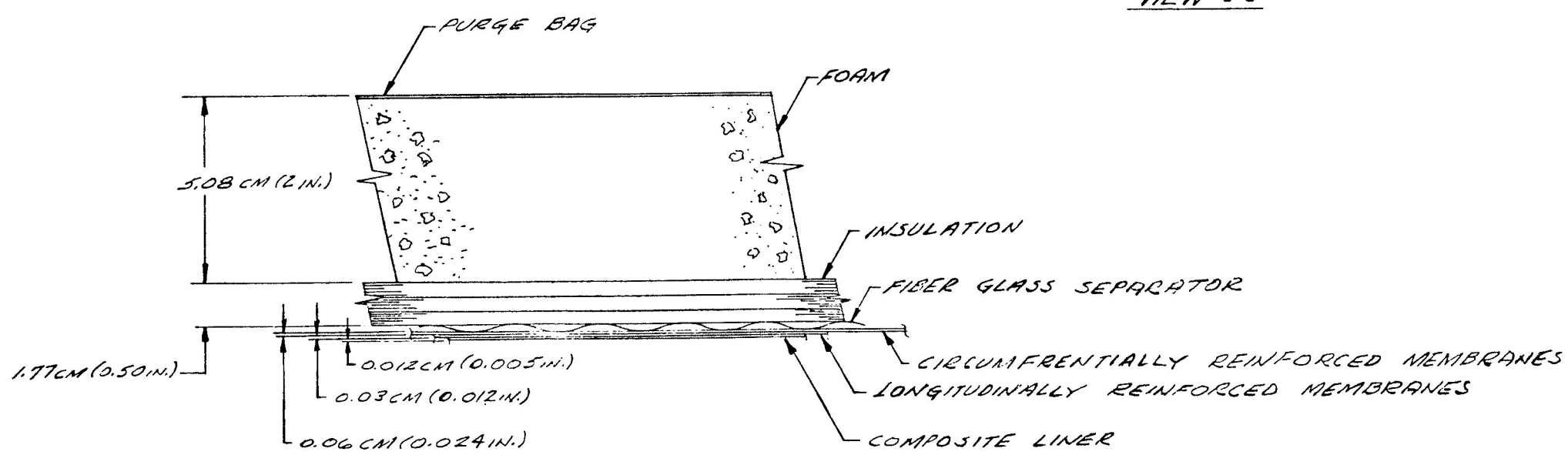

VIEW K

FIGURE 2.3-1 BASELINE CONFIGURATION (SHEET 4 OF 8)

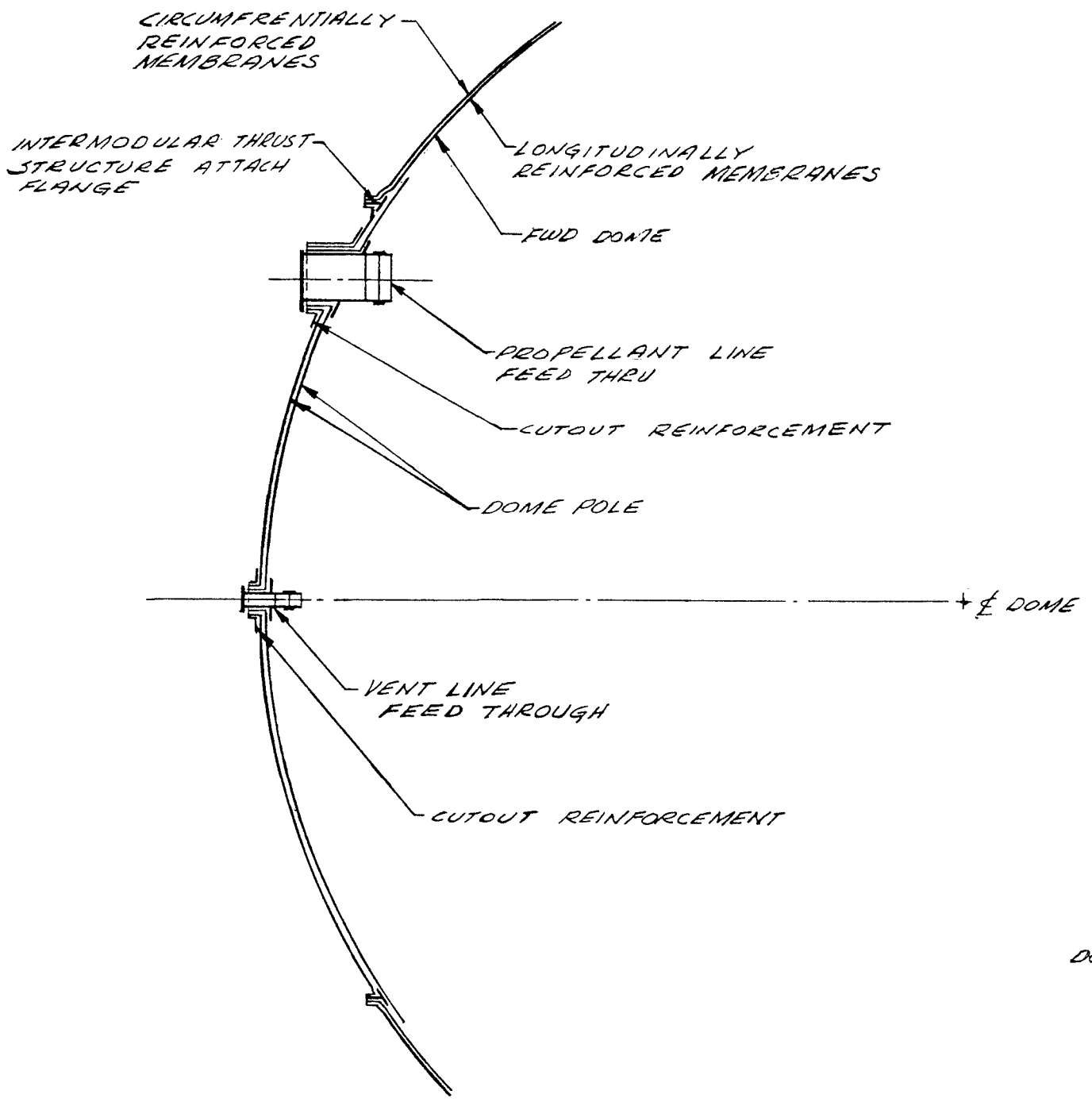

FWD DOME POLE LAYUP

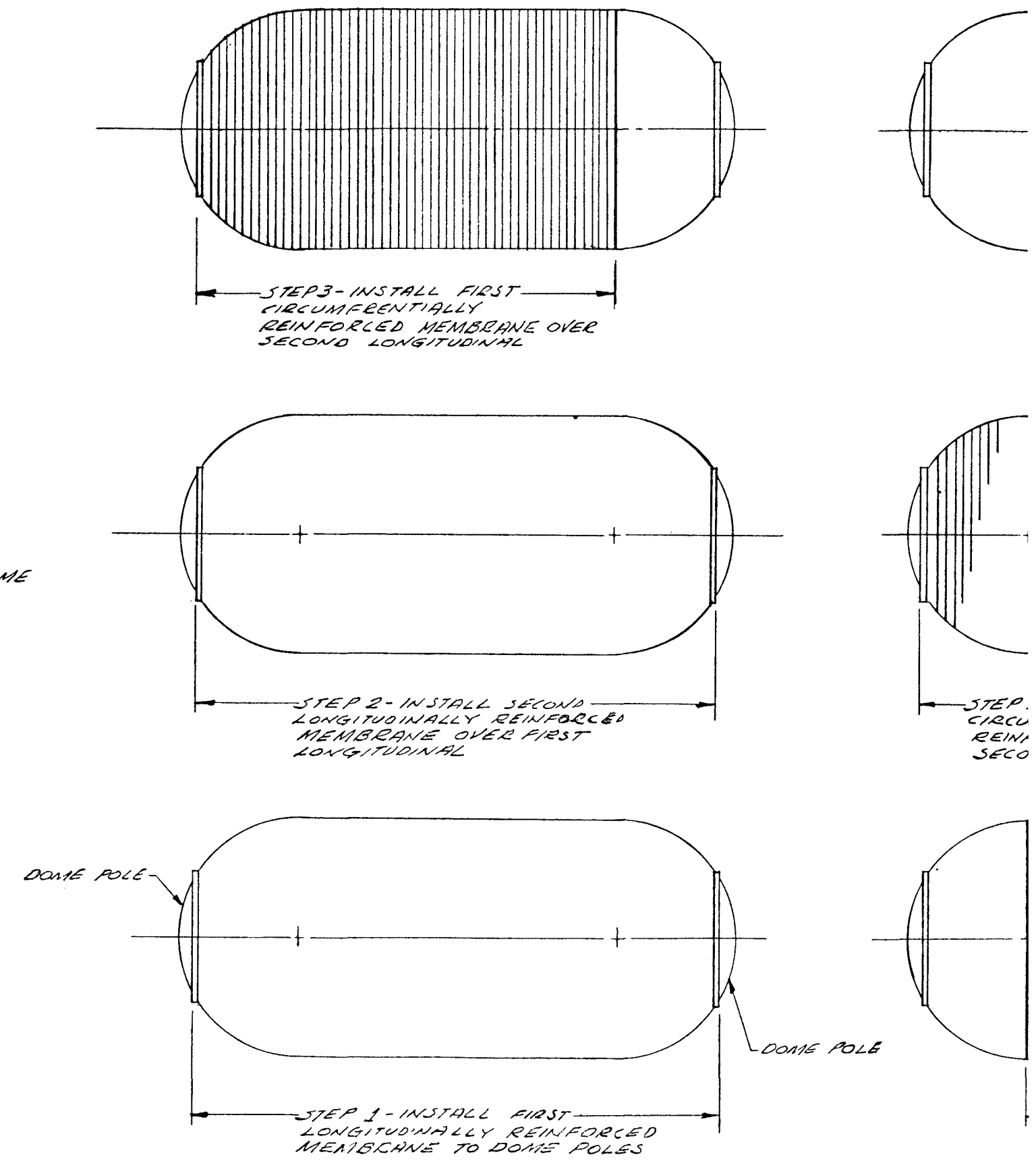

TANK CYLINDER ASSEMBLY SEQUENCE

NGITUDINALLY
INFORCED MEMBRANES

UD DOME

PELLANT LINE
ED THRU

ITOUT REINFORCEMENT

E POLE

+ ℄ DOME

UGH

REINFORCEMENT

FWD DOME POLE LAYUP

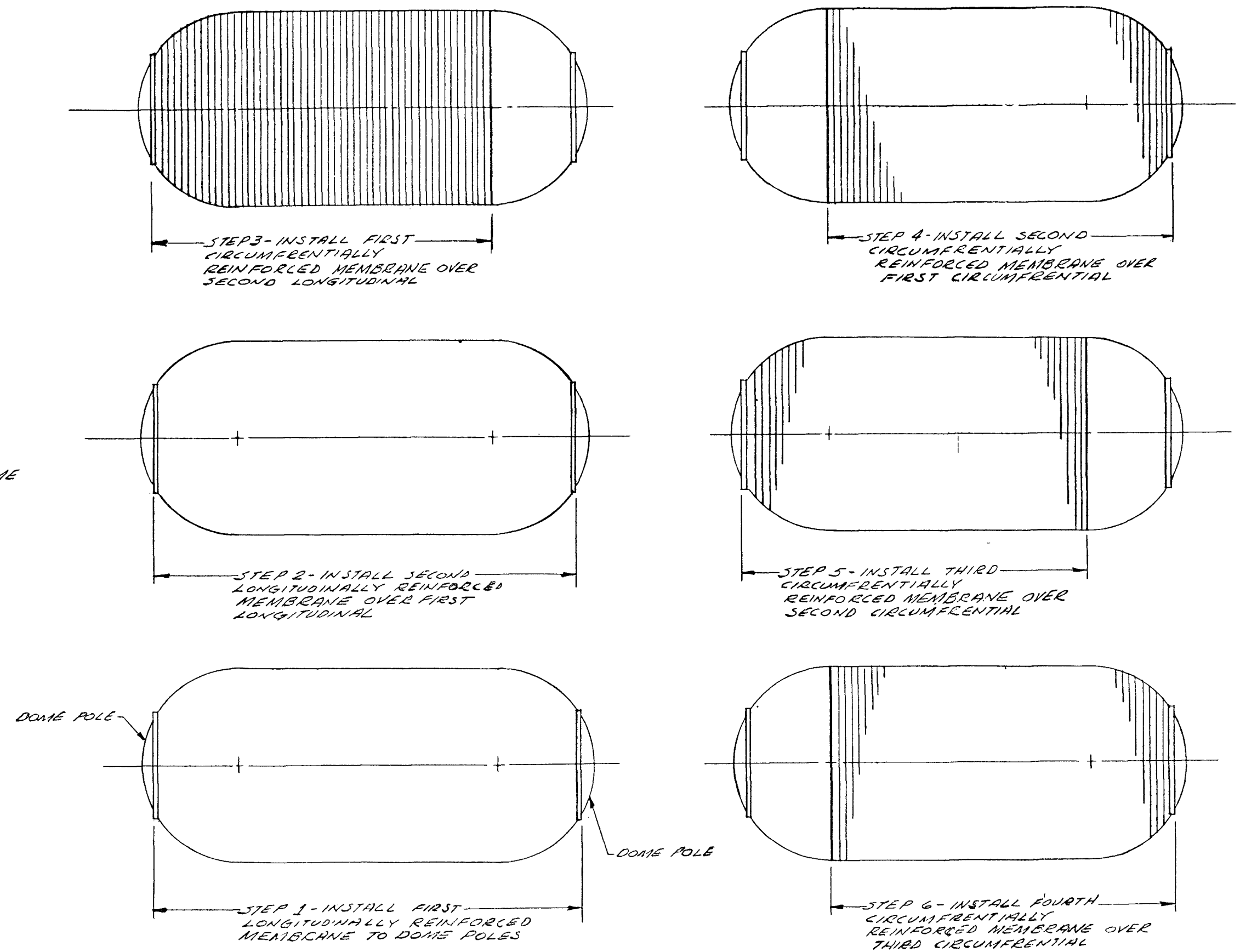

TANK CYLINDER
ASSEMBLY SEQUENCE

FIGURE 2.3-1 BASELINE CONFIGURATION (SHEET 5 OF 8)

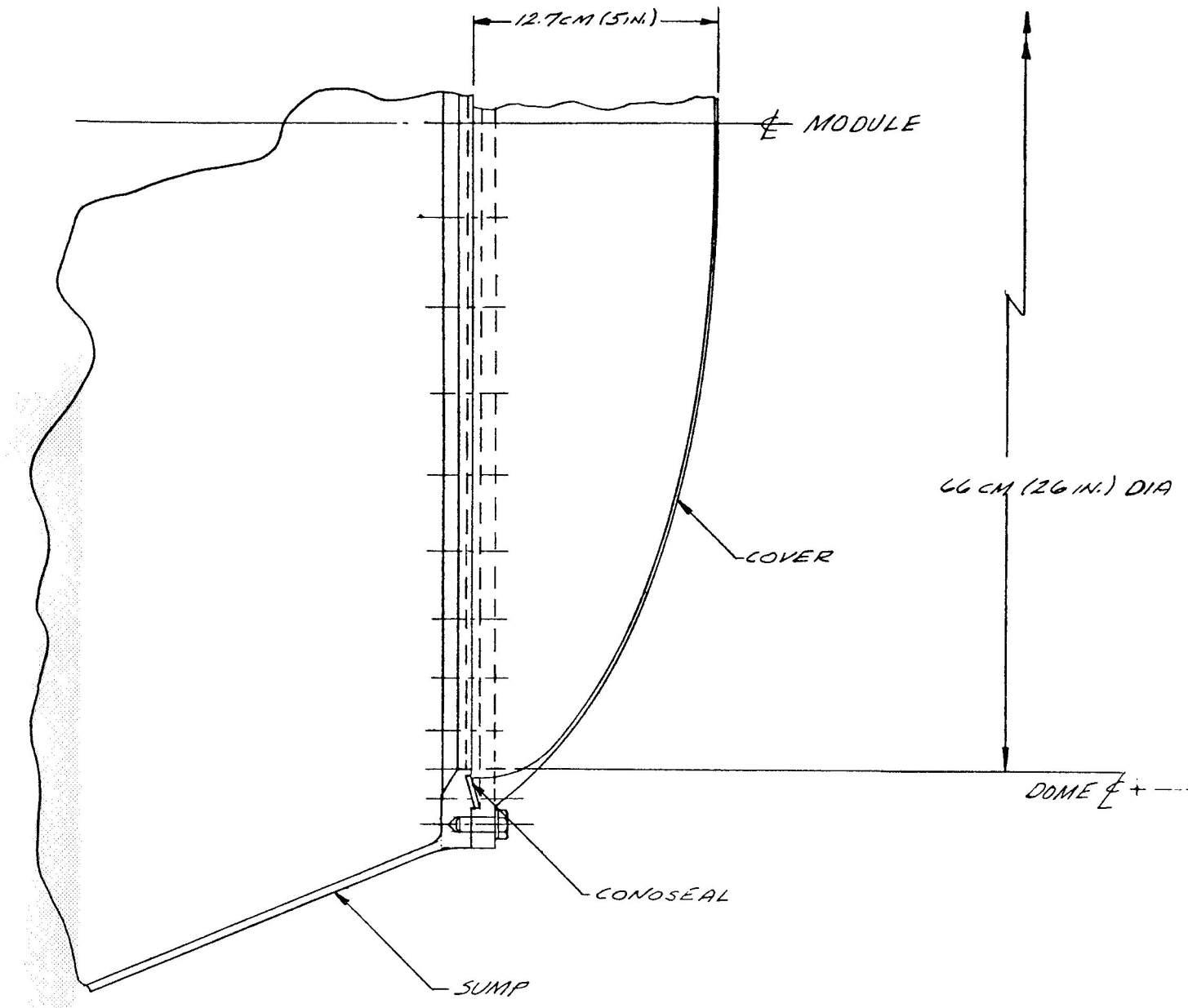

VIEW L

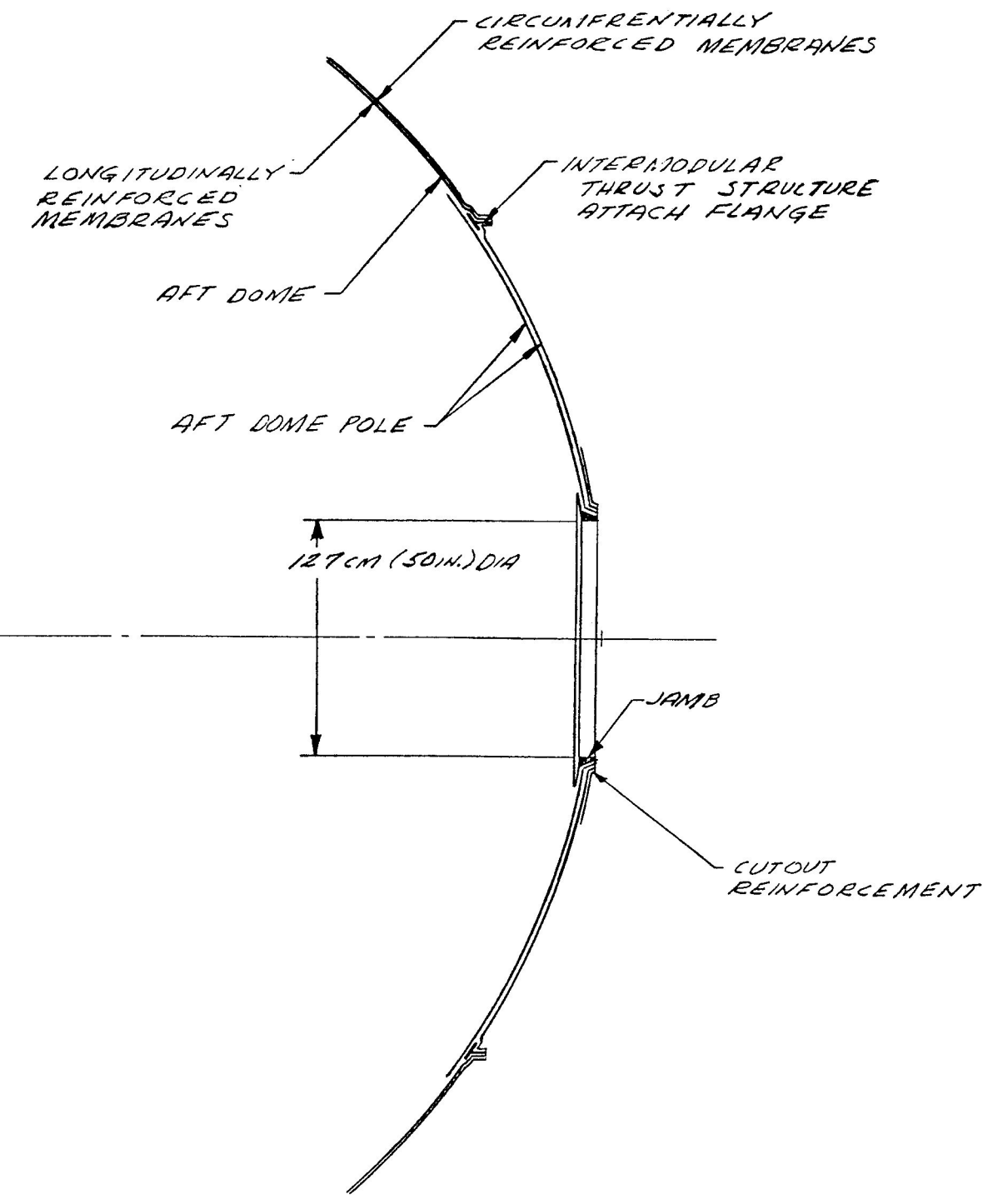

AFT DOME POLE LAYUP

FIGURE 2.3-1 BASELINE CONFIGURATION (SHEET 6 OF 8)

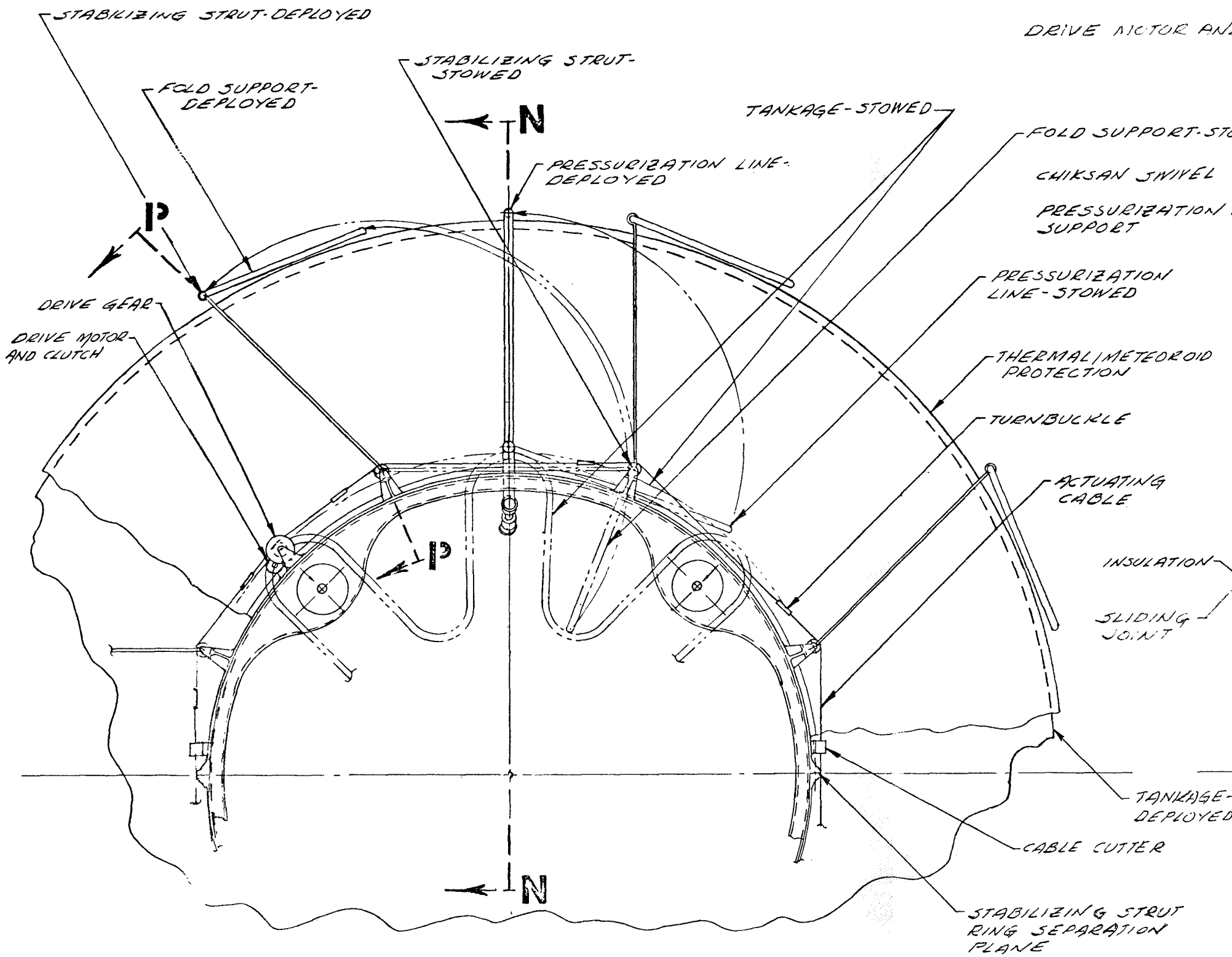

VIEW **M-M**

WITH STABILIZATION SYSTEM SHOWN

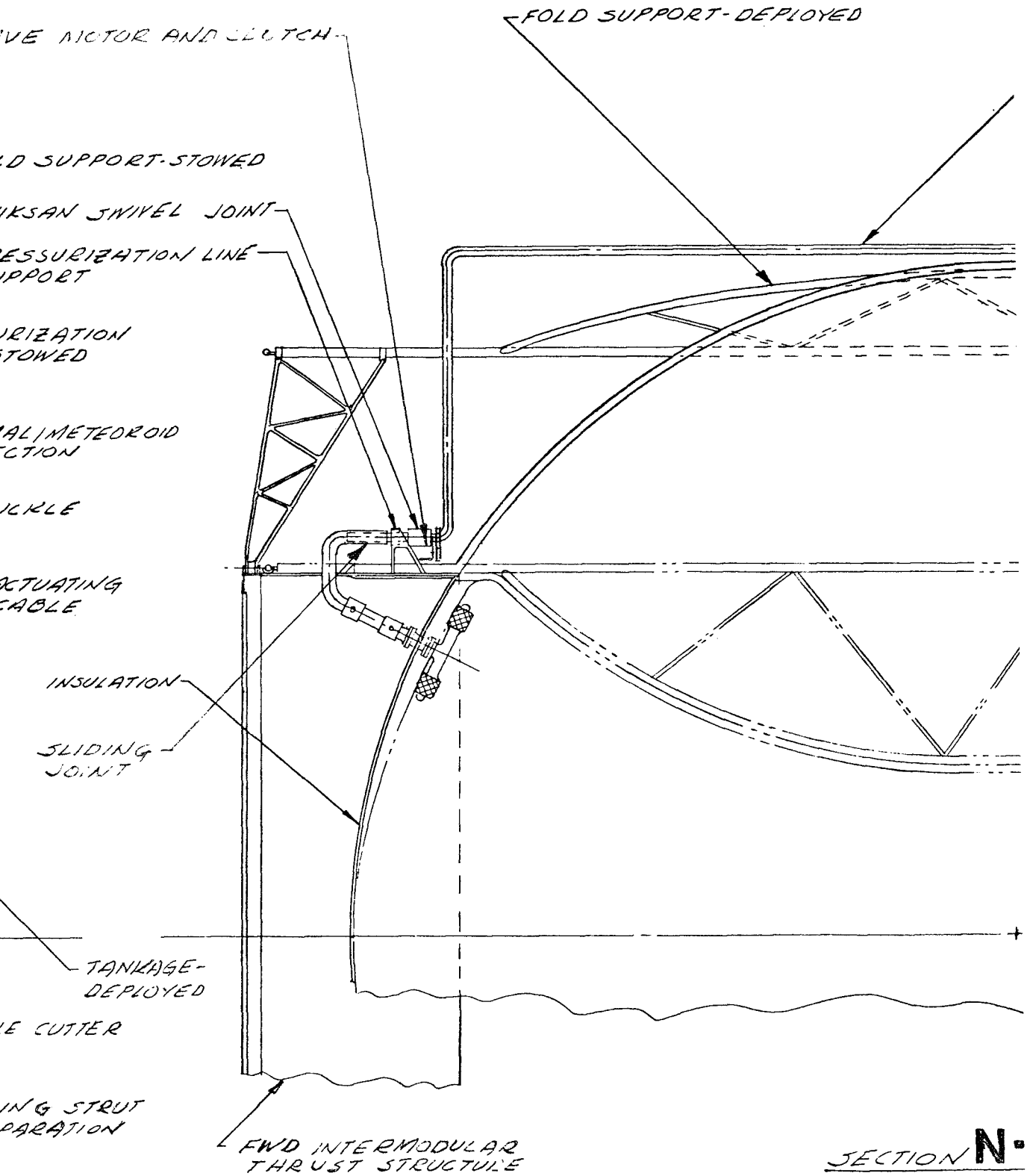

SECTION **N-**

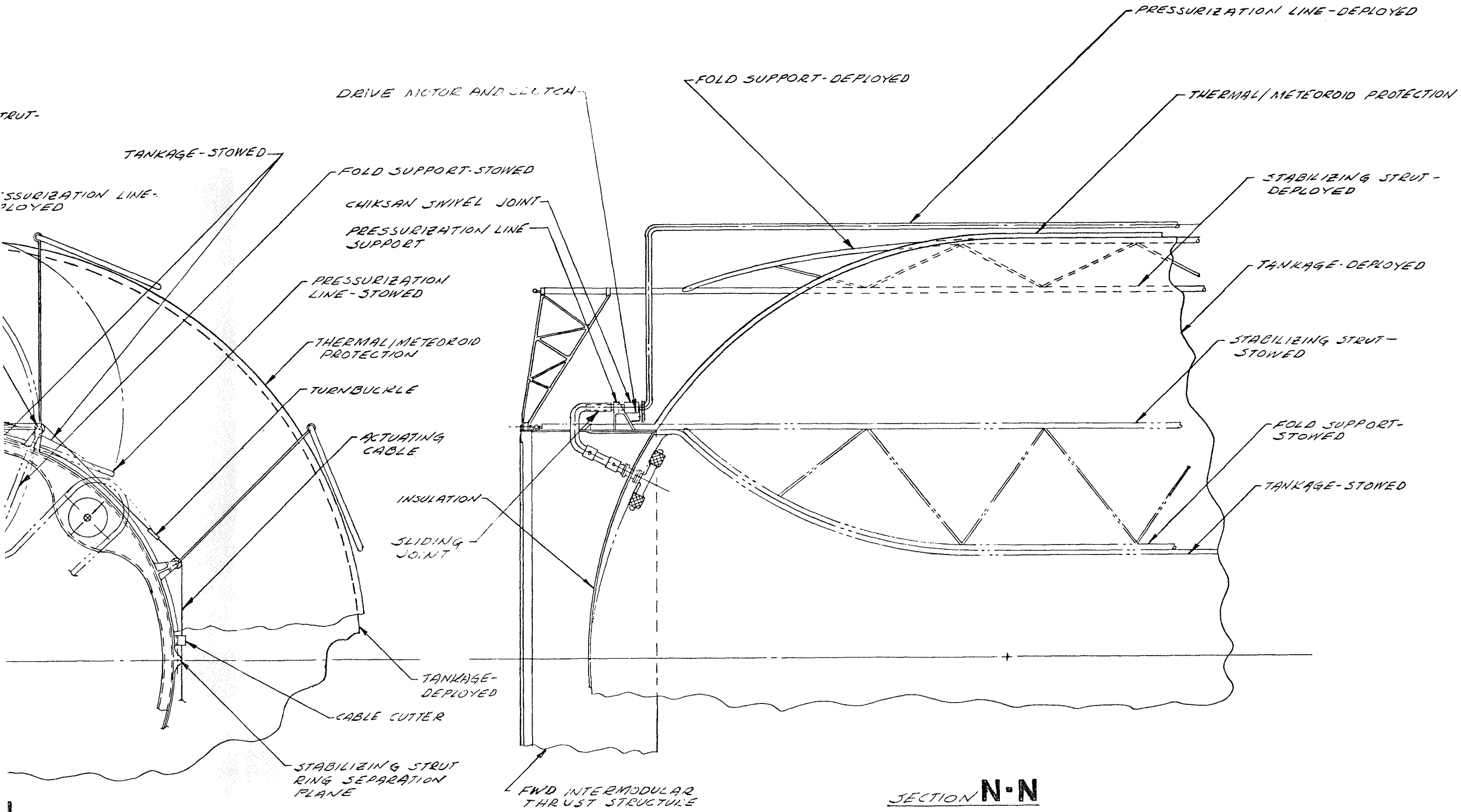

ATION

FIGURE 2.3-1 BASELINE CONFIGURATION (SHEET 7 OF 8)

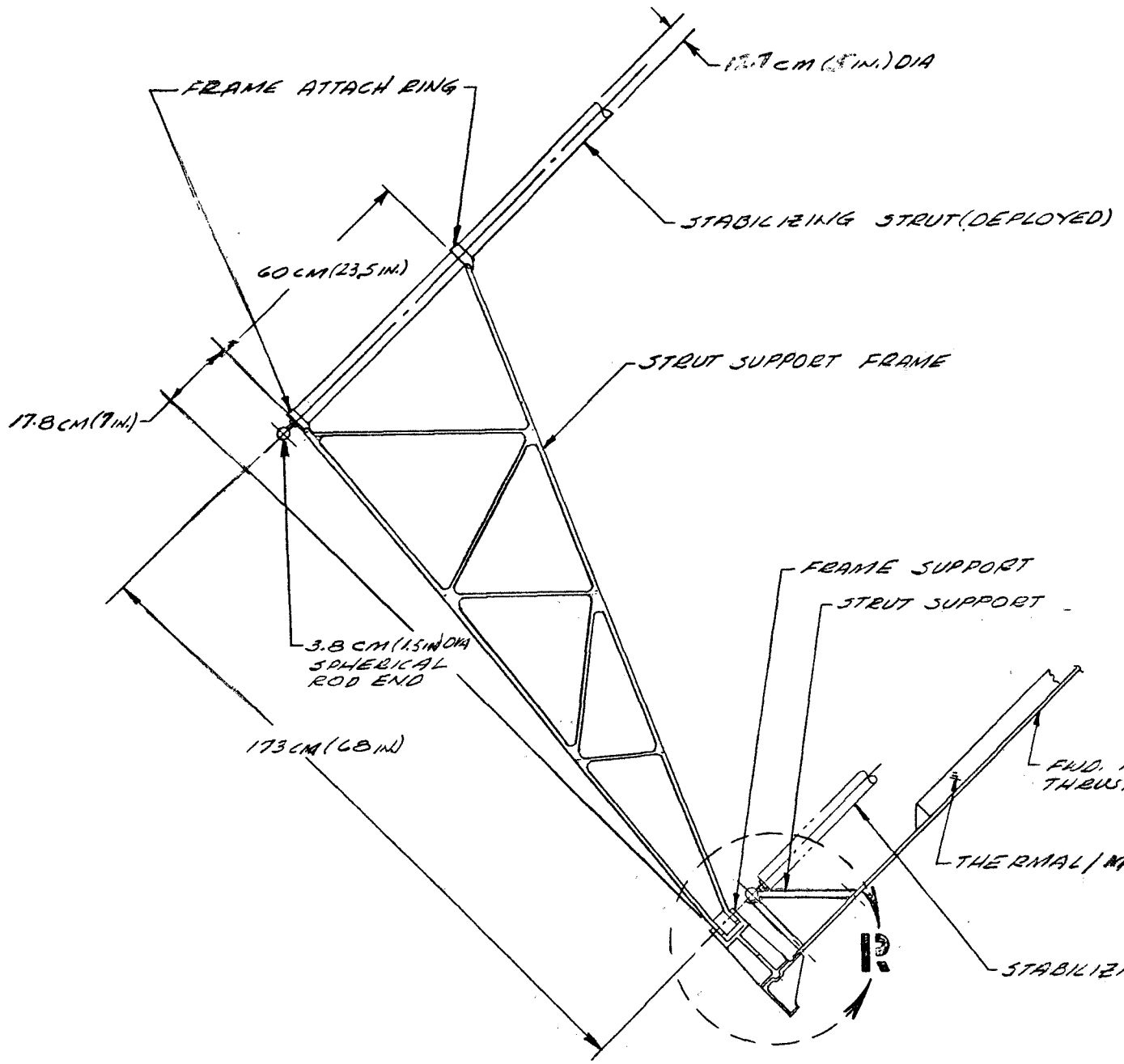

SECTION P-P

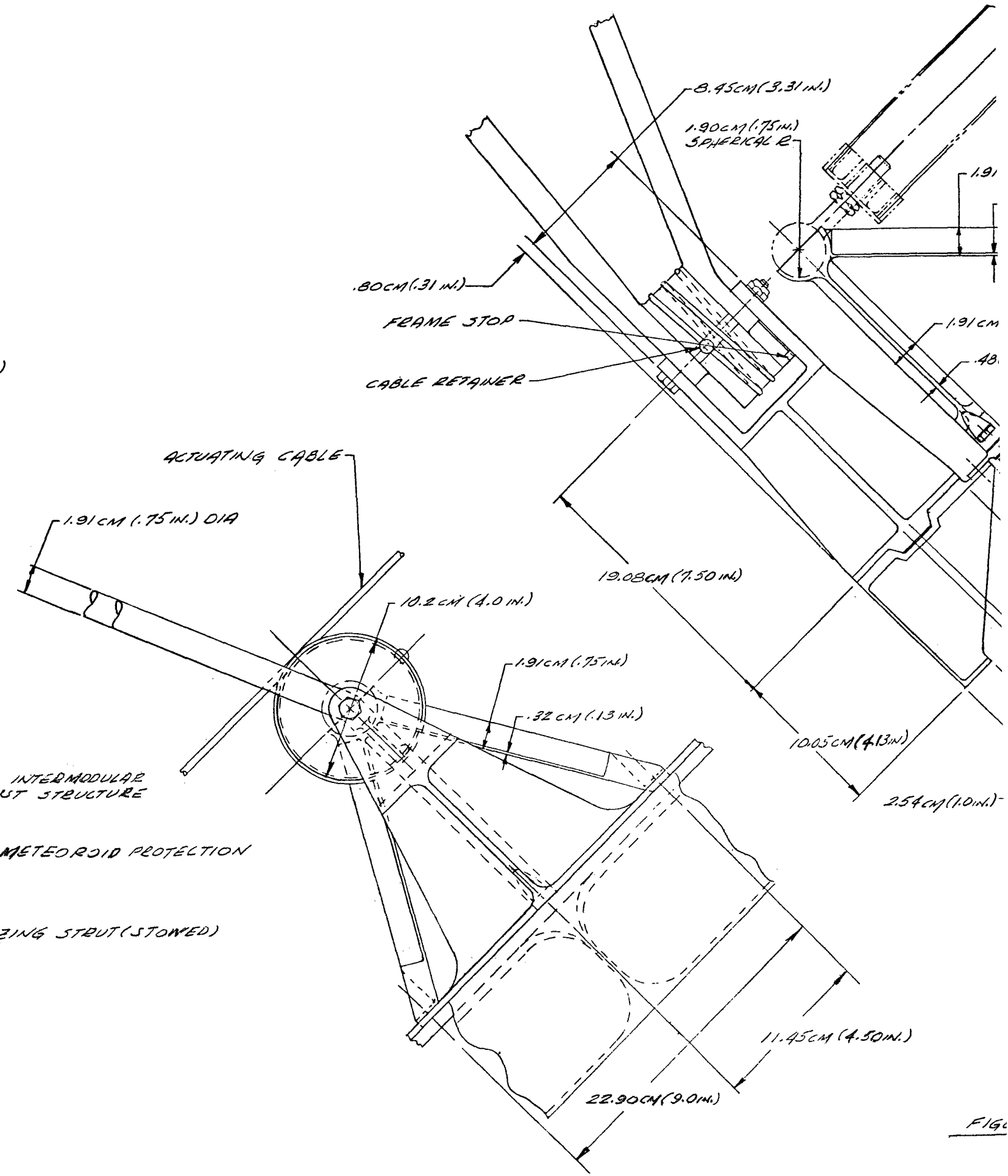

FIG

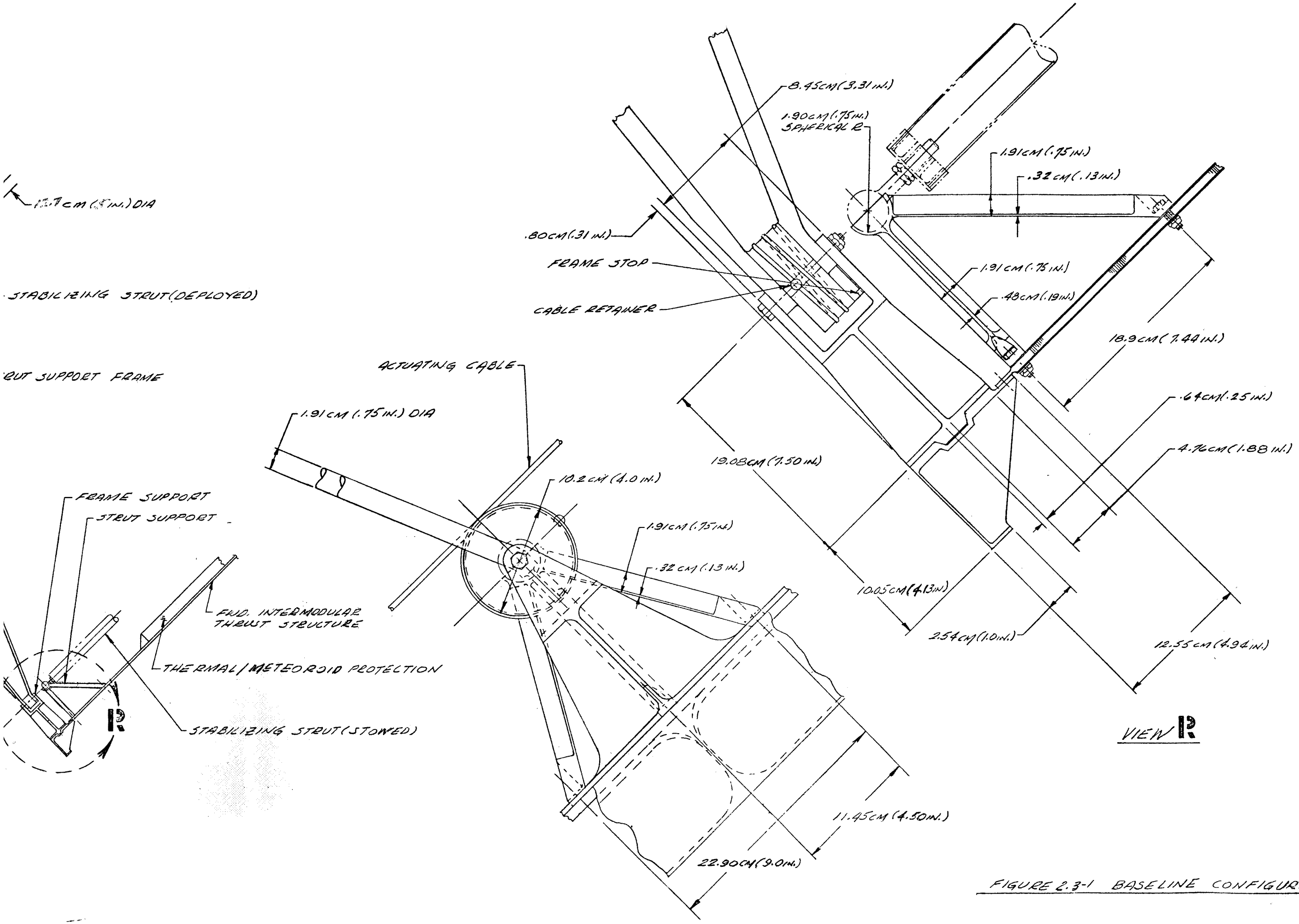

FIGURE 2.3-1 BASELINE CONFIGURATION (SHEET 8 OF 8)

The assembly sequence for the longitudinally and the circumferentially reinforced membranes is shown on Sheet 5. The longitudinals are installed first because the circumferentials would restrain the reinforcing pieces from separating and for ease of fabrication since the spherical segment at one end of the membrane must be stretched to the full diameter of the tank. Also shown on Sheet 5 is the forward dome pole layup including the layup around the feed throughs and the inter-modular thrust structure attach flange. All feed throughs incorporate bi-metallic weld joints internal to the tank. The aft dome pole layup is shown on Sheet 6. It is similar to that of the forward dome pole. A bolted connection is employed to attach the cover (View L Sheet 6) to the sump. Sealing of the two components is provided by a metal gasket.

The stabilization system and the pressurization line are shown in both their deployed and stowed positions in View M-M and Section N-N, Sheet 7. The stabilization system consists of eight L-shaped supports, each support comprised of a stabilizing strut and a fold support both extending the length of the module, plus two triangular shaped transverse support frames. The support frames at the forward end of the module are fabricated from forgings and are pully configurated at their apex. They attach to fittings machined into the stabilizing strut ring. A single motor driven cable is employed for support deployment. The cable is tensioned between supports by turnbuckles and utilizes a ball terminal driving against a slot in the support frame apex to rotate the support assemblies. Both the drive motor and reduction gear assembly are mounted on the stabilizing strut ring.

Two stabilizing strut rings, one at the forward end of the module and the other at the aft end are employed in the design. Each ring is fabricated from two 3.14 rad (180 degree) segments which utilize bolts and explosive nuts for segment attachment. The rings have integrally machined tongues which nest in mating grooves in the closing frames of the intermodular thrust structures (IMTS). This provides a closed load path between the forward and aft thrust structures and maintains interface parallelity during the space curing operation. After the module has cured the cable is severed by redundant sets of cable cutters, which are mounted on the support ring. The explosive nuts

are then ignited and the support assembly jettisoned in half sections. The separation force is provided either by mechanical springs or pyrotechnic devices installed between the support ring segments.

In the stowed condition the fold supports, which have a 5.1 cm (2 in.) diameter and a well thickness of 0.16 cm (0.40 in.), nest in the valleys or troughs of the star fold and conform to the contour of the fold. The stabilizing struts which resist the inertial loads during launch are 12.7 cm (5.0 in.) in diameter with a 0.127 cm (0.005 in.) wall. They have spherical rod ends which are adjustable to compensate for manufacturing and installation tolerances. When the module is stowed each rod end nests into a hemispherical receptacle machined into a tripod support which is attached to the IMTS. The struts are locked in their stowed position by restraining bands which are jettisoned after the module has been deployed from the Space Shuttle. A truss framework is utilized to stabilize the longitudinal members.

The pressurization line has a hat-section configuration external to the module. It incorporates a chicksan swival joint at each end and has a sliding seal at its forward end to accommodate the 17.8 cm (7 in.) relative motion between the tank and the line. Two gimbal joints are installed between the dome exit and the line penetration of the IMTS. In its stowed position the line is routed tangent to the IMTS and adjacent to one point of the star fold. It has a motor drive and is rotated approximately 1.92 rad (110 degrees) after deployment of the stabilization system.

A weight statement for the structural subsystem of a single propellant module is presented in Table 2.3-1.

Table 2.3-1

STRUCTURAL WEIGHT

ITEM		WEIGHT kg, (LB)	
Propellant Tank Assembly		940	(2,070)
Tank	[780 (1,720)		
Liner	[160 (350)		
Forward Intermodular Thrust Structure		105	(230)
Aft Intermodular Thrust Structure		105	(230)
Anti-Slosh Baffles		70	(150)
Equipment Support Structure		50	(110)
Access		25	(60)
Stabilization System Structure		380	(835)
Total (Including 130 kg (290 lb) Contingency)		1,805	(3,975)
Less Jettison of Stabilization System Structure		380	(835)
Total Operational Weight		1,425	(3,140)

Future Work

Design of the baseline configuration will continue through the next report period. Particular attention will be given to the thermal/meteoroid protection subsystem design. Additional detail and induced loads resulting from the second stage cure will be generated for the stabilization subsystem. The configuration of the dome pole transition region will be defined in greater detail and the method of accommodating relative motion between the pressurization line and the tank will be reviewed.

Section 3

TASK 3 -- MANUFACTURING FEASIBILITY AND COST ASSESSMENT

This task was initiated during the past quarter.

3.1 MANUFACTURING FEASIBILITY ASSESSMENT

The manufacturing approach to fabricate the RNS propellant module is given below:

1. Utilize state-of-the-art wherever practical.

2. The proposed vehicle will mirror the mandrel. Consequently, the mandrel quality and alignment will be a paramount manufacturing consideration.

3. All module "hardpoints", alignment and structural index points, fittings and flanges will be located on the mandrel.

4. Provide adequate and valid vehicle integrity test procedures throughout the manufacturing cycle.

A conceptual schematic of the module is shown in Figure 3.1-1.

3.1.1 Tooling

The philosophy conceived for the manufacture of the mandrel was determined by the manufacturing flow plan and the processes required to fabricate the proposed vehicle. The mandrel for the manufacture of the proposed vehicle should have the following characteristics:

1. Semi-rigid
2. Dis-mantling capability
3. Expansion capability
4. Ingress and egress of personnel and equipment
5. Maintain vehicle orientation and alignment during the manufacturing process

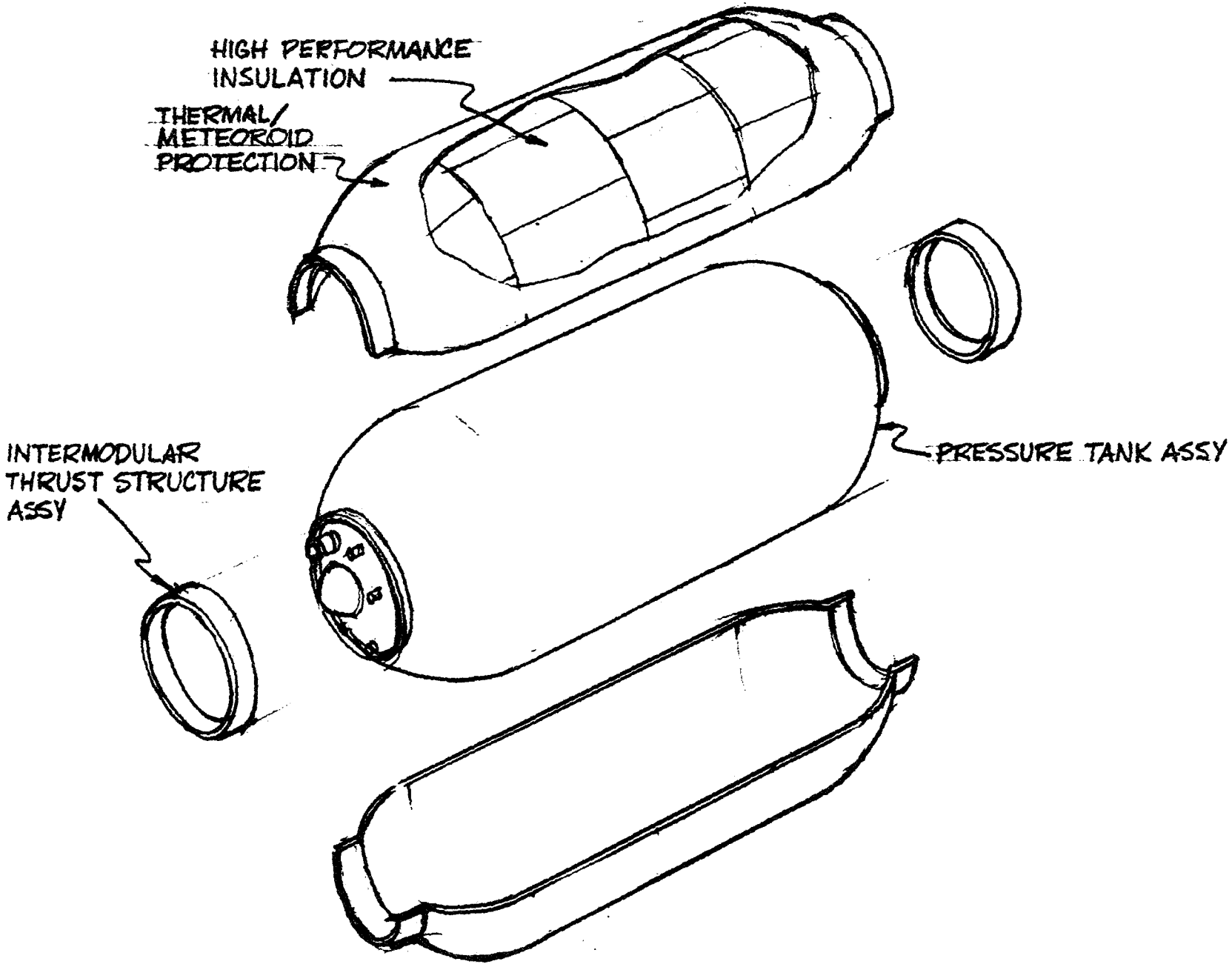

Figure 3.1-1 PROPELLANT MODULE SUBASSEMBLIES

Considering these requirements, two mandresl are presently being considered. A description of each of these mandresl is given in the following sections.

3.1.1.1 Mandrel Option 1

This mandrel is depicted in Figure 3.1-2. It is a semi-rigid, inflatable and segmented mandrel with the following major components:

1. Spindle
2. Tank Body Segments
3. Dome Gore Segments
4. Internal Spokes
5. Inflatable Seal
6. Inflatable Bag

A brief description of each of the above noted components is described in the following sections under their individual headings.

Spindle

The spindle is a lightweight dual walled metallic structure reinforced with longitudinally oriented corrugations and polyurethane foam filled. The spindle will have an internal wall opening of approximately thirty-six inches which will allow for ingress and egress. The outer diameter of the spindle is approximately forty-eight inches and the overall length is approximately thirty-two feet long.

Tank Body Segments

The tank body segments are fabricated from a wire mesh impregnated with a semi-rigid rubber. Each of the tank segments will have interlocking capability with the adjacent segments. These panels are held rigid and are indexed to the spindle with spokes.

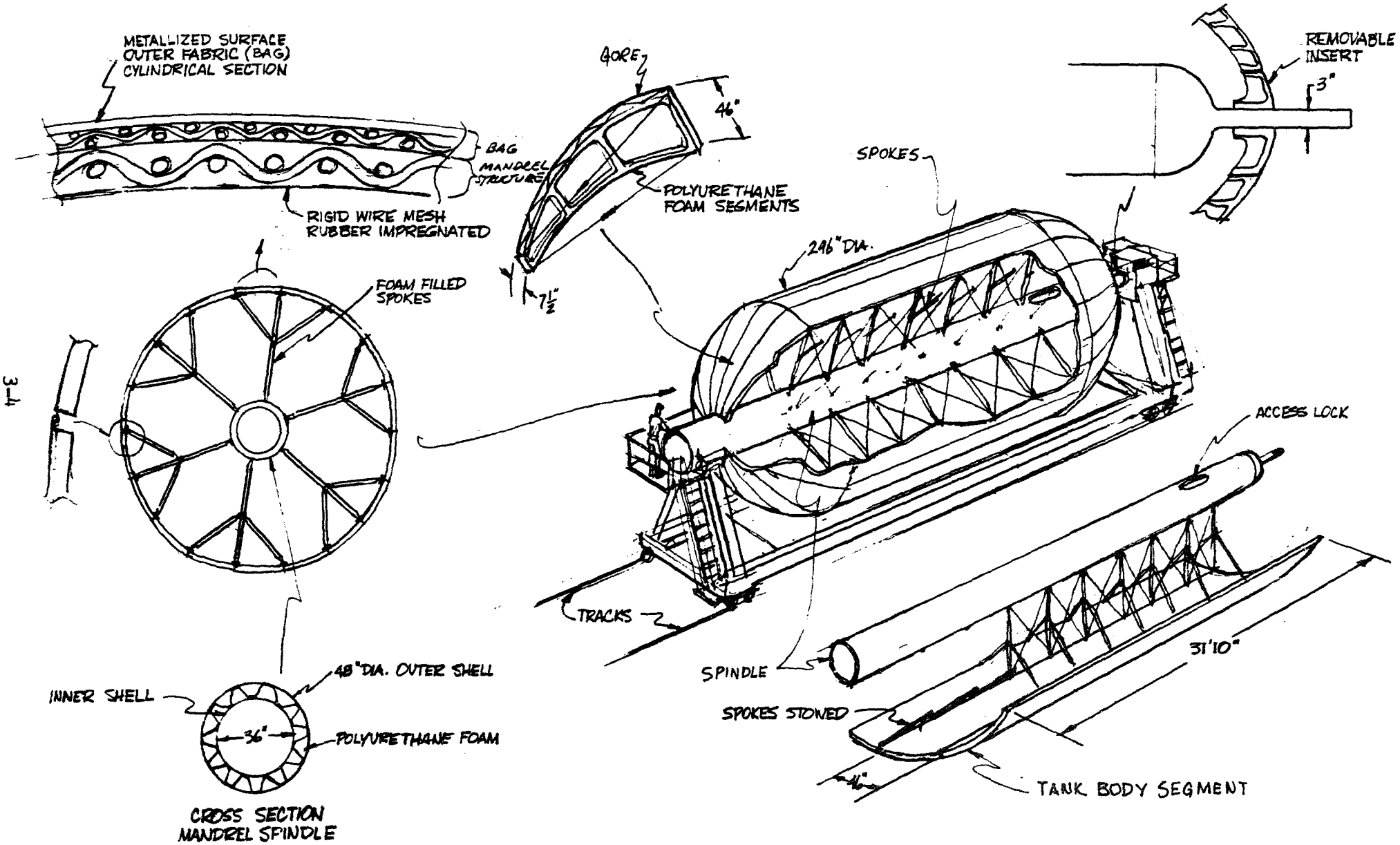

Figure 3.1-2 SUPPORTED INFLATABLE MANDREL (OPTION 1)

Dome Gore Segments

The hemispherical domes of the mandrel consist of 20 gore segments. The manufacturing mode conceived for the gore segments is as follows:

1. Fabricate trusses from thin-walled tubing. These trusses will be fabricated to the shape of the gore segment.

2. Reinforce the trusses with polyurethane foam.

Each of the fabricated gores will have interlocking capability and the final gore segment will be a "keystone" capability for assembly and dismantling purposes.

Internal Spokes

The internal spokes will be light-wall tubing and will be filled with urethane foam. The spokes will aid the mandrel in maintaining concentricity and alignment.

Inflatable Seals

The inflatable seals are located between the tank body segment ends and the gore equatorial plane ends. These seals will be used to rigidize the mandrel.

Inflatable Bag

The inflatable bag goes over the gore segments and tank segments of the mandrel. The bag may be segmented into two or more segments for installation over the mandrel. The bag will be capable of holding 5 psi. The bag will be fabricated from a silicone rubber impregnated wire mesh with the outer surface metallized.

Mandrel Assembly

The dome gore segments and tank body segments are individually installed, interlocked, and spoked into position on the spindal. After all segments are installed, inflatable seals located circumferentially between the dome and tank body parting planes are inflated. The outer inflatable bag is then positioned on the mandrel and leak checked. The mandrel is now ready for application of the parting agent.

Mandrel Dismantling

The mandrel is dismantled in the same manner and in the same sequence employed during assembly.

3.1.1.2 Mandrel Option 2

Figure 3.1-3 depicts the second option for the mandrel. The principle difference from Option 1 is the omission of the inflatable bag and the addition of mechanically expanding ring mandrels located inside the mandrel at the dome and tank body equatorial planes. These ring mandrels will allow expansion of the mandrel during the manufacturing process.

3.1.2 Manufacturing Plan

The preliminary manufacturing plan is depicted in Figure 3.1-4 and a descriptive narrative of each of the positions is described by position number.

Position #1

Position the mandrel on a power operated rotissiere type dolly. Transport the mandrel and dolly to an environmentally controlled area and apply a parting agent on the mandrel.

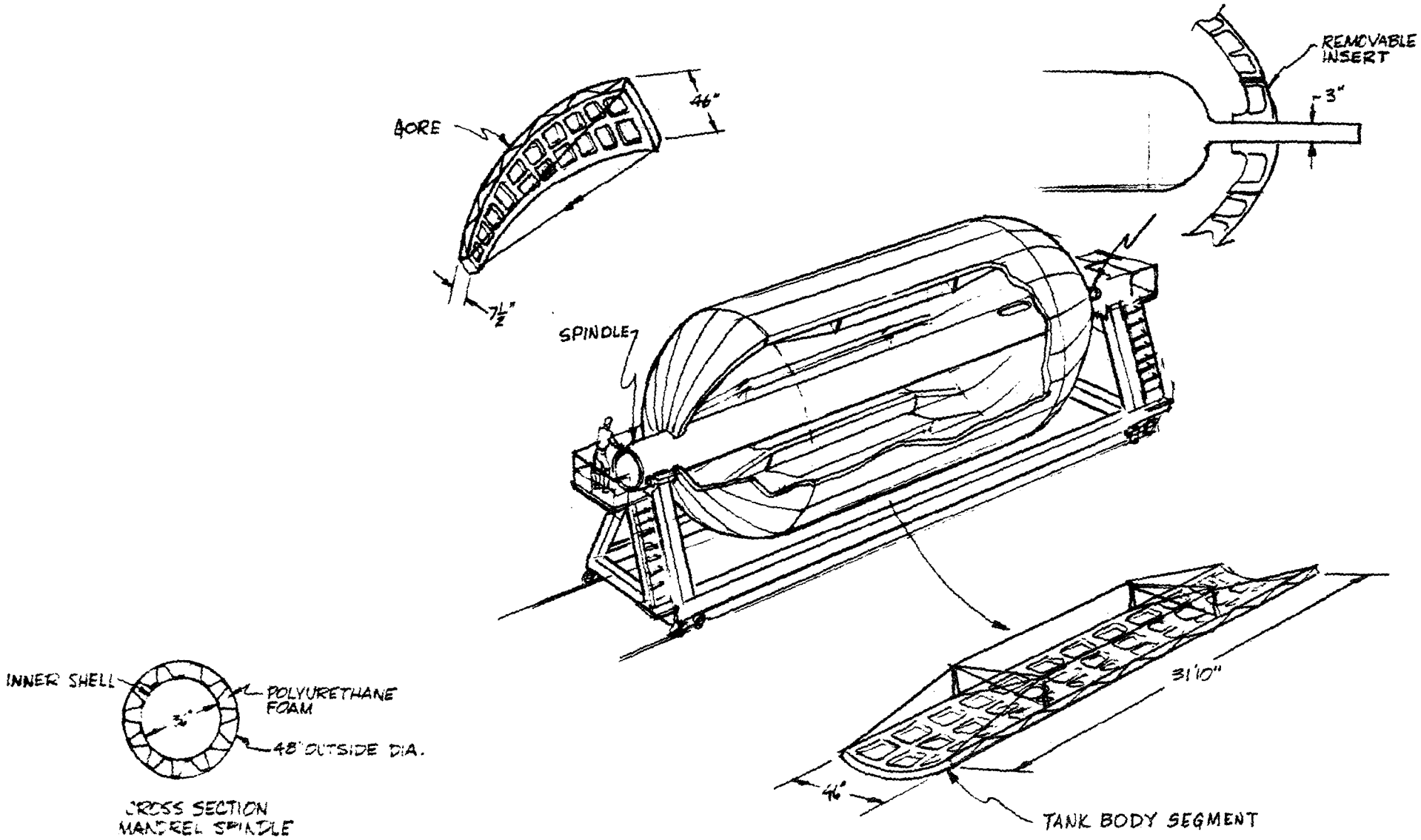

Figure 3.1-3 NON-INFLATABLE MANDREL (OPTION 2)

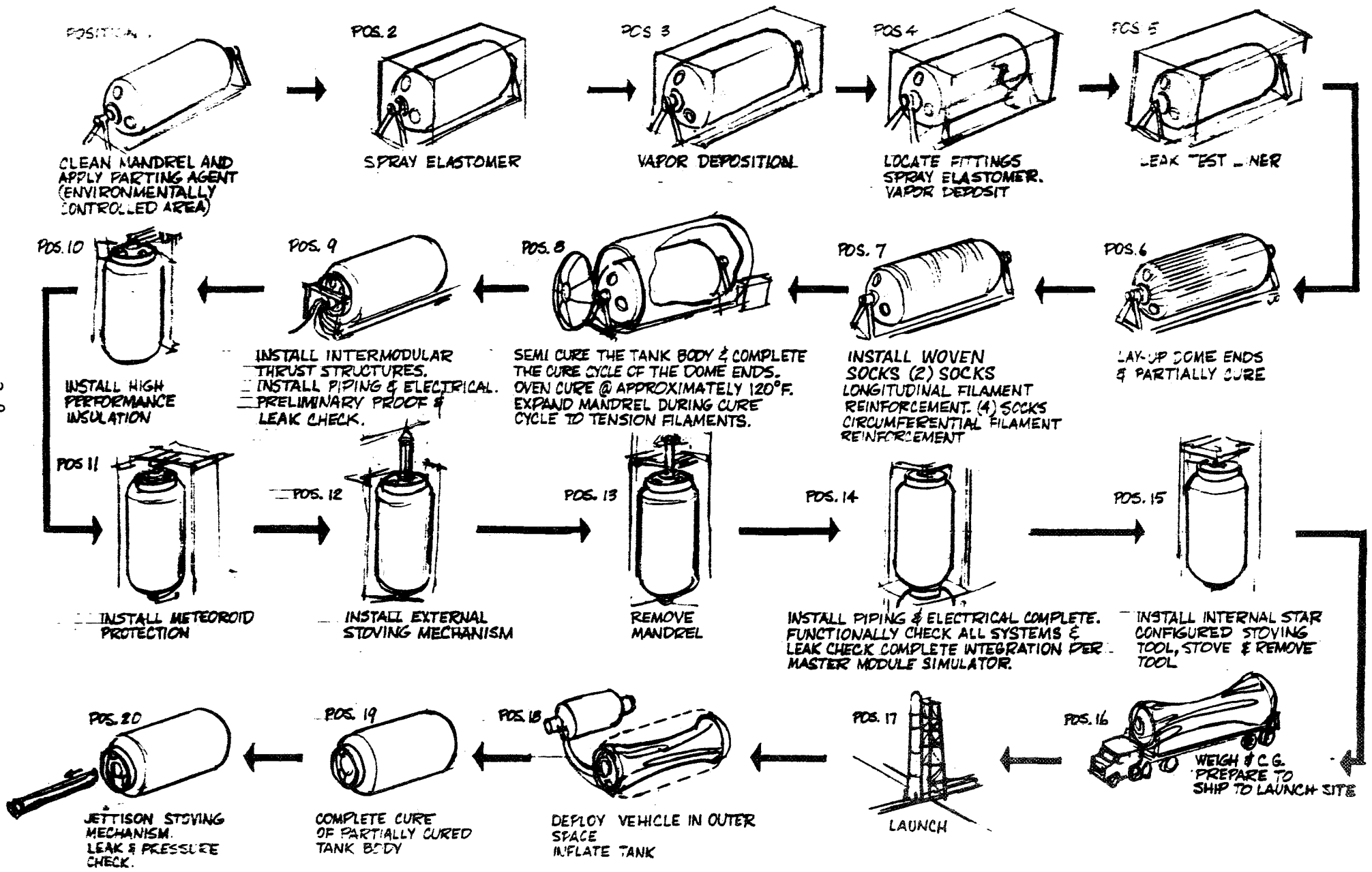

Figure 3.1-4 MANUFACTURING FLOW PLAN

Position #2

Apply 0.038 mm thickness of polyurethane polymeric elastomer over the entire surface of the mandrel in an environmentally controlled area and cure.

Position #3

Place the mandrel into a vacuum chamber and vapor deposit 600 Å of nickel on the surface.

NOTE: Repeat positions #2 and #3 until the desired liner thickness is attained.

Position #4

Locate all atach fittings, flanges, and jamb openings per tooling locators (Figure 3.1-5). The fittings will be matched to the previously sprayed and vapor deposited liner by applying a coating of polyurethane polymeric elastomer on the mating faces of the fittings and the liner. The fitting is then floated into position and secured per tooling locators. The spray techniques described in Positions #2 and #3 are then repeated. The spray operation will continue until the desired thickness is achieved.

Position #5

The liner is leak tested by one of three proposed methods; pressure decay, tracer gas probe or thermistor probe.

Position #6

Wet lay-up the forward and aft domes on a female mold and then index the molds to the mandrel per tooling points. The mandrel is then placed into an oven and the domes are semi-cured (approximately 25%). The semi-cured condition is described as having developed strength and rigidity to prevent any delamination during subsequent steps.

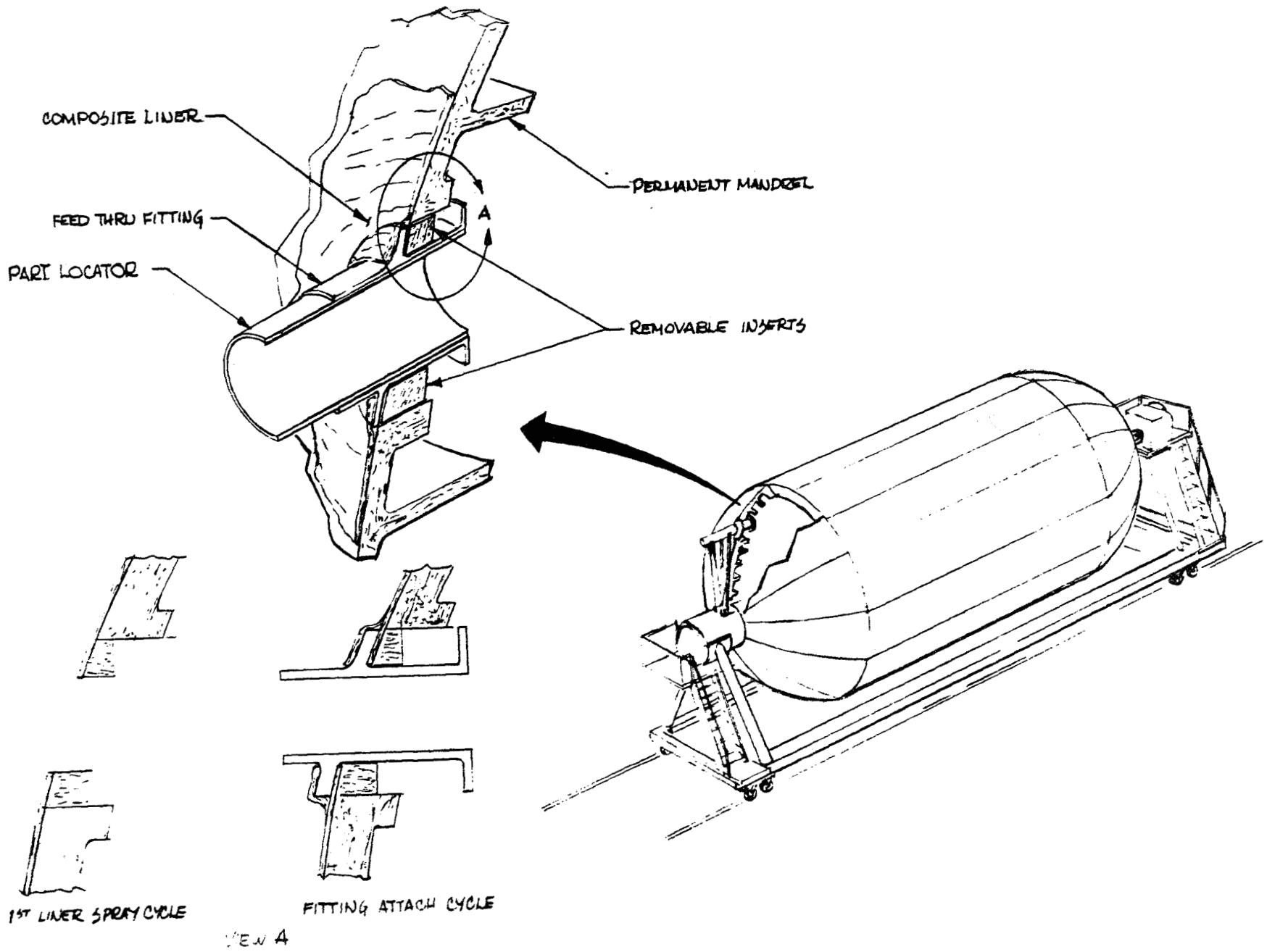

Figure 3.1-5 FEED THROUGH INSTALLATION

Position #7

Stretch two previously woven longitudinally oriented filament socks over the mandrel. Stretch four previously woven circumferentially oriented filament socks over the previously installed longitudinal socks. The socks will be impregnated with the resin one at a time as they are installed.

Position #8

The tank lay-up is then placed into an oven and cured at approximately 120°F. Upon completion of this cure cycle, the dome ends are fully cured and the tank body is in a 1st step cure condition. During the cure cycle the mandrel is expanded a pre-determined amount to tension the filaments. Upon completion of this cure cycle, gradient cures may be accomplished by initiating heating elements in selected areas.

Position #9

Install the intermodular thrust structures (a subsystem flow plan is shown on Figure 3.1-6). Install piping and electrical equipment to the highest level feasible. Perform a preliminary proof and leak test (reference product acceptance test plan).

Position #10

Install previously manufactured high performance insulation blankets and secure them to the tankage structure.

Position #11

Install the flex foam meteoroid protection system and attach it to the tankage structure.

Position #12

Install the previously manufactured and sub-assembled external stoving mechanism per previously located structural fittings.

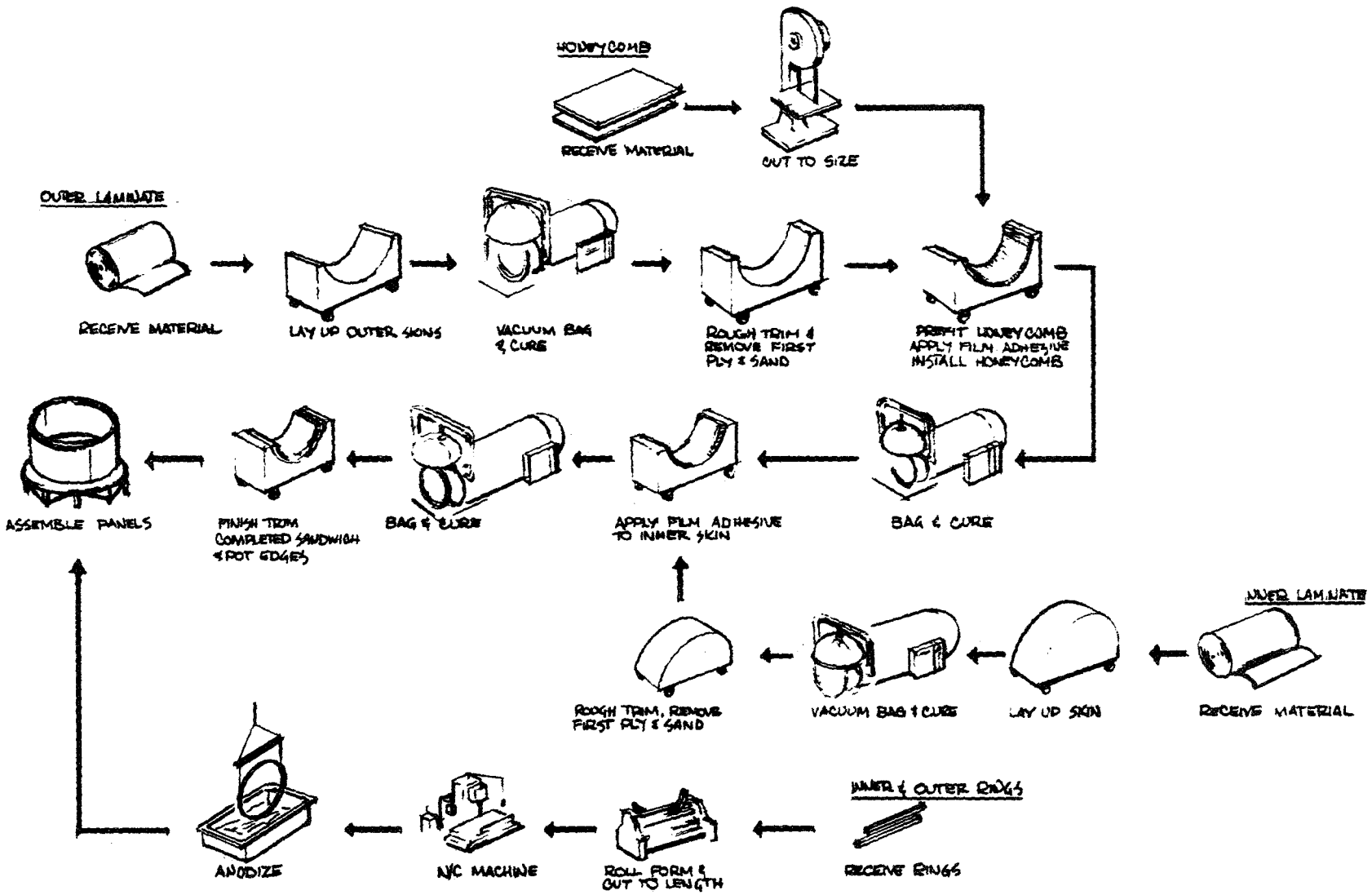

Figure 3.1-6 FLOW PLAN FOR INTERMODULE THRUST STRUCTURE

Position #13

Disassemble the mandrel and remove from the tank structure.

Position #14

Complete the installation of the piping and electrical, install all internal screens, fittings, etc. Install sump. Mate the assembly to the master module simulator and complete integration. Leak and pressure check completed vehicle.

Position #15

Install the star configured internal stoving tool. Actuate the external longitudinal stoving members individually and then restrain with straps. The external stoving actuating cables are installed and the internal stoving tool is removed.

Position #16

Weigh and establish the center-of-gravity. The stowed module is then placed into a shipping container that will have purging capability, sealed and shipped to the launch site.

Position #17

The vehicle is placed into the cargo bay of the space shuttle orbiter and launched into space.

Position #18

In space, the vehicle is deployed, the stoving mechanism is rotated outward and then the vehicle is inflated to size.

Position #19

The final cure of the tank body matrix is accomplished by initiating the heating elements previously installed in the tank by an auxiliary power source from a support vehicle.

Future Work

Mandrel assessment will be performed to determine the most promising method of tensioning the reinforcing fibers during first step cure. Methods of fabricating and installing the thermal/meteoroid protection subsystem will be investigated and flow plans of the selected methods generated. The fabrication process, mode of attachment and operation of the stoving mechanism will be determined. In addition, the requirement for a temporary internal stoving tool will be investigated.

3.1.3 Inspection and Testing

The complex ground and earth orbit fabrication procedures proposed for the propellant tanks places unusual requirements on the nondestructive inspection of the tanks. The final cure of the tanks in earth orbit requires a high confidence in the prelaunch fabrication and acceptance test procedures. The objective of the propellant tank acceptance test program is to ensure the uniformity and usability of the final product by providing detailed information during the initial manufacturing processes, prior to launch, and again after cure in space.

The tank acceptance test program may be divided into four main phases, manufacturing, prelaunch, deployment and reuse, each having different objectives (Table 3.1-1). The final acceptance testing of the tank will take place in earth orbit. The earth orbit testing will be conducted without the use of any extra-vehicular activity (EVA).

Table 3.1-1

PROPELLANT TANK ACCEPTANCE TEST PROGRAM

Phase	Description
Manufacturing	Acceptance after specific fabrication steps up to the folding operation
Pre-Launch	Acceptance of folded tank for launch
Deployment	Acceptance of fully cured tank in orbit (particularly leak and proof testing)
Reuse	Monitoring of tank response during use and qualification of tank prior to each mission

An acceptance test program must first address itself to identifying the defects that can cause the failure of a vehicle. After the defect is identified, nondestructive techniques can be applied for its detection. A number of nondestructive testing techniques are considered for the detection of each defect of interest. The techniques considered are drawn from both the current state-of-the-art and new technology requiring further development. Technique selection will be based upon sensitivity to the defect of interest, applicability to the unique configuration, ease of operation, and remote sensing capabilities for space testing.

The cost effectiveness of suggestive NDT techniques must be considered. Techniques which require elaborate tooling or cause significant manufacturing perturbations must be justified on the basis of the usefulness of the data. It is equally important to maintain the flexibility of modifying the manufacturing procedures where a significant amount of data, ease of gathering data, or an otherwise not obtainable but necessary piece of data can be obtained.

Although all portions of the propellant tanks are vital to its operation, the principal areas of concern for this discussion are the structural integrity and uniformity of the tank, leak integrity of the liner, and uniformity of the thermal insulation system. In addition to these areas of inspection, it will be necessary to monitor material changes occurring during use to predict incipient failure.

3.1.3.1 Manufacturing Acceptance Testing

Several manufacturing steps (Table 3.1-2) are considered as major milestones in the tank fabrication procedure, and are selected as logical points for incorporating the NDT inspection program. It will be assumed that all precursor materials for the tank fabrication have undergone a thorough inspection program.

Table 3.1-2

MANUFACTURING TESTING SEQUENCES

Manufacturing Step	Description	Defects	Techniques	Remarks
Liner Fabrication	Polyurethane deposition	Thickness fluctuations	Eddy current	1
	Nickel deposition	Thickness fluctuations	Resistance	1
	Complete liner	Leak	Pressure decay	1
			Tracer gas probe	1
			Thermistor probe	2
			Restrained hard vacuum/mass	1
			Spectrometry	
			Quantitative PPM Leak	
Dome Poles	Cured dome poles Over liner	Composite nonuniformities (porosity and delaminations)	Ultrasonic	1
			Radiographic	1
			Holography	2
			Infrared	2
		Dome-liner unbond	Pulse echo	1
			Holography	2
			Infrared	2
Longitudinal Sock	First longitudinal sock over liner	Sock-liner unbond	Holography	2
			Infrared	2

1 - State-of-the-Art

2 - New technology needing development

Table 3.1-2

MANUFACTURING TESTING SEQUENCES (CONT'D)

Manufacturing Step	Description	Defects	Techniques	Remarks
First Stage Cured Sock	Complete composite fabrication	Composite nonuniformities (porosity and delaminations)	Ultrasonic	1
			Radiographic	1
			Holography	2
			Infrared	2
		Dome-liner unbond	Holography	2
			Infrared	2
		Leak	Pressure decay	1
			Tracer gas probe	1
			Thermistor probe	2
			Restrained hard vacuum/mass	1
			Spectrometry	1
			Quantitative PPM leak	1
HPI	Installation of HPI	Tears, loss of metal coating, and compression	Induction coil	2
Folded Tank	Folding of tank prior to launch	Liner composite Bond at folded radii	Holography	2
			Infrared	2
		Crack at Ni layers	Eddy current	2
		Crushing of HPI	Induction coil	2

1 - State-of-the-Art

2 - New technology needing development.

Table 3.1-2

MANUFACTURING TESTING SEQUENCES (CONT'D)

Manufacturing Step	Description	Defects	Techniques	Remarks
Fully Cured Tank	Deployment and cure in earth orbit	Leak Structural integrity HPI crushing	Pressure decay Proof test Induction coil	2 2 2
Reuse	During and after each mission	Requalification of tank and aging anomalies	Acoustic emission Strain monitoring Ultrasonic Measurements	2 2 2

1 - State-of-the-Art

2 - New technology needing development

Liner Fabrication

After each deposition of polyurethane and nickel, a thickness check will be conducted to establish that the individual layer thicknesses are within tolerance. The methods considered for these inspections are eddy current for the polyurethane and electrical resistance measurements for the nickel.

The eddy current technique is based on probe liftoff due to the thickness of the nonconductive layer over a conducting substrate (Ref. 3.1). Electrical resistance measurements between two knife edge contacts are currently being used as an acceptance procedure for vapor deposited metallic coatings. However, if close nickel layer tolerances are required, other techniques having greater sensitivity may be required. Although these methods are planned for only spot check purposes they can be automated.

With the completed liner deposited on the mandrel it is desirable to perform an initial leak test. The acceptance leak tolerance levels will be determined by overall mission requirements and development testing. A number of feasible leak test procedures and techniques are briefly discussed in the following paragraphs.

It is necessary to distinguish between the permeation leak rate and a leak through a pinhole defect. The permeation leak is a diffuse process which cannot be located by current state-of-the-art techniques and can only be quantitatively determined through a total tank leak rate method. The pinhole is a singular defect causing flow conditions around itself and may be detected by scanning or other isolation methods. The approach has therefore been defined to first determine an overall integral tank leak rate followed by isolation methods to locate any single out of tolerance leak. This approach will provide maximum assurance that repair can be accomplished in the most favorable manufacturing position.

Leak tests must be performed on the mandrel-liner combination because the elastomeric liner is not self supporting. Leak testing may be possible by selecting the mandrel release agent so that upon slight heating it would outgas sufficiently to provide an adequate differential pressure for testing. However, this approach would require allowing the liner to expand unrestrained away from the mandrel. This may make the method undesirable.

An alternate approach providing continuous support for the liner is that of constructing the mandrel from a permeable material which would still provide the desired surface finish for the polyurethane. The pressure can be obtained by either pulling a partial vacuum on the inside of the mandrel, applying pressure from the outside, or a combination of the two. The mandrel will be surrounded by a suitable bag for collecting the gas or applying pressure.

The test gas for the total integral leak rate test can be helium or gases containing sulphur difluoride, or radioactive tracers. If this rate is not within tolerances, a second test to scan the exterior surface of the liner can be conducted. Current tracer gas methods using gathering devices are not practical here since they would require internal pressurization and access to the liner.

A new method currently under development at MDAC under Contract NAS1-10184 entitled "Study of Damage Control Systems for Space Station" potentially could provide an accurate means for inspection. This method uses a device which operates by detecting choke flow conditions with a thermister thermoconductivity cell (Ref. 3.2).

A radioactive gas check using Krypton 85 may be applicable. Krypton 85 can be introduced in the exterior bag with a partial vacuum on the interior of the mandrel. The exterior bag is flushed and the liner scanned for tracers of the radioactive gas. A possibility of performing both the total leak rate check and location of defects may be possible with this technique. Generally, the leak test area is one which requires further developmental studies.

Dome Pole Ends

Inspection of the dome pole ends can be initiated after the first composite layer is layed up on the liner to ensure a lack of unbond areas. After the remaining layers are layed up on the liner and the dome pole ends are fully cured, the composite and composite-liner interface should be inspected. A number of techniques for these inspection areas are discussed below.

Ultrasonic and radiographic methods have been used at MDAC to detect composite defects, porosity, and delaminations.(References 3.3 and 3.4). Basically the ultrasonic technique relies on introducing an ultrasonic pulse into a composite and measuring its loss of amplitude (attenuation) or the delay time (velocity). Porosity has been detected in unidirectional composites by both these methods (Figure 3.1-7). An ultrasonic pulse echo method would be applied to the tank composite so that only single surface access would be necessary. The radiographic technique could be accomplished by using a gamma ray source on the interior of the mandrel and placing the recording film on the outside surface. While the radiographic technique is routine, further development would be required for the ultrasonic pulse echo method of obtain the desired sensitivities.

Infra-red radiometry is a potential technique for detecting composite defects and lack of interface bond. By observing heat flow patterns in the specimen which has been heated above ambient (ΔT of 4° to $8^\circ F$) material integrity may be monitored. The thermal input could be achieved from the exterior surface or by small heat source internal to the mandrel. The thermal technique may have limited sensitivities due to the heterogeneous nature of the composite.

A more promising technique which has been applied to pressure vessels is that of interferometric holography (References 3.5 and 3.6). This technique compares two three-dimensional images of a specimen which are recorded under two different levels of applied stress. The resulting differences in the dimensions of the test object are visualized in the form of an interference fringe pattern, the character of which is influenced by the integrity of the specimen. The simplest stressing technique

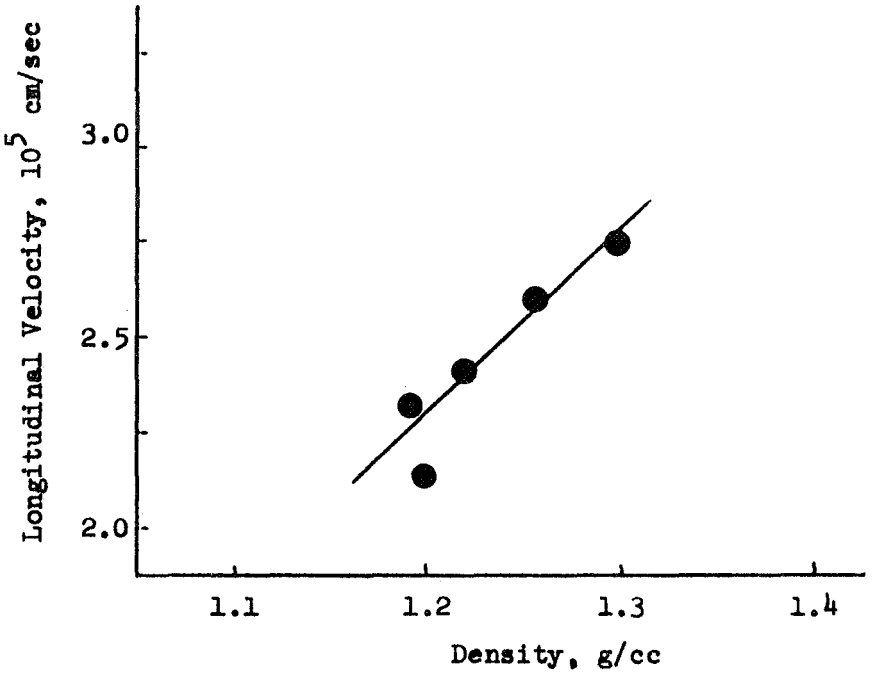

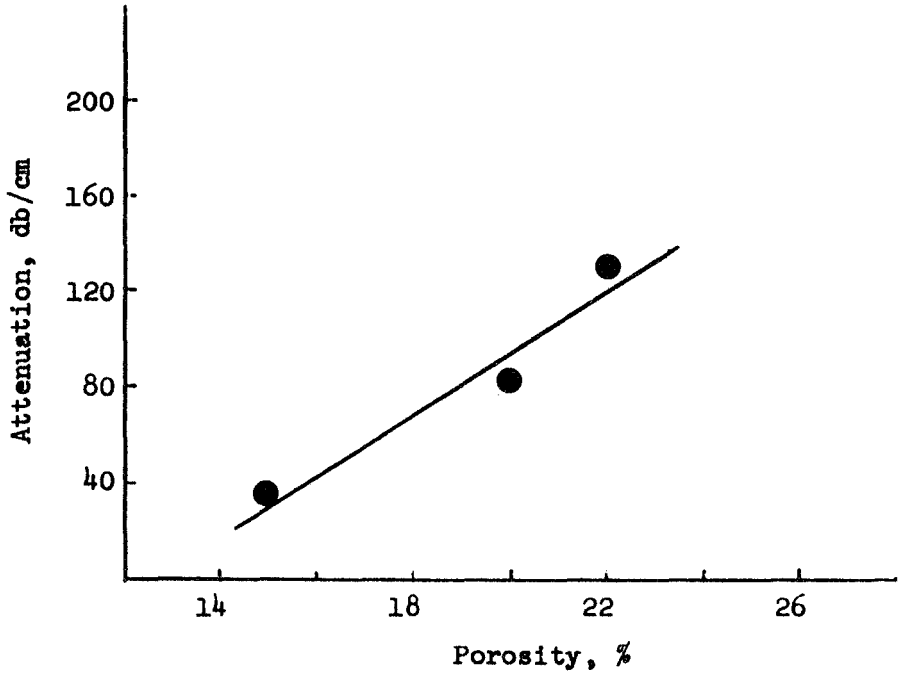

Figure 3.1-7 ULTRASONIC PROPERTIES OF A PYROLYZED UNIDIRECTIONAL CARBON-CARBON COMPOSITE

may be heating the specimen approximately 5°F above ambient. A hologram of a metallic pressure vessel containing a flow is shown in Figure 3.1-8.

Longitudinal Sock

The interfacial bond between the first longitudinal sock and the liner must be inspected to ensure lack of unbonded areas. As in the previous inspection, interferometric holography and infra-red radiometry are potential methods of detecting the unbond.

First Stage Cured Sock

With the last circumferential sock placed on the tank, a final tank inspection prior to folding is necessary. Since the tank is self supporting at this point, internal pressurization or access is possible. Leak integrity, defects, within the composite, and lack of interface bond are the important conditions to be detected. The NDT techniques previously described for the composite defect and lack of interface bond detection can again be applied for the inspections (Table 3.1-2).

Total integral leak rates can be obtained by the same techniques and procedures as used for the initial liner inspection. Since the tank is now self supporting, internal pressurization procedures are probably more attractive. The detection techniques may be the same as described for the liner tests.

With the composite system over the liner, any leak in the liner will be difficult to detect due to its diffuse nature at the exterior surface.

To obtain information on composite properties, a sample which had been processed along with the tank should be cured and destructively tested. Although this does not qualify the tank, it will provide data which would indicate proper processing procedures.

UNFLAWED FLAWED

$\Theta = 67^0$

$\Theta = 122^0$

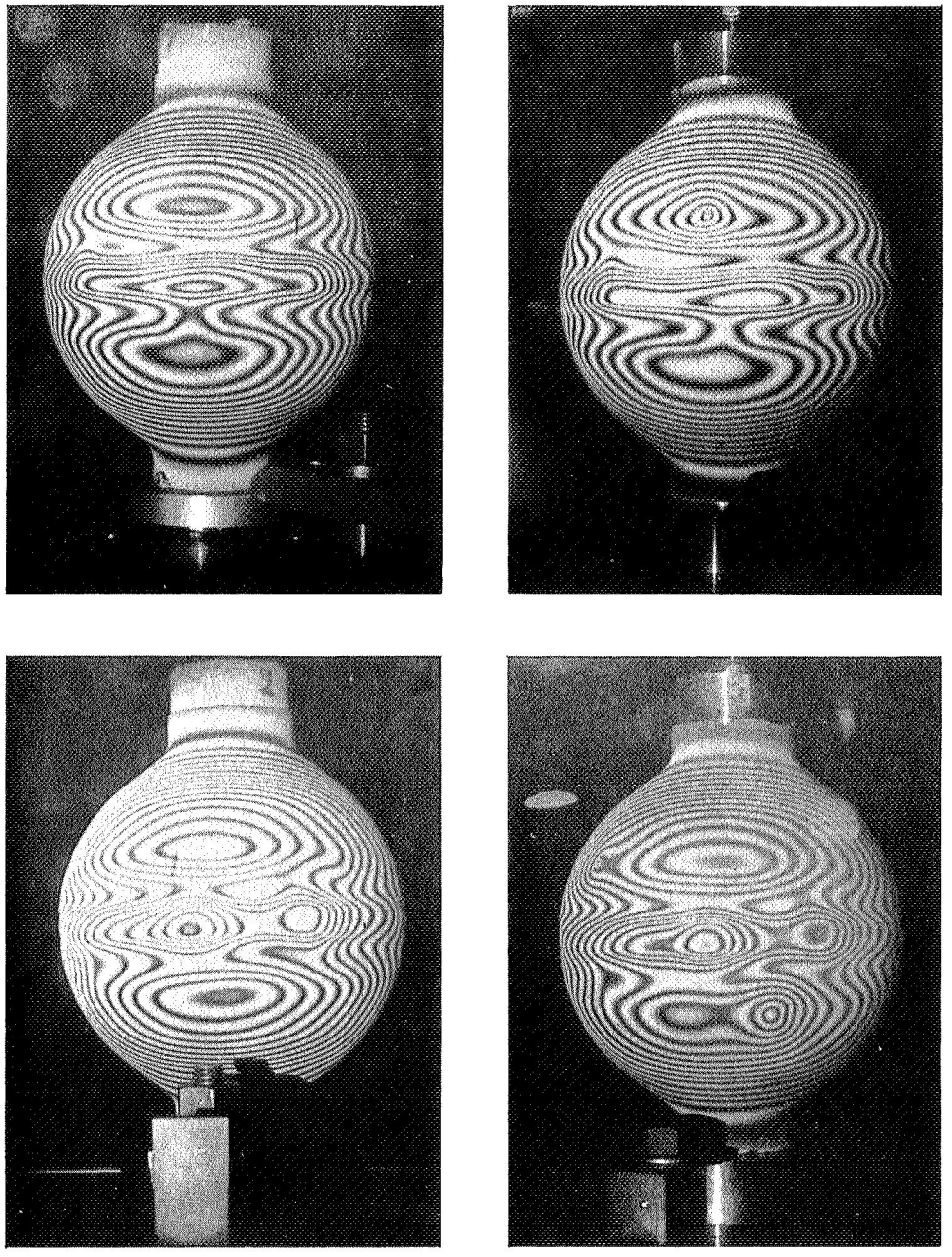

Figure 3.1-8 HOLOGRAPHIC INSPECTION OF 15 cm TITANIUM PRESSURE VESSEL
$\Delta P = 2.76 \times 10^5$ N/m^2 (40 psi)

An initial proof test of the first stage cuted tank will be conducted to ensure that the tank is capable of sustaining the inflation pressures required for deployment in orbit. This test will also provide assurance that the internal tank, purge, storage and shipping pressures are within safety limitations. This proof test is not intended as a final structural test, since this can only be accomplished when the tank is fully cured in earth orbit.

Installation of HPI

The defects that may be introduced into the HPI system during installation are tears, loss of metal coating, excessive compression, and separation of butt joints. A technique which appears applicable for inspecting HPI is an induction coil technique (Reference 3.7). This technique developed at MDAC employs an induction coil held in proximity to the installation. The coil impedance is sensitive to the physical condition of the insulation system. After the HPI is installed, visual and induction coil inspection procedures can be used to ensure the absence of any defects. The inspection could be accomplished by using additional fixturing which would allow scanning of the entire insulated surface of the tank.

3.1.3.2 Pre-Launch Acceptance

The prelaunch inspection procedures are to qualify the folded tank for Space Shuttle launch. Folding of the tank may cause separating at the liner composite interface and cracking of the nickel layers at the sharp bend radii. Crushing of the HPI insulation at these points is also possible. Assuming internal access to the folded tank, holographic and infrared radiometric techniques may be applied to the local bend areas for detection of interface unbonds. Eddy current methods could be applied to the detection of nickel layer discontinuities (cracks). The HPI system could conceivably be inspected for open butt joints, tears and layer density anomalies in the folded condition by the induction coil technique. This inspection can probably be conducted from the exterior surface through the foam layer.

3.1.3.3 Final Module Acceptance

After the tank has been put into earth orbit, deployed, and cured, the operational leak and proof tests must be conducted and monitored to ensure tank integrity. The most feasible leak test procedure in earth orbit is a pressure decay method using hydrogen gas. If the tank does not meet the leak rate tolerances, probe scanning to locate the leak and repair procedures from within the tank may be initiated. However, these tests and repair procedures would require EVA.

A proof test at liquid hydrogen temperatures to a predetermined level above the operating pressure will be conducted and monitored by onboard sensors. These sensors may include ultrasonic transducers for acoustic emission monitoring and strain gages for strain measurements. The location of these sensors must be selected so as to provide adequate coverage of the entire tank. The sensors would be installed directly on the composite surface at the first stage cure manufacturing position (prior to launch).

Acoustic emission from the stress wave produced in materials by the energy released as the specimen deforms or fractures can be used to predict tank failure (References 3.8 and 3.9). A typical composite acoustic emission response in tension is shown in Figure 3.1-9. Anticipating future research on acoustic emission properties of composites, the proof test emissions may be related to fiber or matrix fracturing. This information along with the strain measurements may provide a means of predicting ultimate tank strength and reuse life.

Incorporating a number of fine metal wires into the precursor unidirectional composites may provide a means of detecting fiber breakage and crack growth in specific areas of the tank. Changes in electrical resistance of the wire might be a measure of strain, and loss of electrical continuity would indicate breakage.

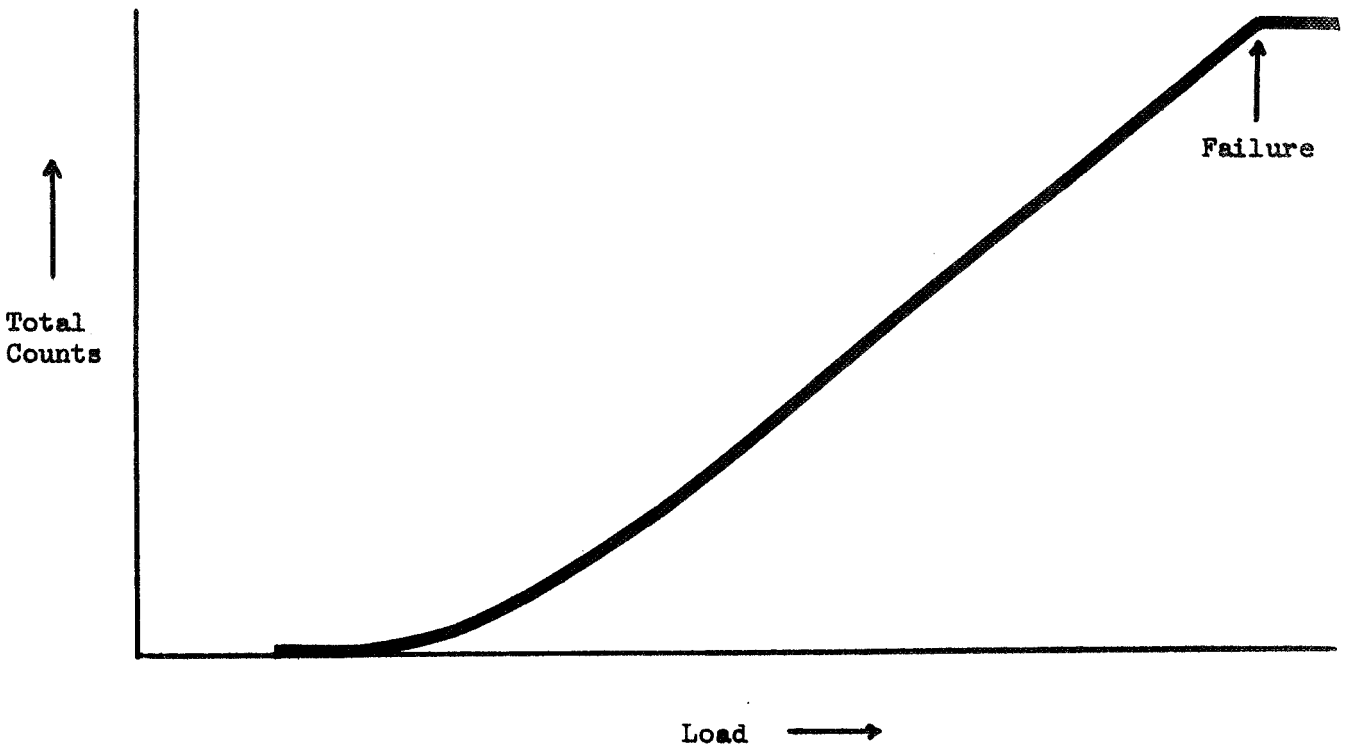

Figure 3.1-9 TYPICAL ACOUSTIC EMISSION RESPONSE OF CARBON-CARBON COMPOSITE IN TENSILE TEST

The ultrasonic transducers can be used in an active mode to generate ultrasonic signals which can be used to measure ultrasonic velocity and attenuation. This information can be indicative of the cured composite uniformity as previously discussed. Measurements made during the proof test may be correlated to a composite response property or be used to predict reuse properties. For example, the ultrasonic properties of a composite under stress may be related to a quantitative amount of material damage which would reduce future properties of the composite. Preliminary work in the area of measuring material damage in composites by NDT methods has been done at MDAC (Reference 3.10). One aspect of this damage assessment program was the correlation of residual compressive strength to ultrasonic attenuation of a plate-slap tested composite (Figure 3.1-10).

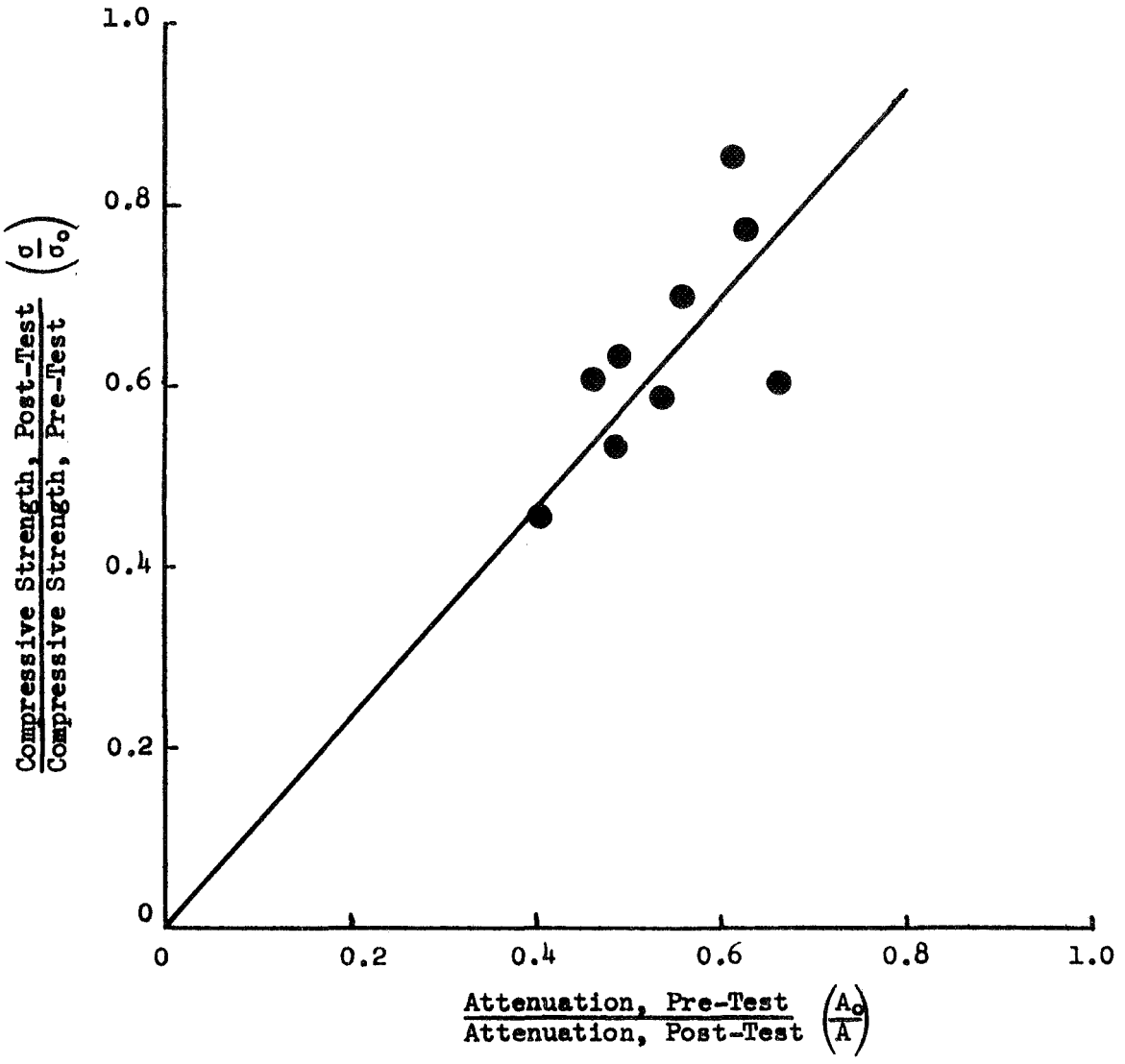

Figure 3.1-10 CORRELATION BETWEEN STRENGTH AND ATTENUATION FOR PLATE-SLAP TESTED COMPOSITE

3.1.3.4 Reuse Qualification

The onboard sensors used during final proof test procedures can be utilized to monitor tank response during the mission and for reuse qualification. Cyclic thermal and structural loads in a space environment may produce again mechanisms in the composite systems which may alter the physical properties of the composite. By using the acoustic emission, ultrasonic property, strain, and crack measuring sensors, continuous data acquisition is possible. The information obtained may provide insights into design and material properties of the tank which can then be used for the design of future propellant tanks.

3.1.3.5 Future Work

The feasibility and trade-off analyses will be continued to establish multiple acceptance test options. From these options, a baseline or reference test plan will be selected. The selection of reference test procedures and techniques will be based on sensitivity to the defect of interest, utility with existing manufacturing sequences, remote sensing capabilities, and cost effectiveness. The reference test plan will be used to establish the ground and orbit support requirements.

3.2 COST ANALYSIS

3.2.1 Bases for Cost Estimates

The analyses performed in support of cost estimating falls into two major categories. The first is a detailed evaluation associated with the cost of developing and producing the expandable propellant module with special emphasis placed on the unique structural subsystem. The second category is that associated with a system level evaluation of the cost effectiveness of the advance RNS concept. In performing these analyses the following ground rules will be imposed.

1. State of the art: 1980's.
2. All costs are expressed in constant 1971 dollars without fee.
3. Production requirements will be based on an operational program of 6 missions per year over a ten year period.
4. Each module of the advanced RNS will be designed to operate for 10 missions.
5. The RNS will interface with the space shuttle for transportation to earth orbit and a space tug with assembly support provisions for orbital support.

The elements for the work breakdown structure associated with the advanced RNS are identified in Figure 3.2-1 and defined below:

NSX-03-00-00 **Advance RNS Project (RNS-X)**

The RNS-X is composed of three distinct modules: one propulsion module, one set of three propellant modules and one command and control module. Its characteristics are:

Thrust = 334,000 N (75,000 lbs)

Specific Impulse = 825 sec

Propellant Capacity = 131,000 Kg (300,000 lbs)

NSX-03-01-00 **Propulsion Module**

Provides acceleration to the RNS-X. It is identical to Phase III propulsion module. It is composed of NERVA, propellant run tank, propellant and astrionic controls. It is mated to the flight vehicle in orbit. Its technical characteristics are:

Dry Weight = 14,350 Kg (31,685 lbs) including shield

Design Life = 3 years

Operating Life = 10 hrs

Overall Dimensions = 4.57 m dia. x 18.3 m long (15 ft x 60 ft)

NSX-03-02-00 **Propellant Module**

LH_2 storage vessel. Three propellant modules in tandem contain about 131,000 Kg (289,000 lbs) of LH_2. The propellant modules employ radial expansion in orbit to establish a 7.52 m (24.6 ft) diameter. The propellant modules are mated in orbit. The technical characteristics of a module are:

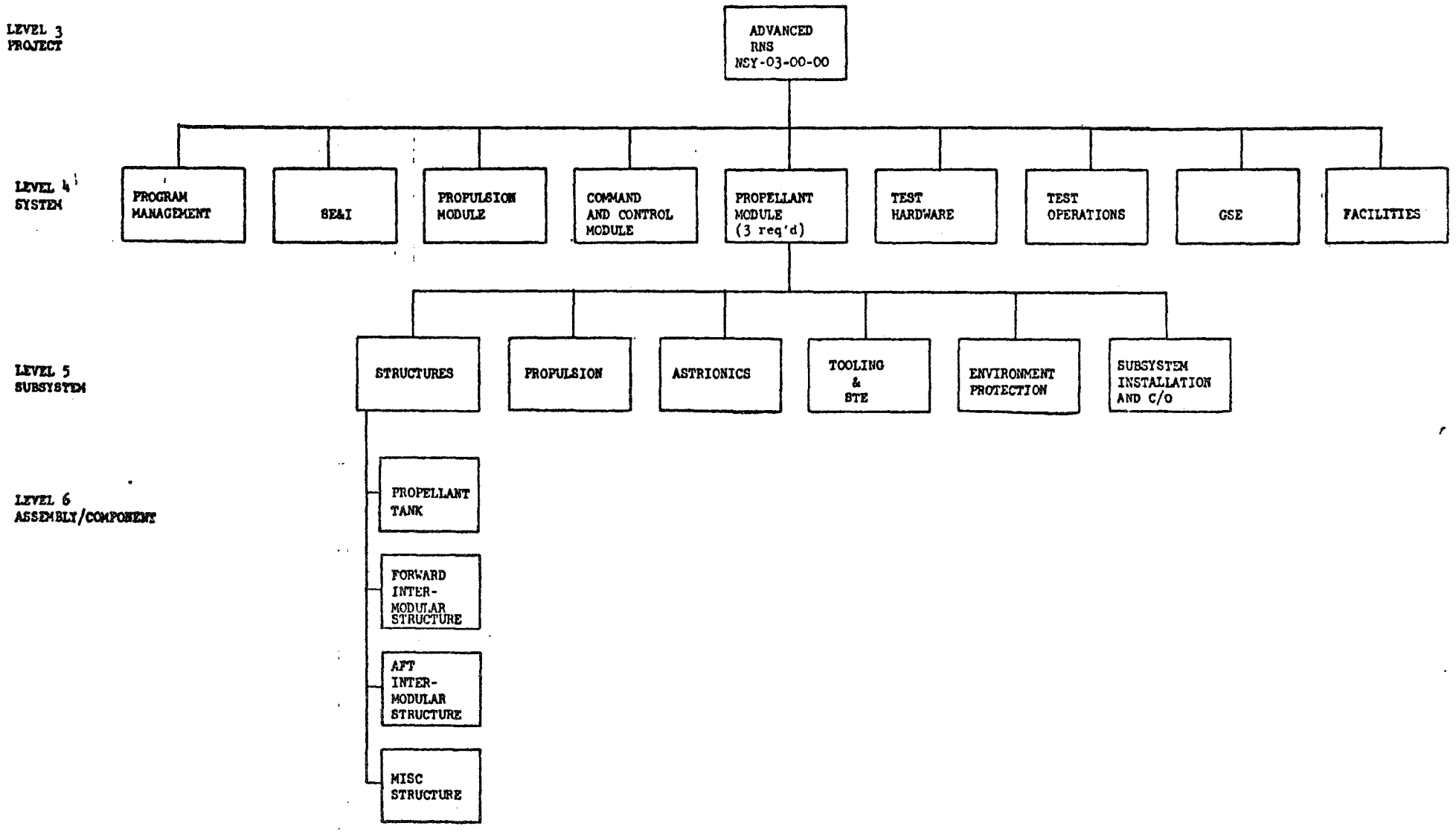

Figure 3.2-1 WORK BREAKDOWN STRUCTURE

Design Life = 3 years

Propellant Capacity = 43,700 Kg (96,400 lbs) LH_2

Design Pressure = 20,650 N/m^2 (30 psi)

NSX-03-02-01 Structures

Propellant Tank Assembly

The propellant tankage is fabricated from a composite consisting of PRD-49-3 filaments and an epoxy matrix. An impermeable liner is bonded to the inside of the tank. The central portion of the domes (spherical segments having a 4.23 m (13.8 ft) diameter) are rigidized on the ground. The remainder of the tankage is left flexible, packaged in an 8 point star fold, and transported to orbit in the cargo bay of the space shuttle. Once in orbit it is removed from the cargo bay deployed by pressurization and rigidized by heat. The pressurization and heat sources are provided by orbital GSE contained in an orbital support vehicle. The propellant tank characteristics are:

Dry Weight = 940 Kg (2070 lb)

Surface Area = 407 m^2 (4380 ft^2)

Material

Tank Wall - Fiber glass filaments/epoxy matrix composite

Tank Liner - A composite of six urethane elastomer layers, five having 600 to 1200 Å of vacuum deposited nickel.

Production Experience - none

State of Art - Major development work is required

Forward Intermodular Thrust Structure (FITS)

The FITS is a cylindrical heat block whose function is to minimize heat flow into the tank and accommodate loads. At the forward end is an integrally machined frame with provisions for mounting docking probes/drogues and structural latches for joining propellant modules. The technical characteristics of the FITS are:

Dry Weight = 105 Kg (230 lb)

Material:

Heat Block - Fiber glass honeycomb sandwich

Forward Ring - Aluminum machined frame

Aft Attach Ring - Fiber glass epoxy machined

Production Experience - moderate

State of Art - Within current state of the art

Aft Intermodular Thrust Structure (AITS)

Identical to FITS.

Miscellaneous Structure

This category includes antislosh baffles, equipment supports, access structure, docking, stabilization, etc.

Dry Weight = 650 Kg (1430 lb)

Material = Mainly aluminum

Contingency

Allowance for variation in tankage assembly

Weight = 130 Kg (290 lb)

NSX-03-02-02 Propulsion (Lines, Valves, and Misc.)

The propulsion LVM reflect the functional subsystems required to provide: propellant feed, pressurization, fill and drain, orbit refuel and flight vent. The pressurization line is rotated to its operational position via motor drive. The remaining elements are positioned for operation while on the ground

Weight = 210 Kg (453 lbs)

NSX-03-02-03 Astrionics

This group includes the supporting avionics subsystems. The source of control is in the command and control module. Typical of this group are instrumentation sensors, and signal conditioning, remote decoders, and power distribution networks.

Group Weight = 75 Kg (165 lbs)

NSX-03-02-04 (Not Used)

NSX-03-02-05 Tooling and STE

This category includes all subassembly and assembly tools, checkout towers, and special test equipment required to support the module production effort. The cost shall reflect a direct estimate made by advance manufacturing engineering.

NSX-03-02-06 Environment Protection

The thermal/meteoroid protection sybsystem consists of multi-layer high performance insulation, a blanket of flexible foam, and a mylar shroud or purge bag.

Subsystem Weight = 1017 Kg (2,240 lbs)

Insulation = 350 Kg (772 lbs)

Meteoroid
Protection = 667 Kg (1470 lbs)

NSX-03-02-07 Subsystem Installation and Checkout

This effort consists of mating and final assembly of structural subassemblies, installation of all other subsystem hardware into the module and factory checkout of the completed module.

NSX-03-03-00 Command and Control Module (CCM)

The CCM contains the functional subsystems providing electrical power, guidance navigation and control, data management, instrumentation and auxiliary propulsion. It is identical to the Phase III RNS CCM.

The remaining work breakdown structure (WBS) elements will be defined at a later date.

NSX-03-04-00	Test Hardware
NSX-03-05-00	Test Operations
NSX-03-06-00	Facilities
NSX-03-07-00	Support Equipment (Ground & Orbital)
NSX-03-08-00	System Engineering and Integration (SE&I)
NSX-03-09-00	Project Management

3.2.2 Recurring Costs

The recurring costs associated with the advance RNS are summations of manufacturing labor, related support, raw materials, and purchased parts required for 6 flight articles. The methodology used in evaluating the costs is divided into two primary categories: (1) use of existing data resulting from the Phase III RNS study NASA Contract NAS8-24714, and (2) use of detail manufacturing plans which defined the required manufacturing labor.

For the advance RNS configuration the costs of the propulsion module and the command and control module fall into category one. The aforementioned study define the propulsion module cost to be 14.7 million dollars at the first unit. Included are 13.0 million dollars for the NERVA engine. For the assumed program model 6 units are required resulting in a total recurring cost of 101 million dollars including sustaining engineering. The command and control module first unit cost is 13.6 million dollars with the total recurring cost of 162 million dollars for six unit and including sustaining engineering.

In defining the recurring costs for the propellant modules the use of both categories is invoked. As was shown in Figure 3.2-1, the propellant module is made up of structures, propulsion, astrionics and thermal protection subsystems as well as tooling and STE, and subsystem installation and checkout. There are 3 units per flight vehicle for a total of 18 during the program. The costs for the propulsion and astrionics subsystems were derived on the basis of the comparable Phase III subsystems. The results are:

	T_1 ($\$10^6$)	Total Recurring ($\$10^6$)
Propulsion	0.24	5.7
Astrionics	0.34	7.9

The remaining element of the propellant module will be derived as functions of detail manufacturing evaluations. Typical of this process is the method used for evaluating the thermal/meteoroid protection subsystem. The High Performance Insulation (HPI) consists of stacked pairs of reflections (aluminized) mylar) and spacers (nylon or dacron net) held together by button pin fasteners. A preliminary but detailed fabrication plan is presented below. Based on that plan operations engineering estimated the time required for fabrication, and installation of the HPI. For the propellant module size in question 7.1 hrs/sq ft were required for fabrication and 3 hr/sq ft for installation. The resulting cost at the first unit is $455,000. During the next study period this approach to costing will be followed in the areas of structures, tooling, subsystems installation and checkout.

Insulation Blanket Fabrication

a. Receive and inspect mylar rolls, dacron rolls, Velcro loop, and Velcro hook pile.

b. Place rough trimmed inner cover sheet on layup tool and align.

c. Unroll one (1) dacron sheet, cut off on flat table; hold with weights on selvage edges.

d. Unroll a second dacron sheet, cut off, stack on top of 1st sheet; hold with weight on selvage edges.

e. Unroll one (1) mylar sheet, cut off, stack on dacron sheets.

f. Center mylar template on stack. Rough trim using an Exacto knife. Hand punch grommet holes. Apply reinforcing tape to contour cut terminations.

g. Remove mylar template. Make contour cuts from tape spot to rough trimmed edge by and using an Exacto knife. Remove tape.

h. Move stack of 2 dacron and one mylar, align using studs on layup tool (on top of previously located inner cover sheet); overlap and tape down outer edges at contour slit cuts.

i. Repeat (c) - (h) thirteen more times (total of fourteen times) alternating contour cut patterns from layer to layer.

j. Last set of mylar/dacron will be 2 dacron, one mylar, and 2 dacron to take care of extra layer of dacron on top - same operations as (f) - (h).

k. Locate outer cover sheet on top of stack on layup tool using aligning holes. Tape outer edges in place.

l. Apply 3/8" spacers and female template onto the male contour layup tool.

m. Receive and inspect buttons, washers and grommets.

n. Push hollow needle through guide (slip-bushing) of apply template, blanket, and into foam backing block (prevents forcing layers into holes of layup tool).

o. Remove foam backing block.

p. Insert button pin into blanket using the needle as a guide. Remove slip bushing - snap on button cap, cut off button excess shank, heat seal button using a modified soldering gun.

q. Repeat (n) - (p) for all button locations.

r. Remove female apply template.

s. Insert contoured cutting surfaces between blanket inner cover and layup tool.

t. Final trim edges using 4 individual contoured edge trim tools (1 for each edge) indexed to layup tool.

u. Lift edges, insert grommets, and snap on washers - 6 places.

v. Locate and apply Velcro tape on external surface of trimmed blanket-hand layout.

w. Locate and apply Velcro to internal surface of blanket - lift edge of blanket, locate Velcro by marks on HF1 tool, press edge onto located Velcro to attach. Sew Velcro at edge location.

x. Repeat (v) and (w) as required on each edge.

y. Place on mockup tool for edge tolerance checks.

z. Remove completed blanket, handling with a contoured storage/shipping fixture.

3.2.3 Nonrecurring Costs

The nonrecurring cost for the advanced RNS is a summation of the one time expenditures associated with the engineering, fabrication, and testing in support of design and development. As in the case of the recurring cost analyses, the data to be generated will reflect previous Phase III RNS cost data and information unique to the development of the advance RNS. The development costs for the propulsion module and command and control module are 42.5 and 149.2 millions of dollars based on the previous Phase III RNS study. During the remaining study effort the development requirements for the expandable propellant module will be identified, specifically testing, tooling, and support equipment peculiar to the advance structural concept. The resulting cost will then be estimated.

Section 4

TASK 4 -- MATERIALS INVESTIGATION

This task was completed during the last quarter with specification of materials and properties for the baseline RNS configuration.

4.1 MATERIALS SUMMARY

Three major materials and process technology areas were analyzed as part of the requirements for the RNS; (a) an improved organic matrix for use in a filamentary reinforced structure, (b) an improved reinforcement, and (c) a non-permeable liner.

The criteria used in analyzing and selecting the materials and processes were (a) the materials and processes would be available within the 1980s, (b) the materials had to be compatible with either existing or potential processing techniques, (c) the materials and processes had to be compatible with the conceptual structural design, and (d) the materials and processes had to be compatible with either existing or anticipated manufacturing methods.

The materials and processes are not part of the current state of the art, however, they are logical combinations and extensions of available technology and are amenable to research and development to bring them to fruition by the 1980s.

Two organic matrices and rigidization processes have been selected based upon the major requirement of being able to fold the RNS tank for launch followed by rigidization (cure) after expansion in earth orbit. These are: (a) a two-step cure, modified epoxy - capable of being cured to a non-tacky, foldable first step cure followed by a second step cure after expansion in earth orbit to yield a rigid structure, and (b) controlled evaporation/volatilization of solvent and/or plasticizer from a plastic material.

The filamentary reinforcement selected is based on a new, longitudinal weave, woven in the form of a "sock." Socks woven to provide both longitudinal and circumferential reinforcement will provide the benefits of a

filament wound tank, but obviate the manufacturing problems associated with filament winding very large structures. The material selected as a baseline for the woven socks is DuPont's new PRD-49-3 fiber.

The non-permeable membrane concept consists of a multi-layered urethane-nickel composite. The composite is constructed by casting a film of urethane (0.038 mm), curing the urethane, vapor depositing nickel (600-1200 Å), and repeating the process to provide a non-permeable membrane. A major advantage of a multi-layered urethane-nickel membrane is that it can be formed to shape and sealed around penetrations without the problems associated with pre-cured film materials.

4.2 ORGANIC MATRIX

An improved organic matrix is required for use in the filamentary reinforced structure of the RNS. In addition to providing load transfer within the composite, the organic matrix must be compatible with the liner at cryogenic temperatures and must be processible by a two-step procedure to allow for folding, packaging, and launch in ambient earth environment followed by expansion and rigidization in earth orbit environment.

4.2.1 Requirements

The requirements for the organic matrix summarized below can be logically grouped into two categories, structureal requirements and processing and manufacturing requirements.

4.2.1.1 Structural Requirements

a. The organic matrix must form and maintain an integral bond with the tank liner. The bond strength must be greater than the stresses created by differences in thermal contraction between the composite and the liner upon cycling between 20°K and 400°K and must maintain structural integrity upon pressurization and depressurization.

b. Resin strins vary between 3 and 20 times composite strains depending on resin concentration resulting in crazing and cracking. The resin strains must be minimized.

c. Crazes must not be allowed to result in crack formation. Appropriate particulate fillers must be incorporated in the organic matrix to provide triaxial dissipation of strain energy and prevent crack propagation.

4.2.1.2 Processing and Manufacturing Requirements

a. The organic matrix must be either liquid or soluble in a suitable solvent in the uncured state so that the filamentary reinforcement can be impregnated.

b. The pot life of the formulated organic matrix must be sufficiently long under ambient conditions to permit completion of processing and manufacturing steps without gelling.

c. It is desirable that the processing and manufacturing phases be carried out under ambient conditions without having to resort to refrigeration to prevent the organic matrix from curing beyond a useful flexibility.

d. The organic matrix must be curable, or be capable of being transformed by some suitable means (first step cure) into a pliable, preferably non-tacky material, which will maintain dimensional stability under its own weight within ambient earth environment.

e. The rate of the first step cure reaction leading to a pliable, non-tacky matrix must be quantitatively controllable so that sufficient manufacturing time will be available.

f. The pliable, non-tacky characteristics of the organic matrix must be stable for sufficient time to complete the RNS construction, then fold, package, launch, and finally expand the tank in orbit.

g. The organic matrix must be capable of forming an integral bond with the impermeable tank liner while in the pliable state.

h. The organic matrix, while in the pliable state, must be foldable, packageable, and expandable, but be cured sufficiently to maintain the structural integrity of the filamentary reinforcement.

i. After the organic matrix has been cured to a flexible, non-tacky state (first step cure), the HPI and meteoroid shield must be installed. Therefore, the final rigidization process (second step cure) must take into account the fact that the tank is completely enclosed.

j. Any volatile materials liberated from the organic matrix during first step cure to the pliable state, during subsequent ground hold and launch operations, or during final rigidization (second step cure) in orbit must be compatible with, and not degrade the efficiency of, the aluminized Mylar HPI.

k. The filamentary reinforced, pliable organic matrix must be foldable and packageable without acquiring a permanent compression set or undergo other damage which would prevent the tank from being expanded into a uniform structure.

l. The filamentary reinforced organic matrix must be rigidizable (second step cure) by a simple, quantitatively definable process.

m. The rate of the second step cure reaction must be defined so that the tank can be unfolded in space environment, pressurized, and then rigidized within an acceptable time by a simple process.

4.2.2 Candidate Matrix Materials

A number of candidate resin systems have been considered for use as an organic matrix to meet the requirements for the RNS. The type of resin, the type of curing agent, the type of additives, and the solvency requirements of the components in a resin formulation, will all vary depending upon the process or processes which might be used to obtain a practical two-step process of curing/rigidization. A large number of resins and various combinations of resins must be considered:

Epoxies: Various epoxies have been considered which might lead to flexible systems within ambient earth environment but which could be rigidized in earth orbit. The classes of epoxides considered were alicyclic, aliphatic, glycidyl ethers of polyhydroxy compounds (bisphenols, glycols), and glycidyl amines (aniline, methylene dianiline).

The modulus of cured epoxies and the rate of cure can be determined by the type and chemical structure of the curing agent. Therefore, a variety of curing agents were considered: aliphatic diamines, aromatic diamines, compounds having both aliphatic and aromatic amino functionality, polyamides, anhydrides, acids, and acid complexes.

Two-step curing epoxy systems might be derivable from a catalyzed co-reactant epoxide system. Thus, mixtures of epoxides with polyhydroxy compounds and anhydrides are viable candidates.

Urethanes: The properties of cured urethanes can be varied widely by changing the chemical structure of the isocyanate moiety or by changing the structure and reactivity of the curing agent. Polyether-type urethanes have excellent cryogenic properties. In addition, they can be formulated with epoxies to yield tough materials having physical and mechanical properties in between the properties of the two components. When diepoxides and diisocyanates are heated in the presence of a catalyst an oxazolidone polymer is formed. By appropriate control of the reaction conditions, prepolymers can be obtained which lead to cured materials having excellent properties.

Soluble Resin Systems: There are conditions of temperature and choices of solvents or plasticizers which will dissolve or plasticize most resins. Since there is no single resin which will fulfill all of the established requirements, copolymers containing a variety of chemical groups and "polymer alloys" must be considered. Thus, copolymers and polymer alloys of the following resin systems are candidates: polyacrylates, polymethacrylates, polyesters, polyacrylonitrile, polyolefins (butylene, methylpentene, butadiene, ethylene, propylene), polycarbonates, polysulfones, polystyrenes, silicones, and polyamides; vinyl polymers (vinyl chloride, vinyl chloride-vinyl acetate copolymers, vinylidene chloride, vinyl formal, vinyl butyral, vinyl chloride-propylene copolymer, polystyrene-acrylonitrile copolymer, (SAN), polyacrylonitrile-polybutadiene-styrene (ABS). In a similar manner, the fluorine-containing monomers can be copolymerized with many of the above materials to provide copolymers which are soluble and have unique properties.

Additives: Additives may be necessary to improve the cryogenic fracture toughness and the strain compatibility of the selected resin system. Some additives which might be used are pre-cured, finely divided particles of elastomers (urethane, flexible epoxy, polyamides) and hollow spheres or microballoons (glass, phenolic, epoxy).

4.2.3 Low Temperature Fracture Toughness

Glassy polymers display a variety of responses to stress. For example, three obvious responses result from a tensile stress: (1) brittle fracture after elongation, (2) cold drawing involving extensive deformation, and (3) crazing (Reference 4.1).

Kambour (Reference 4.2) has observed that crack propagation involves the formation and breaking of a craze. Figure 4.2-1 taken from his excellent paper illustrates this phenomena.

Crazes result when glassy polymers are subjected to stresses less than the fracture stress. Craze formation is a function of the polymer molecular weight, is time dependent, and is accelerated by the presence of a plasticizing environment.

A craze is a plate-like region plastically deformed in the direction of the stress. The craze consists of interconnected spheroidal holes 200Å in size imbedded in a matrix of oriented polymer. Annealing the polymer above the glass transition temperature results in a "healing" of the craze.

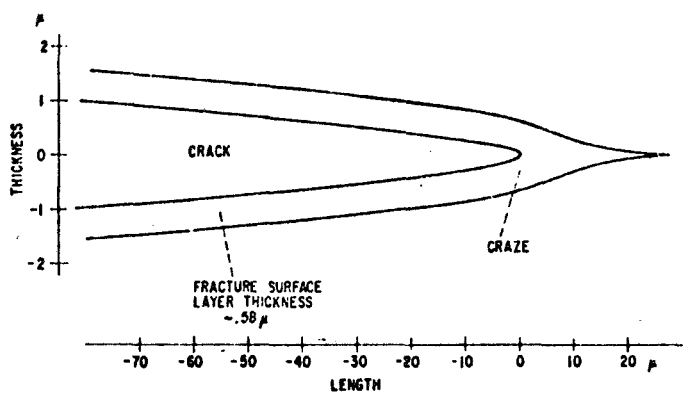

Figure 4.2-1 CRACK PROPAGATION BY CRAZE FORMATION AND BREAKING

Since all polymers contain at least trace amounts of low molecular weight species, traces of solvent impurities, traces of unreacted curing agents, etc., and one or all of which can act as a plasticizer, craze formation and incipient crack formation will be promoted provided time under stress is sufficiently long and providing there is no annealing temperature cycle. The seriousness of incipient crack formation and propagation can be mitigated by (1) appropriate choice of polymer structure which will provide relaxation phenomena below the glass transition temperature; relaxation phenomena are generally the result of polymer segmental motion and (2) incorporation of substances within the polymer which will prevent crack propagation.

Polyether-based urethane rubber has a structure which undergoes stress relaxation at low temperatures, and it is known that particles of elastomer incorporated into a glassy polymer will help prevent crack propagation. Therefore, all of the rigidized organic matrix materials discussed above should be formulated with about 2-5 percent of a finely divided urethane elastomer. Such a formulation will decrease the ultimate tensile strength about 10 percent, but should prevent catastrophic crack propagation during cyclic uses.

4.2.4 Processing

The rigidizing processes which appear feasible in terms of a 1980 time frame are: (a) two-step catalytic cure process, (b) volatilization of a solvent and/or a plasticizer from a plastic, (c) the use of a latent catalyst, i.e., a material which has no positive catalytic effect until affected by some physical or chemical agent to develop its properties, (d) a negative polymerization catalyst, i.e., a material which prevents polymerization from occurring until the material is neutralized or removed by vaporization, (e) complex formation, i.e., where one or more of the polymerizable components is chemically complexed, preventing cure. These rigidization, or curing processes are discussed separately below. It must be emphasized, however, that the present state of the art indicates that there is no unique material or process which will currently meet the established requirements for the organic matrix.

The following discussion of the various rigidization processes is ranked according to the methods which could probably be most readily quantized and brought to practical fruition by the 1980s.

Although the dual curing system is ranked first indicating that it would probably require less research and development effort, method (b) "Volatilization of a solvent and/or a plasticizer from a plastic," would probably provide a more quantitatively controllable process.

4.2.4.1 Two-Step Catalytic Cure Process

Most reactions of thermoset polymers can be thought of as a two or more step catalytic cure. For example epoxies react at some intermediate temperature to give a B-stage material which can be stored at low temperatures for extended periods of time without appreciable reaction occurring. If the B-staged material is warmed, further staging (or advancement, or cure) will occur. If the temperature is raised further, the rate of the cure reaction will increase, the rate of cure approximately doubling for each 10°K rise in temperature. These phenomena are depicted in Figure 4.2-2.

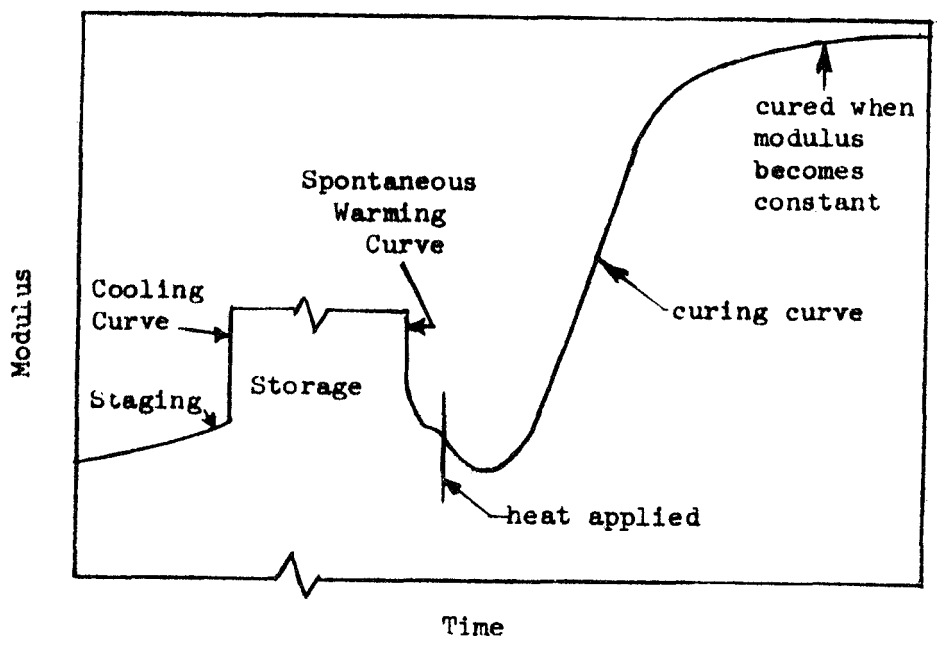

Figure 4.2-2 THERMAL EFFECTS ON EPOXY RESIN

Unfortunately, for the application intended for RNS, the usual materials and staging conditions cannot be used readily. B-staged epoxies are tacky, or if they are staged beyond the tacky state, they are "boardy," i.e., they break if an attempt is made to bend them without warming.

There are a number of epoxy resin systems which have a potential for being developed into the type of two-step cure process necessary to meet the established requirements.

Ciba-Geigy has recently announced a new developmental epoxide (Reference 4.2) which has been described as curable in a two-step process.

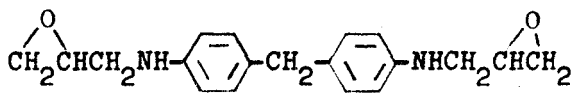

A proprietary system has been partially defined which has some of the desired characteristics (Reference 4.4). A polyepoxide was caused to react with a polyhydroxy compound in the presence of an amine catalyst at relatively low temperatures to yield a rubbery, non-tacky material, which upon heating to 408°K, caused a final anhydride cure to yield a material having 25 percent elongation at room temperature.

Thus, the process envisioned would involve the reaction of a mixture of a polyepoxide, a polyhydroxy compound, an anhydride, and an amine catalyst. Upon heating at a relatively low temperature (ca. 350°K) a first step cure would occur leading to a rubbery, non-tacky material. The rate of reaction of the polyepoxide with the polyhydroxy compound is greater than the rate of reaction with the anhydride. Upon raising the temperature, the second step cure occurs, involving reaction of the anhydride, yielding the final, rigidized material.

In order to optimize the properties for use at liquid hydrogen temperatures and provide the greatest possibility for the cured epoxy to exhibit stress relaxation phenomena, polymer structure disorder can be accomplished by using a mixture of structurally dissimilar epoxies, mixtures of polyhydroxy compounds, mixtures of anhydrides, and mixtures of curing agents.

A baseline composition for the two-step cure process might be formulated as follows:

a. Mixture of Epoxides
   diglycidyl ether of bisphenol A
   triglycidyl ether of glycerol
   bis (2,3 - epoxycyclopentyl) ether

b. Mixture of Polyhydroxy Compounds
   ethylene glycol
   diethylene glycol
   dipropylene glycol
   glycerol

c. Mixture of Anhydrides
   phthalic anhydride
   pyromellitic dianhydride
   methyl tetrahydrophthalic anhydride

d. Mixture of Curing Agents
   triethylenetetraamine (TETA)
   triethanol amine
   methylene bis (o-chloroaniline) (MOCA)

The use of mixtures of triethylenetetraamine and triethanol amine is known to produce a synergistic lengthening of pot life (Reference 4.5). It is very important that the organic matrix have a sufficiently long pot life to allow completion of the processing and manufacturing steps before gellation occurs.

4.2.4.2 Volatilization of a Solvent and/or a Plasticizer

Extensive literature is available describing the use of plasticizers to improve the flexibility of plastics. The major investigative efforts have been directed to the development of polymer-plasticizer compatible systems where the plasticizer would not "bleed" out, or vaporize out of the polymer.

The design of materials where solvent and/or plasticizer could be used to flexibilize a polymer and then be quantitatively removed by vaporization in

a controlled two-step process would require a basic synthetic organic and physical chemical investigation. However, certain logical assumptions can be used to arrive at the type of process which would be required.

A study of Stuart-Briegleb molecular models (Reference 4.6) of various polymers, copolymers, and cross-linked polymers in conjunction with models of various plasticizers, has indicated the type of experimental studies which would be required to quantize the solvent/plasticizer volatilization method of rigidization. For example, the rate of volatilization of the plasticizer is a function of both the vapor pressure of the solvent/plasticizer and the rate at which the solvent/plasticizer diffuses (or migrates) to the surface. Some of the chemical, physical, and mechanical parameters which affect the rate of diffusion include:

a. The chemical nature of the groups within the polymer chains, i.e., ketone, ester, amide, ether, etc.
b. The free volume within the bulk polymer.
c. The cross-link density, i.e., the number of interconnections between polymer chains per repeating unit.
d. The molar volume, chemical structure (shape), and the chemical nature of the functional groups within the plasticizer.
e. The degree of crystallinity of the polymer.

McDonnell Douglas Astronautics has expended several man-years developing and computerizing information about the compatibility of materials, with special reference to functional fluids and elastomers, using solubility parameters (Reference 4.7).

In addition, a study of techniques to calculate physical properties of materials based on a matrix algebraic establishment of additive group contributions to physical properties was highly successful (Reference 4.8).

In order to optimize a polymer for use as the organic matrix in a hydrogen tank wall, the Tg should be as low as possible, or various polymer segmental motions must be available to allow a stress relaxation to occur at temperatures below the glass transition temperature. This cannot be accomplished by simply copolymerizing two different monomers; the Tg of a copolymer is generally intermediate between the Tg's of the individual polymers.

It appears possible that copolymers having controlled cross-linking could be predicted using solubility parameters, and applying the matrix algebraic methods to Tg and relaxation phenomena, both in conjunction with studies of Stuart-Briegleb models. Synthesis of suitable systems would follow for verification and iterative optimization.

A process involving a two-step system would probably involve dissolving the polymer in a three component solvent. The three components would be a low molecular weight solvent to allow impregnation of the reinforcement, a less volatile solvent which could be removed in a quantitative and controlled manner to yield a pliable, non-tacky, foldable structure, and a plasticizer which would be removed by volatilization after the tank is deployed in orbit.

The techniques outlined which would lead to a rigidization process based on the quantitative and controlled volatilization of solvent/plasticizer provide the most logical approach to the development of a 1980 polymer technology fitting the established requirements for the organic matrix.

4.2.4.3 Latent Catalyst Process

There are a number of latent catalysts which might be used to cause the cure of a thermoset material. For example, ethanolamine-boron trifluoride reacts only very slowly with epoxy resins under ambient conditions, but causes a rapid cure to occur at 348-373°K. The reactivity of amine-boron trifluoride complexes can be controlled by varying the chemical structure, and hence, the basicity, of the amine (References 4.9 and 4.10).

4.2.4.4 Negative Catalyst Process

There are many materials which inhibit or prevent chemical reaction; such materials are referred to as negative catalysts. For example, some silicones will not polymerize if there is an amine present and some acrylates polymerize only slowly in the presence of oxygen, but cure rapidly when oxygen is excluded. The activity of negative catalysts is generally manifested by the formation of a complex with one of the reactants. If the negative catalyst is removed or inactivated by reaction with a suitable material which is not part of the polymerization reaction, then the desired reaction can proceed. Amines or Lewis acids such as boron

trifluoride which normally catalyze the cure of epoxies which form weak complexes with various functional groups (double bonds, ketones, esters, etc.) which would normally be involved in a polymerization reaction, can function as negative catalysts. A systematic study of negative catalysts, or inactivation of a necessary component in a polymer reaction by complex formation could lead to the development of technology necessary to meet the established requirements for an organic matrix. However, the study, at least in the beginning, would be highly empirical and less sure of success.

4.2.4.5 Complex Formation

There are many possible chemical complexes which are stable within ambient earth environment but which can be caused to liberate one or more polymerizable components by some suitable process or combination of processes. For example, complex formation involves the reaction of two or more substances,

$$A + B + C \underset{}{\overset{K}{\rightleftharpoons}} A - B - C$$

The dissociation of the complex, ABC, can be caused by increasing the temperature, by removing one of the reactants by complexing with a third substance to form a thermodynamically more stable complex, by precipitation, by volatilization, etc.

Quantitative data necessary to design a rigidization process based on complex formation and dissociation are not available. In addition, many complexes are solid and might sublime if a mixture were exposed to space vacuum. However, complexes of polymeric substances are known, such as the Lewis acid complexes of polymeric amines, and therefore, the use of complexes could be a viable process.

4.2.5 Properties of the Organic Matrix

The properties of the organic matrix in the flexible state, and in the final rigidized state should be essentially the same regardless of the process used. The ranges of properties for the matrix are shown in Table 4.2-1. It would be desirable to have a material with very high strength and toughness and therefore it is anticipated that the organic matrix will be formulated with 2-5 percent of a finely divided polyurethane elastomer or other additive

to prevent catastrophic crack propagation during cyclic use. Such a formulation will probably decrease the room temperature ultimate tensile strength by about 10 percent.

Table 4.2-1

ORGANIC MATRIX PROPERTIES

	FLEXIBLE STATE		RIGID STATE	
	UTS MN/m^2 (ksi)	E MN/m^2 (ksi)	UTS MN/m^2 (ksi)	E MN/m^2 (ksi)
Resin	34.5-68.9 (5-10)	55.1-172 (8-25)	62-82.6 (9-12)	2760-4100 (400-600)

4.3 Filamentary Reinforcement

An improved composite tank wall for the RNS is dependent upon an improved filamentary reinforced composite and new assembly concept.

4.3.1 Requirements

The selection of a reinforcement has been determined by a consideration of the various filamentary materials available, the existing properties of filamentary materials and the properties anticipated by the 1980 time frame, compatibility with the structural design, compatibility with the proposed processing and manufacturing sequence, compatibility with the two-step cure process necessitated by the requirement to fold within an earth environment and then expand and rigidize within earth orbit environment. In addition, a comparison of specific strengths and moduli and strain compatibilities of various reinforcement materials was considered. A conceptual analysis of the RNS indicates that the reinforcement must meet the following requirements:

a. The filamentary reinforcement must have as high a specific strength as possible to provide a minimum weight tank.

b. The filamentary reinforcement must have as high a specific modulus as possible to provide a structurally stable tank.

c. The strain incompatibilities between the reinforcement and the matrix must be minimized at cryogenic temperatures.

d. The reinforcement must be wet by the uncured organic matrix.

e. The reinforcement must bond to the organic matrix during the first step cure and maintain the bond during fold, launch, and expansion in earth orbit.

f. The reinforcement must remain bonded to the organic matrix during the final rigidization in earth orbit environment.

g. The filamentary reinforcement must withstand thermal cycling between 20° and 400°K.

h. The filamentary reinforcement must be capable of being woven into a "sock" of the size and shape of the tank.

i. The "sock" must have sufficient abrasion resistance to be handled and installed on the tank without damage.

4.3.2 Candidate Reinforcement Materials

A survey of various filamentary and woven materials was made and boron, graphite, S -glass, and PRD-49-3 fibers were selected as viable candidates. Present and predicted fiber properties are shown in Tables 4.3-1 and 4.3-2. Composite properties are shown in Tables 4.3-3 and 4.3-4.

The assumption was made that the fibers and matrix are integrally bonded together such that the longitudinal strain in the matrix and fibers are equivalent. The following terms were defined:

σ_f = stress in the fibers

σ_m = stress in the matrix

e_f = strain in the fibers

e_m = strain in the matrix

E_f = Young's modulus of the fibers

E_m = Young's modulus of the maxtix

Hooke's law for a uniaxial stress is:

$$\sigma = eE$$

By applying Hooke's law to the fibers and matrix and equating the strains in the matrix and fibers, the following relation is obtained:

$$\frac{E_f}{E_m} = \frac{\sigma_f}{\sigma_m}$$

This relation indicates that the stress applied to a composite, parallel to the reinforcing fibers, is redistributed in the proportion to the relative moduli of the matrix and the filamentary reinforcement. Thus, in the case of organic matrix composites reinforced with high modulus fibers, essentially all the load is carried by the fibers, as the ratio of the moduli exceed 100:1.

The calculation of the predicted moduli and strengths of composites for the 1980's is based upon the rule of mixtures:

$$E_c = E_f V_f + E_m (1-V_f)$$

and

$$\sigma_c = \sigma_f V_f + \sigma_m (1-V_f)$$

Table 4.3-1

PRESENT AND PREDICTED 1980 FIBER PROPERTIES

(Uniaxial at Room Temperatures - International Units)

FIBER IN ORGANIC MATRIX	PRESENT PROPERTIES					EST 1980 PROPERTIES				
	ρ 10^3 Kg/m^3	E 10^{10} N/m^2	UTS 10^8 N/m^2	$\frac{\rho}{E}$ 10^7 m	$\frac{UTS}{E}$ 10^5 m	ρ 10^3 Kg/m^3	E 10^{10} N/m^2	UTS 10^8 N/m^2	$\frac{\rho}{E}$ 10^7 m	$\frac{UTS}{E}$ 10^5 m
Boron-Tungston Core	2.63	41.3	31	15.7	11.8	2.48	44.8	34.5	18.1	13.8
Graphite*	1.4-2.0	17.2-51.7	12.4-25.8	12.3-25.9	8.9-12.9	1.94	69.0	34.5	35.6	17.8
S-Glass	2.49	8.5	44.8	3.4	18.0	2.49	8.6	44.8	3.5	18.0
PRD 49.3	1.47	13.8	23.4	9.4	15.9	1.47	17.3	27.6	11.8	18.8

*High strength-high modulus graphite fiber is not presently available. The process used to produce graphite fiber can be optimized to yield either high strength or high modulus material.

Table 4.3-2

PRESENT AND PREDICTED 1980 FIBER PROPERTIES
(English Units)

POTENTIAL REINFORCEMENT	PRESENT PROPERTIES					EST 1980 PROPERTIES				
	ρ Lbs/in.^{3}	E 10^6 psi	UTS 10^5 psi	$\frac{E}{\rho}$ 10^6 in.	$\frac{UTS}{\rho}$ 10^6 in.	ρ Lbs/in^3	E 10^6 psi	UTS 10^5 psi	$\frac{E}{\rho}$ 10^6 in.	$\frac{UTS}{\rho}$ 10^6 in.
Boron-Tungsten Core	0.095	60	4.5	632	4.78	0.086	65	5.0	756	5.81
Graphite*	0.051-0.072	25-75	1.8-3.75	490-1042	3.55-5.21	0.070	100	5.0	1430	7.14
S-Glass	0.090	12.4	6.5	138	7.22	0.090	12.4	6.5	138	7.22
PRD-49-3	0.053	20	3.4	376	6.42	0.053	25	4.0	472	7.54

* High strength-high modulus graphite fiber is not presently available. The process used to produce graphite fiber can be optimized to yield either high strength or high modulus material.

Table 4.3-3

PRESENT AND PREDICTED 1980 COMPOSITE PROPERTIES

(Uniaxial at Room Temperature - International Units)

	Present Properties					Est. 1980 Properties				
Fiber in Organic Matrix	ρ 10^3 Kg/m^3	E 10^{10} N/m^2	UTS 10^8 N/m^2	$\frac{E}{\rho}$ 10^7m	$\frac{UTS}{\rho}$ 10^5 m	ρ 10^3 Kg/m^3	E 10^{10} N/m^2	UTS 10^8 N/m^2	$\frac{E}{\rho}$ 10^6 m	$\frac{UTS}{\rho}$ 10^4 m
Boron-tungsten core	1.91	22.8	17.1	11.9	8.95	1.83	26.9	20.7	14.7	11.3
Graphite	1.22-1.55	9.53-28.5	6.82-14.2	7.8-18.4	5.58-9.17	1.61	41.3	20.7	25.6	12.9
S-Glass	2.06	6.00	31.2	2.9	15.2	2.06	6.0	31.2	2.9	15.2
PRD-49-3	1.35	8.40	16.4	6.2	12.2	1.36	12.1	19.3	8.9	14.2

Table 4.3-4

PRESENT AND PREDICTED 1980 COMPOSITE PROPERTIES
(Uniaxial at Room Temperature - English Units)

	PRESENT PROPERTIES						EST. 1980 PROPERTIES					
FIBER IN ORGANIC MATRIX	ρ Lbs/in^3	E 10^6psi	UTS 10^5psi	$\frac{E}{\rho}$ 10^6in.	$\frac{UTS}{\rho}$ 10^6in.	VOL. % FIBER	ρ Lbs/in^3	E 10^6psi	UTS 10^5psi	$\frac{E}{\rho}$ 16^6in.	$\frac{UTS}{\rho}$ 16^6in.	VOL. % FIBER
Boron-Tungsten Core	0.069	33	2.48	478	3.6	55	0.066	39	3.0	591	4.55	60
Graphite	0.044-0.056	13.8-41.3	0.99-2.06	314-738	2.04-3.68	55	0.058	60	3.0	1040	5.17	60
S-Glass	0.075	8.70	4.55	116	6.15	70	0.075	8.70	4.55	116	6.10	70
PRD-49-3	0.049	14.0	2.38	292	4.96	70	0.049	17.5	2.8	357	5.7	70

where

E_c = modulus of the composite

V_f = volume fraction of the fibers in the composite

E_m = modulus of the matrix

Since it is assumed that the organic matrix does not contribute to the properties of the composites, the above relationships reduce to

$$E_c = E_f V_f$$

$$\sigma_c = \sigma_f V_f$$

4.3.3 Evaluation

A comparative evaluation has been made of boron, graphite, S-glass, and PRD-49-3 fibers in terms of the established requirements.

Boron Fialments

The processing technology for boron filament reinforced composites has advanced significantly and is being used on flight hardware. Although the specific strength of boron composites is not as great as for graphite, S-glass, and PRD-49-3, the strength increases at cryogenic temperatures. The thermal contraction characteristics for boron are similar to those of S-glass and therefore, the strain compatibilities would be similar. The anticipated 1980 properties indicate that boron filaments will probably not improve as much as graphite and PRD-49-3.

Boron filaments cannot be woven simply and cannot be used to provide a sock as described in Section 4.3.4, below.

Graphite

A variety of graphite filaments are available with moduli ranging from 25 to 75 million psi and strengths ranging from 375,000 psi to 180,000 psi. The processes used to prepare graphite filaments can be optimized to provide either high modulus or high strength material. It is anticipated that new and improved techniques will lead to a graphite fiber having a modulus of 100 million and a strength of 500,000 psi by 1980.

S-Glass

S-glass reinforced pressure vessels have been studied extensively and the properties of S-glass fibers are better known than the other candidates. S-glass filamentary reinforced composites undergo strength degradation due to cyclic loading or sustained loading, especially when the loads are a high percentage of ultimate forcing a lower design allowable. However, some recent data (Reference 4.11) has indicated that the cyclic fatigue performance at cryogenic temperatures may actually improve.

A comparison of the properties of S-glass indicates that is has the highest specific strength of the candidate fibers. However, it is not anticipated that the properties of S-glass will improve significantly by 1980.

PRD-49-3

PRD-49-3 is a new fiber introduced recently by DuPont.

The fracture toughness of epoxy composites has been reported to be greater than for either boron or graphite composites and the fiber ultimate tensile strength is 340,000 psi at 1.8 percent elongation. In addition, considerable improvement can be expected by the 1980's (Reference 4.12).

Work at the Boeing Airplane Company has resulted in the following conclusions: (Reference 4.13).

a. Mechanical property data generated in the program verifies that the (PRD) composites evaluated have the highest specific strength of any known material.

b. Cryogenic temperatures do not degrade composite mechanical properties.

c. Potential for using the composites in structural tension applications, such as filament-wound pressure vessels, is considered excellent.

Composite reinforced propellant tanks are being evaluated by Grumman using boron, graphite, S-glass, and PRD-49-1 fibers. Their preliminary data indicate that the PRD fiber is outstanding (Reference 4.14).

The contraction curves for epoxy composites derived from the candidate fibers are shown in Figure 4.3-1 to provide a comparison of the relative structural changes anticipated upon cooling the various materials to cryogenic temperatures.

The outstanding properties and anticipated improvements suggest that PRD-49-3 fiber is the reinforcement material of choice for the RNS.

4.3.4 Assembly Concept

The reinforcement material and assembly have been selected to match the operational stress field in the tank. Since the load in the circumferential direction is twice that in the longitudinal direction, there must be twice as many circumferential layers of reinforcement as longitudinal layers.

A unidirectional reinforcement was selected over a woven cloth because the tensile strength of cloth composites is only about 30-40 percent of the strength of unidirectional reinforced composites.

The structure of the reinforcement has been chosen so that it can be handled like a woven "sock" having the correct shape and dimensions, but approach the strength of a filament wound tank. A recent development by Woven Structures Division of HITCO (Reference 4.15) in making longitudinal weaves and cylinders using longitudinal weaves will be used. The longitudinal weaves have 90-94 percent of the fibers in one direction and are tied togegher with 6-10 percent transverse yarns.

The socks are designed so that they structurally tie the end domes into the tank.

The first layer of longitudinal reinforcement will be slipped over the mandrel using a Teflon sleeve to reduce frictional drag. The first sock will be impregnated with the organic matrix and then the second layer of longitudinal reinforcement will be installed using a Teflon sleeve. The second layer will be impregnated and then four layers of circumferential reinforcement will be installed in the same manner. After all of the socks are installed and impregnated the mandrel will be pressurized to tensile the filaments to about 12 percent of ultimate before the first step cure.

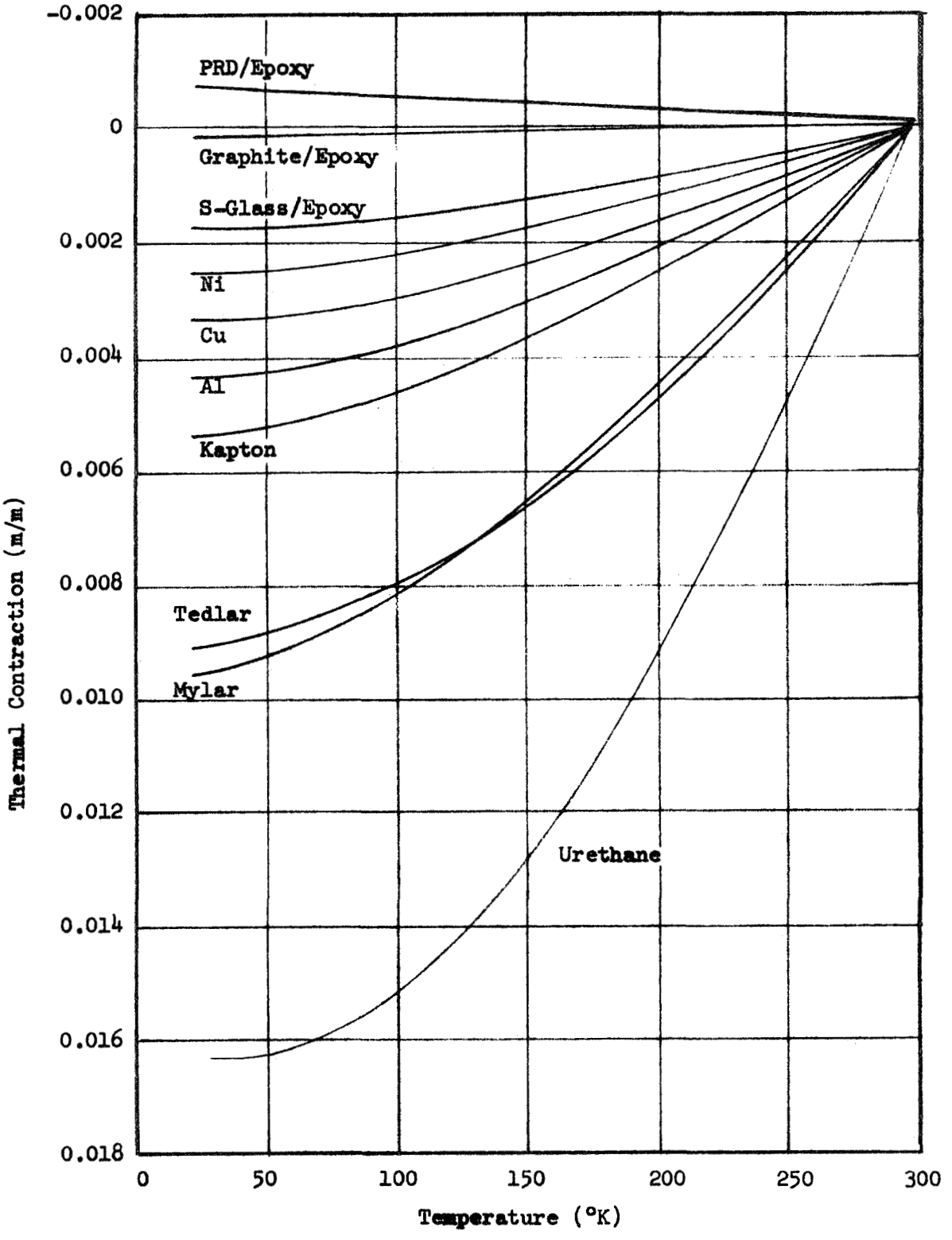

Figure 4.3-1 CONTRACTION CURVES FOR POTENTIAL MATERIALS

4.4 Tank Liner

An impermeable membrane must be provided as a tank liner to contain the LH_2 propellant. The liner is necessary because filamentary reinforced organic matrices craze and crack under composite strains of 0.5 to 2 percent of the composite strain and it has been shown by Kies (Reference 4.16) that resin strains can be as high as 3 to 20 times composite strains, depending upon resin content. Therefore, the liner must bridge the resulting discontinuities and provide an impermeable barrier to both liquid and gaseous hydrogen.

4.4.1 Requirements

The requirements for a liner for the RNS are:

a. A compatible coefficient of contraction of the liner and composite is necessary to minimize differential stresses. (Figure 4.3-1).

b. The liner must be capable of cyclic loading to 1.8 percent strain and maintain physical and mechanical integrity.

c. During the construction of the tank, the membrane will act as the outer surface of a mandrel.

d. After the installation of the filamentary reinforcement and the impregnation of the reinforcement with organic matrix, the organic matrix will be submitted to a first step cure. The membrane must form an integral bond with the organic matrix.

e. The membrane must remain bonded to the organix matrix while the tank is folded, packaged, launched and unfolded.

f. An integral bond betwen the membrane and the tank wall must be maintained during and after the second step cure.

g. The membrane must be capable of multiple cycling from 20 to 400°K.

h. The membrane will not be a load carrying member of the structure.

i. The membrane must be processible so that it can be formed around lead-throughs and provide a seal around the lead-throughs.

j. The major limiting factor on the allowed leak rate (permeability) of the membrane is determined by the insulative degradation of the HPI.

4.4.2 Candidate Liner Materials

A number of materials have been investigated for use as impermeable liners for filament wound pressure vessels for cryogenic applications. (References 4.17 and 4.18).

Electrochemically deposited copper, silver, and nickel foils and hand-formed aluminum foil have been investigated.

Non-metallic films which have been investigated include Mylar, Tedlar, Kapton, polyurethane, and a glass flake-backed polyester. Vacuum deposited metals on various organic films were included for consideration and evaluation as potential liner materials.

4.4.3 Evaluation

There are several drawbacks to the use of a metal foil as a liner material:

a. The metal exhibits low (0.25 to 0.5 percent) elastic strain and any additional strain necessary to match the strain in the composite during pressurization must occur by plastic deformation. Upon depressurization, the metal liner can recover the 0.25 to 0.5 percent strain elastically and then one of three possible situations may prevail:
   1. The adhesive bond betwwn the metal liner and the composite remains intact and the liner undergoes plastic deformation to return to the original state.
   2. The adhesive bond remains intact but the adhesive is incapable of causing plastic deformation in the liner and therefore the liner fails.
   3. The liner buckles and fails due to an adhesive failure.

b. Electrodeposited liners (no seams) can be cycled at both ambient temperature and at 20°K without failure. On the other hand, aluminum foil liners with a bonded seam all leaked at the seam at cryogenic temperatures.

c. Complex curvature metal liners are difficult to fabricate.

d. Metal foil liners would be very difficult to fold without undergoing permanent plastic deformation at the complex curvature fold.

Most of the non-metallic films which have been investigated have low total elongation at 20°K which make them unsuitable for use as liner materials designed to take all of the tensile strain in filament wound vessels.

A major problem with Mylar, Tedlar, and Kapton is that joining (seam formation) is difficult and obtaining an integral bond between the liner and the composite is difficult. These materials are available only as precured films and are not heat sealable, are not soluble in solvents, and cannot be adhesively bonded such that the adhesive bond will withstand the thermal contraction. The glass flake backed polyester can be adhesively bonded but is an inherently low strength material. The polyurethane film forms an excellent adhesive bond but is permeable.

An approach presently being investigated by Boeing Airplane Company under NASA Contract No. NAS3-13326 is to deposit gold onto Kapton, then put two layers together and diffusion bond the gold to form a homogenously bonded candidate liner. (Reference 4.19).

Most of the materials which have been investigated are difficult to join, difficult to bond for reliable performance at cryogenic temperatures, difficult to obtain with complex curvatures, difficult to fold and difficult to seal around lead-throughs.

A consideration of the joining problems, the complex curvature, and the necessity of folding the RNB tank suggested that a liner material be

considered which could be formed simply to the correct size and shape. Hence, thin coatings of metal on various nonmetallic substrates were considered.

Lead, aluminum, and nickel appear worthy of consideration for vacuum deposition onto a film. All three metals had been deposited onto Kapton, Mylar, and Tedlar, and lead and aluminum had been deposited onto urethane (Reference 4.20), but nickel had not.

However, a consideration of the overall technology involved suggested that it would be possible, and the practical advantage of the improved corrosion resistance of nickel over aluminum was one of the deciding factors in its consideration. Lead can probably be deposited with fewer "pin holes" than with aluminum or nickel but was not given serious consideration because of the additional weight.

4.4.4 Selected Concept

A liner concept consisting of a multilayer, metal-urethane composite was selected as most likely to meet all of the requirements (Figure 4.4-1).

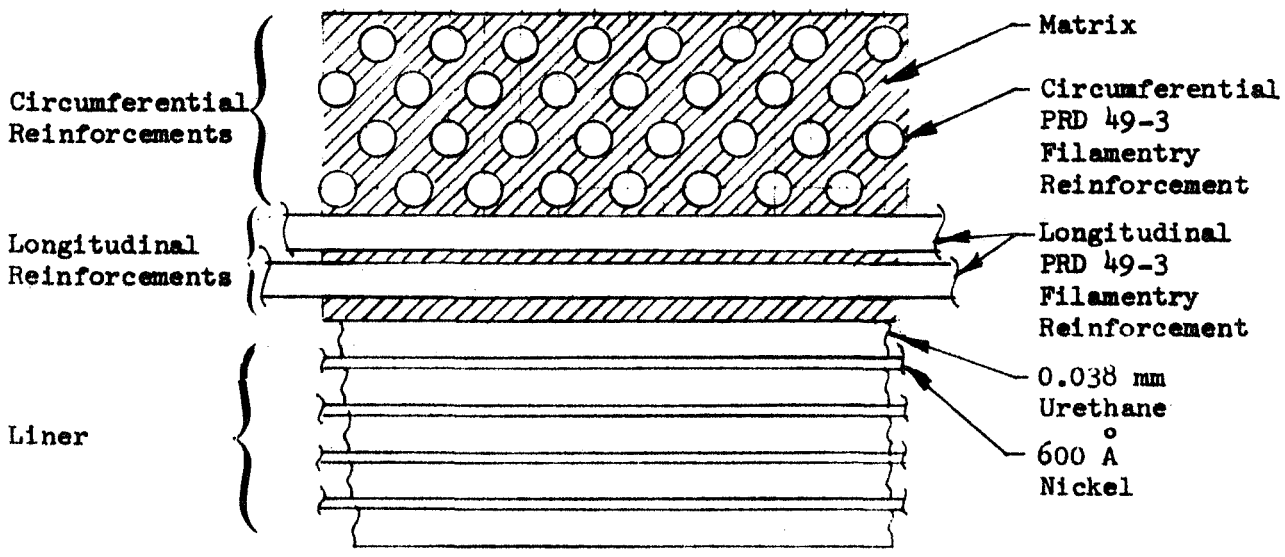

Figure 4.4-1 TOTAL MATERIALS SELECTION FOR RNS TANK WALL

The thickness required for the urethane layers cannot be analytically predicted, but has been selected at about 0.038 mm as a practical thickness which can be controlled by either spray or brush coating.

The multi-layer construction was selected to minimize the problem with pin holes which normally result when thin layers of metal are vapor deposited. Generally, control of metal coating thickness cannot be maintained below about 100 Å with 200 Å being a normal production limit. In comparison, aluminized Mylar used for high performance insulation has a coating thickness of about 1200 Å of aluminum.

A coating thickness of 600 Å has been selected as a thickness which can be controlled and still provide relatively few pin holes. A liner consisting of five layers of 0.038 mm urethane and four layers of 600 Å nickel weighs 0.244 Kg/M^2 ($0.05/LB/FT^2$).

It has been experimentally verified that nickel can be vapor deposited onto a urethane film. Microscopic investigation indicates very few pin holes and the elongation of the material is excellent.

REFERENCES

1.1 "Nuclear Shuttle System Definition Study Phase III Final Report," Volume II, Part B, Book 2, Contract NAS8-24714, Report Number MDC G2134, May 1971.

1.2 "Nuclear Shuttle Systems Definition Study Phase III," Volume II, Part B, Contract NAS8-24715, Report Number LMSC-A984555, May 1971.

2.1 "Buckling of Thin Walled Cylinders," NAS SP-8007, August, 1968.

2.2 D. K. Weidner, ed., "Natural Environment Criteria for the NASA Space Station Program," NASA TMX-53865, October 31, 1969.

2.3 "Investigation of Smooth-Bonded Metal Liners for Glass Fiber Filament-Wound Pressure Vessels," Contract NAS CR-72165, McDonnell Douglas Report DAC-60640, May 1967.

2.4 D. J. Soltysiak and J. M. Toth, "Static Fatigue of Fiber Glass Pressure Vessels from Ambient to Cryogenic Temperatures," DAC-59904, May 1966.

2.5 "Investigations Regarding the Development of a High Performance Insulation System," Contract NAS8-20758, Lockheed Report K-17-68-5, 25 July 1968.

2.6 "Investigation of High-Performance Insulation Application Problems," Contract NAS8-21400, McDonnell Douglas Report MDC-G 1152, 20 July 1969.

2.7 "Investigation of High-Performance Insulation Application Problems," Contract NAS8-21400, McDonnell Douglas Report MDC-G1238, 20 October 1969.

3.1 McMaster, R. C., Nondestructive Testing Handbook, 1959.

3.2 Scherb, M. V., et.al.,"Experimental Evaluation of Three Leak Detection and Location Concepts for Space Stations," Contract No. NAS1-10840, Interim Report, November 1971.

3.3 Cook, J. L., Reinhardt, W. W., and Zimmer, J. E., "Development of Nondestructive Test Techniques for Multidirectional Fiber Reinforced Resin Matrix Composites," AFML-TR-71-187, October, 1971.

3.4 Evangelides, J. J., Meyer, R. A., and Zimmer, J. E., "Investigation of the Properties of Carbon-Carbon Composites and their Relationship to Nondestructive Test Measurements," AFML-TR-70-213 Parts I and II, August 1971.

3.5 Zelik, J. A., "Holographic Flaw and Crack Detection in Metallic Pressure Vessels," To be published.

3.6 Burchett, D. J., "Laser Holography of Carbon Composite Structures," Carbon Composite Technology Symposium, January 30, 1970.

3.7 Development of Light Weight Materials Composites to Insulate Cryogenic Tanks for Thirty Day Storage in Outer Space, Contract NAS8-26006, Report No. MDC G0683, September 1970.

3.8 Blome, J. C., "Development of a Thermal Protection System for the Wing of a Space Shuttle Vehicle," MSC-02562, February 1971.

3.9 Hagemaier, D. J., McFaul, H. J., and Parks, J. T., "Nondestructive Testing Techniques for Fiber Glass, Graphite Fiber, and Baron Fiber Composite Aircraft Structures," Douglas Paper 5549, October, 1969.

3.10 Evangelides, J. S. and Zimmer, J. E., "Evaluation of a Resin Matrix Composite Subjected to Impulsive Loading," MDAC-WD 62990, July 1969.

4.1 S. Newman, Appl. Polymer Symposia 1, 161 (1968)

4.2 R. P. Kambour, Appl Polymer Symposia 1, 215 (1968)

4.3 Personal Communication, Mr. K.C. Johnson, Ciba-Geigy, Inc., July 1971

4.4 Personal Communication, Dr. Henry Lee, Lee Pharmaceutical Inc., July 1971.

4.5 H. Lee and K. Neville, "Handbook of Epoxy Resins," McGraw-Hill Book Company, New York, 1967.

4.6 Stuart-Briegleb Atomic Models are avilable within the United States from Arthur S. LaPine and Company, Chicago, Illinois.

4.7 R. G. Larkin, C. F. Wissman, and R. M. Washburn, unpublished work.

4.8 R. M. Washburn, C. F. Wissman, and R. G. Larkin,"Organic Materials Physical Property Prediction from Molecular Structure," Douglas Report SM-45968, 22 September 1964.

4.9 A. V. Topchiev, S. V. Zavgorodnii, and Ya. M. Paushkin,"Boron Fluoride and Its Compounds as Catalysts in Organic Chemistry,"Pergamon Press, New York, 1959.

4.10 H. S. Booth and D. R. Martin, "Boron Trifluoride and Its Derivatives," John Wiley and Sons, Inc., New York, 1949.

4.11 M. P. Hanson,"Static and Dynamic Fatigue Behavior of Glass Filament-Wound Pressure Vessels at Ambient and Cryogenic Temperatures," NASA TN-D-5807, May 1970.

4.12 E. I. du Pont de Nemours & Co., Inc., Technical Data published by the Pioneering Research Division, Textile Fibers Department, PRD-49-1 High Modulus Fibers and Composites, 1971; also, personal communications, Dr. D. L. G. Sturgeon, Autust 1971

4.13 The Boeing Airplane Company, Cryogenic Filament-Wound Tanks, Contract No. NAS3-13330, April 1971.

4.14 B. J. Aleck, Composite Reinforced Propellant Tanks, Quarterly Technical Progress Narrative No. 1, Contract No. NAS3-14368, September 1971.

4.15 Personal Communication, Mr. M. Black, HITCO, July 1971: Personal Communications, Messrs. W. T. Miller and J. A. McGrath, Woven Structures Incorporated, September 1971.

4.16 J. A. Kies,"Maximum Strains in the Resin of Fiber Glass Composites," U. S. Naval Research Laboratory, Report No. AD 274560, March 1962.

4.17 J. M. Toth, Jr., W. C. Sherman, and D. J. Soltysiak, "Investigation of Structural Properties of Fiber Glass Filament-Wound Pressure Vessels at Cryogenic Temperatures," NASA CR-54393, September 1965.

4.18 J. M. Toth, Jr., and D. J. Soltysiak, "Final Report, Investigation of Smooth-Bonded Metal Liners for Glass Fiber Filament-Wound Pressure Vessels." NASA CR-72165, May 1967.

4.19 Personal Communication, Raymond F. Lark, NASA, Lewis Research Center, August 1971.

4.20 Personal Communication, W. I. Jacobi, G. T. Schjeldahl Company, July 1971.

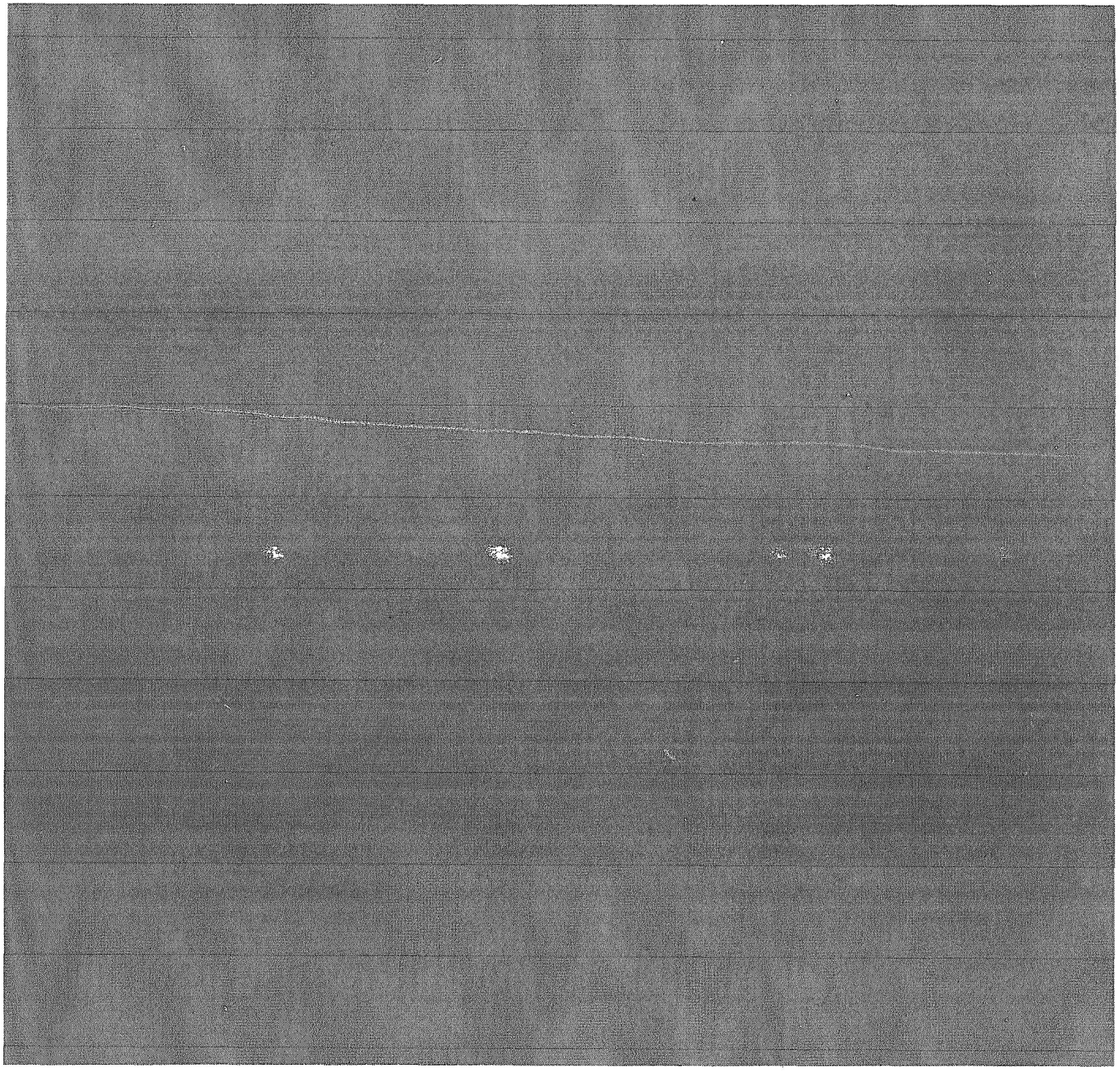

MCDONNELL DOUGLAS ASTRONAUTICS COMPANY

5301 Bolsa Avenue, Huntington Beach, California 92647 (714) 897-0311